Technical University of Munich
TUM School of Medicine and Health

Effects of n-3 Polyunsaturated Fatty Acids and Lipid Mediators on Inflammation Resolution and Remyelination in a Mouse Model of Lysolecithin Induced Demyelination.

Alix S. M. J. Bertrand

Complete reprint of the dissertation approved by the TUM School of Medicine and Health of the Technical University of Munich for the award of the Doktorin der Medizin (Dr. med.).

Chair: Prof. Dr. Marcus Makowski

Examiners:

1. Prof. Dr. Mikael Simons
2. apl. Prof. Dr. Anja Horn-Bochtler

The dissertation was submitted to the Technical University of Munich on 20 December 2023 and accepted by the TUM School of Medicine and Health on 8 May 2024.

Table of contents

List of Abbreviations

AA. Arachidonic acid
Abca1. ATP-binding cassette transporter A1
Abcg1. ATP-binding cassette sub-family G1
AD. Alzheimer's disease
AFN. Atipamezole/ naloxone/ flumazenil
ALOX. lipoxygenase
ApoE. Apolipoprotein E
AQP-4 Abs. Aquaporin-4 Antibodies
ASA. Acetylsalicylic acid
Aβ. Beta-amyloid

BBB. Blood-brain barrier
BPN. Buprenorphine
BS. Blocking Solution

CC. Corpus callosum
CE. Cholesterol ester
Cer. Ceramide
Chol. Cholesterol
CL. Cardiolipin
CNS. Central nervous system
COX. Cyclooxygenase

DAG. Diacylglycerol
DAPI. 4',6-diamidino-2-phenylindole
DHA. Docosahexaenoic acid
DHA-LPC. Docosahexaenoic-acid-Lysophosphatidylcholine
dpi. days post injection

EAE. Experimental Autoimmune Encephalomyelitis
EPA. Eicosapentaenoic acid

FA. Fatty acid

HETE. Hydroxyeicosatetraenoic acid
HexCer. Hexosylceramide
HODE. Hydroxyoctadecadienoic acid

i.p.. Intraperitoneal
IBA1. Ionized calcium-binding adapter molecule 1

KO. Knockout

LB4. Leukotriene B4
LL. Lysolecithin, Lysolecithin
LM. Lipid mediator
LPA. Lysophosphatidate
LPC. Lysophosphatidylcholine
LPE. Lysophosphatidylethanolamine
LPG. Lysophosphatidylglycerol
LPI. Lysophosphatidylinositol
LPS. Lysophosphatidylserine
LT. Leukotriene
LX. Lipoxin

Mar. Maresin
Mfsd2a. Major facilitator superfamily domain containing 2a
MS. Multiple Sclerosis
MSMS. Tandem mass spectrometry
MUFA. Monounsaturated FAs

NF-kB. Nuclear factor kappa-light-chain-enhancer of activated B cells
NMOSD. Neuromyelitis optica spectrum disorders
NPD1. Neuroprotectin D1

List of Abbreviations

OPC. Oligodendrocyte progenitor cell

PA. Phosphatidate
PBS. Phosphate-buffered saline
PC. Phosphatidylcholine
PCA. Principal component analysis
PD. Protectin
PE. Phosphatidylethanolamine
PFA. Paraformaldehyde
PG. Prostaglandin, Phosphatidylglycerol
PGE_2. Prostaglandin E2
PGI_2. Prostacyclin
PI. Phosphatidylinositol
PIM. Pro-inflammatory lipid mediator
PLA2. Phospholipase A2
PMN. Polymorphonuclear neutrophil
PNS. Peripheral nervous system
PPAR. Peroxisome proliferator-activated receptor
PUFA. Polyunsaturated fatty acid

qPCR. Quantitative PCR

RCT. Randomized controlled trial
RT. Room temperature
RvD. Resolvins, D-series
RvE. Resolvins, E-series

s.c.. subcutaneous
SM. Sphingomyelin
Soat1. O-acyltransferase 1
SPM. Specialized pro-resolving mediator
Sulf. Sulfatide

TAG. Triacylglycerol
TGFβ. Transforming growth factor-β

UPLC-MSMS. Ultra-performance liquid chromatography tandem mass spectrometry

WT. Wild type

Abstract

Multiple sclerosis (MS) is the most common inflammatory demyelinating disease of the central nervous system (CNS) and proceeds with inadequate remyelination. Ideally, the acute inflammatory response after myelin damage is self-limited and transitions into resolution and functional myelin repair. Therefore, persistent inflammation might contribute to remyelination failure. N-3 polyunsaturated fatty acids (PUFAs) and derived lipid mediators (LMs) were suggested to mediate the resolution of inflammation. However, their putative role in remyelination has yet to be elucidated.

To explore the involvement of PUFAs in remyelination, we use the lysolecithin model of demyelination, where mice receive injections of lysolecithin (LL) into the corpus callosum (CC), resulting in focal demyelinating lesions. We provide a lipidome characterization of these lesions and identify a PUFA release during the resolution phase. Further, we show that knockout of lipoxygenases (Alox), enzymes processing these PUFAs, leads to sustained inflammation in lesions. Next, we reveal that *fat-1* mice, which feature reduced n-6/n-3 PUFA ratios, exhibit lowered inflammation and fostered remyelination. Likewise, treatment with brain-targeted n-3 PUFA docosahexaenoic acid lysophosphatidylcholine (DHA-LPC), but not with free DHA, also leads to this pro-regenerative phenotype.

In summary, our results elucidate that n-3 PUFAs can foster cerebral inflammation resolution and remyelination after LL-induced demyelination. Our brain-targeted DHA-LPC treatment highlights the importance of using blood-brain barrier traversable (BBB) metabolites. Hopefully, it will contribute to further research and the development of remyelinating and pro-resolving drugs.

Note: Please be aware that literature research for this thesis includes only studies published before the end of September 2021. More recent findings are not included here.

Introduction

1. Polyunsaturated Fatty Acids

The human brain is rich in polyunsaturated fatty acids (PUFAs), which are essential for brain development and health. PUFAs act as structural and functional components of biomembranes and mediate signal transmission during inflammatory processes as lipid mediators (LMs) precursors. Since persisting neuroinflammation is common in several diseases, such as multiple sclerosis (MS), PUFA involvement and its potential therapeutic importance for inflammation resolution are intensely investigated.

1.1. Families, Sources, and Occurrence in Brain Tissue

Long-chain PUFAs can be divided into two groups: N-3 fatty acids, such as eicosapentaenoic acid (EPA, 20:5), and docosahexaenoic acid (DHA, 22:6), and n-6 fatty acids as arachidonic acid (AA, 20:4). In this study, we focus on these three long-chain PUFAs and refer to them as PUFAs.

In contrast to saturated and monounsaturated fatty acids (FAs), mammals cannot synthesize these PUFAs *de novo*. Therefore, they must rely on dietary intake or endogenous synthesis from their precursor FAs in the liver (Sinclair, 1975). DHA and EPA are formed from the essential α-linolenic acid and AA from linoleic acid (Liu et al., 2015). Once available, they are transported into the brain and incorporated into biomembranes in the form of glycerophospholipids (O'Brien & Sampson, 1965; Svennerholm, 1968) with the FAs esterified predominantly in the sn-2 position (Sun et al., 2018).

Among the most abundant FAs in the adult human frontal cortex are DHA and AA, which constitute roughly 15% and 9% of total brain FAs, respectively (McNamara & Carlson, 2006; Svennerholm, 1968; Zárate et al., 2017). The highest DHA concentrations are found in the outer segment of the retina, where the rods are located (Fliesler & Anderson, 1983). EPA, which has the lowest concentration of all brain PUFAs with <1% of total brain FAs, is rapidly used for DHA or lipid mediators biosynthesis after uptake into the brain (Chen & Bazinet, 2015; McNamara & Carlson, 2006). As the accumulation of PUFAs in the CNS is highest from the third trimester onwards and through early infancy (Lauritzen et al., 2016), their sufficient dietary intake is thought to be crucial for neurodevelopment and optimal brain functionality (Basak et al., 2021; Sun et al., 2018; Yavin et al., 2001).

1.2. PUFAs in Health and Disease

As inflammation is one of the main pathological features in numerous widespread cardiovascular and neuroinflammatory diseases, it is hardly surprising that research has turned the spotlight on

PUFAs intending to find potential anti-inflammatory agents. Since the mid-20th century, PUFAs have been investigated for the beneficial effects of dietary supplementation, the consequences of deficiencies, and molecular and cellular functions. Despite the growing understanding, propelled by the discovery of specialized pro-resolving mediators (SPMs), the potential benefits of dietary supplementation of PUFAs throughout adulthood for prophylactic and therapeutic purposes remain controversial and need to be explained more. Thus, their overall usage as an anti-inflammatory or *pro-resolving* therapeutic target remains an area of active research. – The following section will introduce pro-inflammatory and pro-resolving lipid mediators and summarize key findings from PUFA research in cardiovascular and brain disease.

1.2.1. Biosynthesis of Lipid mediators

Through oxidizing pathways of mainly lipoxygenases (ALOX) and cyclooxygenases (COX), PUFAs are transformed into locally active lipid mediators (LM), which are involved in inflammatory and homeostatic processes (Dennis & Norris, 2015). Depending on the releasing tissue and the targeted receptor, these LMs fulfill many functions in initiating, progressing, and terminating local inflammation.

ALOX are non-heme iron-containing dioxygenases, which catalyze the dioxygenation of PUFAs, leading to subsequent hydroperoxides (Haeggström & Funk, 2011; Kuhn et al., 2015). The genome of humans contains six (*ALOX5*, *ALOX12*, *ALOX12B*, *ALOX15*, *ALOX15B*, *ALOXE3*) and of mice seven genes (*Alox5*, *Alox12*, *Alox12b, Alox15*, *Alox15b*, *Aloxe3*, *Aloxe12*) for lipoxygenases (Hajeyah et al., 2020; Ivanov et al., 2015). The functional similarity of human and murine orthologs remains discussed controversially. Also, the nomenclature of these genes and enzymes can be misunderstanding and confusing (Haeggström & Funk, 2011; Ivanov et al., 2015; Mashima & Okuyama, 2015). Therefore, we use in this study italic letters to refer to genes and non-italicized letters for proteins. Capitalized letters refer to humans, and lowercase to mice.

Following an inflammatory stimulus, e.g., oxidation, radiation, or lipopolysaccharide presentation (Sun et al., 2018), phospholipase A2 (PLA2) is activated and releases PUFAs from the biomembrane. AA is preferentially released by the cytosolic subform of PLA2 and DHA by the calcium-independent subform (Sun et al., 2018). AA is transformed by ALOX5, 15, 12/15, and mainly the COX2 isoform, which is inducible by inflammation, into pro-inflammatory lipid mediators (PIMs) such as leukotrienes (LTs) and prostaglandins (PGs) (Faki & Er, 2021; Serhan et al., 2008). EPA, DHA, and also AA can be transformed into anti-inflammatory SPMs such as lipoxins (LXs, AA-derived), E- and D-series resolvins (RvD, RvE, EPA/ DHA-derived), maresins (Mars) and protectins (PDs, synonym to neuroprotectins, DHA-derived) (Serhan et al., 2008; Serhan & Petasis, 2011).

The LM metabolism is not straightforward but requires the combination of several enzyme activities of ALOX and COX isoforms, and hydrolases. In **Fig. 1** are the major steps of the metabolism schematically shown. Their detailed synthesis and chemistry have been described elsewhere (Serhan et al., 2015; Serhan & Petasis, 2011).

Noteworthy, in parallel to endogenous SPMs, their production can be triggered by acetylsalicylic acid (ASA) (Serhan & Petasis, 2011). These aspirin-triggered SPMs (AT-SPMs) have recently been suggested to facilitate ASA-mediated anti-cancer effects by inhibiting the primary tumor and metastasis growth in murine tumor models (Gilligan et al., 2019). In addition, cytochrome P450 enzymes can also be involved in synthesizing certain LM, e.g., RvDs (Dennis & Norris, 2015; Serhan et al., 2008).

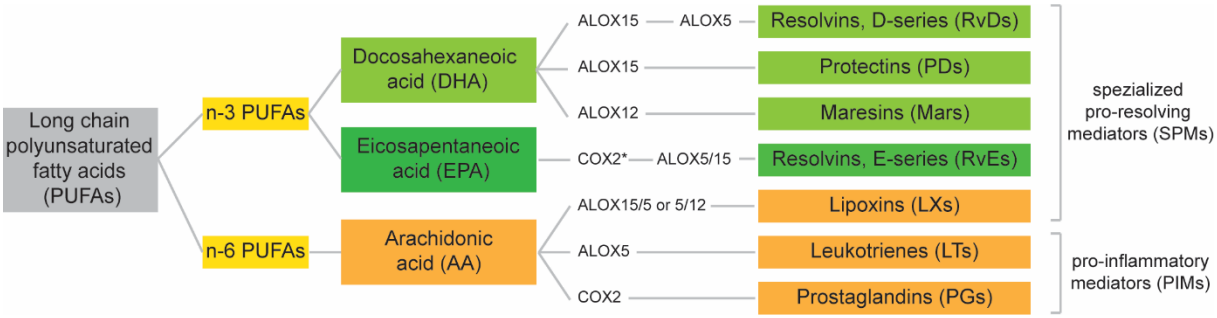

Fig. 1: Schematic overview of human PUFA metabolism to SPMs and PIMs.
The lipoxygenases 5, 15, 12/15 (ALOX), and cyclooxygenase 2 (COX) catalyze oxidations of n-3 PUFA DHA into the SPMs RvDs, PDs, and Mars (light green). Aspirin acetylated COX2 (COX2*), ALOX5, and ALOX15 transform n-3 PUFA EPA to RvEs (dark green). N-6 PUFA AA is metabolized to the PIMs LTs and PGs by ALOX5 or COX2 or to the SPMs LXs by ALOX12/15 and ALOX5 (orange).
Note: This overview does not present the interconnected complex pathways in detail and does not include the metabolism of aspirin-triggered-SPMs and the cytochrome P450 pathways.

1.2.2. Pro-inflammatory lipid mediators (PIMs)

During acute inflammation, the classical clinical signs of inflammation emerge when PIMs are released, leading to vasodilatation, an increase in endothelial permeability, the sensitization of neurons for pain, and the recruiting of inflammatory cells to the tissue site (Dennis & Norris, 2015). Among the most prominent PIMs are ALOX5-derived leukotrienes (LTs), e.g., leukotriene B_4 (LB4), which is a potent activator of the innate immune response, inducing neutrophil recruitment and vascular permeability (Bray et al., 1981; Lämmermann et al., 2013). Well-known COX-derived prostaglandins (PGs) are, e.g., prostacyclin (PGI_2), which mediates pain and acts as an antithrombotic agent (Murata et al., 1997), or prostaglandin E_2 (PGE_2), which induces fever and vascular leakage by mast cell activation (Lazarus et al., 2007; Morimoto et al., 2014).

Historically, pharmacology focused on PGs, and the inhibition of their biosynthesis has been an essential pharmacological target in ancient times when the Greek physician Hippocrates was told to have treated pain and fever with willow bark (Lévesque & Lafont, 2000). The active agent of this phytotherapeutic was later identified (Hoffmann, 1900) as acetylsalicylic acid (ASA), a

COX1/2 inhibitor, which became the active agent for ASA. This finding marked the beginning of the era of non-steroidal anti-inflammatory drugs, commonly used as painkillers. Only in 1996, the dormant potential of leukotrienes was recognized when the first ALOX5-inhibitor zileuton was approved for asthma treatment reducing LB_4-mediated bronchoconstriction (Israel, 1996; Siegert et al., 2017; U.S. Food and Drug administration, 2007).

1.2.3. Specialized pro-resolving mediators (SPMs)

At the beginning of the 21st century, new technologies, such as tandem mass spectrometry-based lipidomics, led to the discovery of anti-inflammatory LMs derived from DHA, EPA, and AA, for which the term *specialized pro-resolving mediators* has been coined (Serhan et al., 2008; Surma et al., 2015). They possess anti-inflammatory features, such as reducing polymorphonuclear neutrophils infiltration (PMN), pain, and inflammatory gene expression, and pro-resolving features, such as increasing the phagocytosis of macrophages and removing inflammatory debris (Serhan, 2014). Bioactive SPMs were identified at picomolar levels in several types of human tissue (Serhan, 2017), and the SPMs and AT-SPMs used in the following studies were administered in nanomolar quantities *in vivo*. In contrast, their precursors, EPA and DHA, exhibit similar bioactivity only at 1000 times higher concentrations (Gilligan et al., 2019; Serhan & Petasis, 2011).

Some examples: RvE1 and RvD1 display antinociceptive actions in relieving inflammatory pain via central and peripheral actions (Xu et al., 2010). RvE1 decreases PMN infiltration and expression of pro-inflammatory genes like tumor necrosis factor or interleukin 12, inducible nitric oxide synthase, and COX2 in an intestinal inflammation model (Arita et al., 2005). RvE1 and PD1 stop leukocyte infiltration and promote macrophage ingestion of apoptotic PMNs (Schwab et al., 2007). The 17S and 17R series resolvins (RvD, AT-RvD) decrease leukocyte infiltration in a dose-dependent manner in nanogram dose ranges *in vivo* (Serhan & Petasis, 2011). MaR1 decreases PMN accumulation, enhances macrophage phagocytosis, and stimulates macrophage efferocytosis (Serhan et al., 2009). It also inhibits pain sensation in mice and stimulates tissue regeneration in a planaria model (Serhan et al., 2012).

The discovery of SPMs changed the understanding of the course of inflammation (**Fig. 2**): First, PIMs cause the immediate inflammatory sign, and then SPMs promote resolution. Therefore, a so-called *class switch* of LMs is required to terminate acute and avoid chronic inflammation (Buckley et al., 2014). Moreover, their discovery underpinned a paradigm change toward the notion that inflammation is a self-limiting process and that the return to homeostasis is not a passive but an actively coordinated process (Serhan, 2017). Thus, SPMs represent a new field of research and a novel mindset of understanding inflammation.

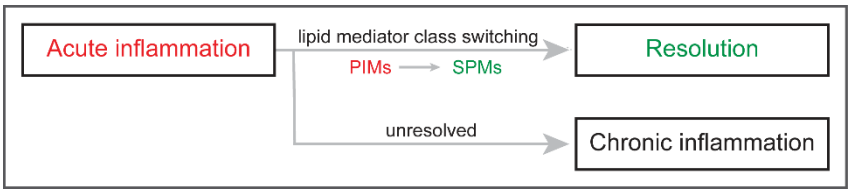

Fig. 2: Lipid mediator class switching marks inflammation resolution.
PIM-mediated processes drive acute inflammation. Its termination is an integral component of inflammation resolution and is initiated by lipid mediator class switching from PIMs to SPMs. Unresolved acute inflammation can lead to chronic inflammation.
Note: Adapted with permission from this publication (Serhan & Petasis, 2011), Copyright (2023) American Chemical Society.

1.2.4. PUFAs in cardiovascular disease

The first observations suggesting that dietary differences in PUFA intake might affect health have been made in cardiovascular disease. Back in 1972, epidemiological studies indicated that the rarity of ischaemic heart disease in Greenland Inuits may be associated with diet habits resulting in altered plasma lipid and lipoprotein levels, including high levels of n-3 PUFAs (Bang & Dyerberg, 1972; Bang et al., 1980). This initial finding has raised the question of whether supplementation of n-3 PUFAs can affect the risk, progression, or treatment of human diseases.

Subsequently, clinical studies were performed examining the association between high n-3 PUFA intake and mortality from cardiovascular events. First major studies, including DART (Diet and Reinfarction Trial, 1989), GISSI-P (the Gruppo Italiano per lo Studio della Sopravvivenza nell'Infarto micardio Prevenzione, 1999), and JELIS (Japan EPA Lipid Intervention Study, 2007) could not provide concordant results (Burr, 2001; Burr et al., 1989; Stone, 2000; Yokoyama et al., 2007). Nevertheless, based on findings in JELIS, the REDUCE-IT trial showed that daily supplementation with an ethyl ester of EPA (IPE, icosapent ethyl) significantly lowers the risk of ischemic events in patients with increased triglyceride levels. The underlying mechanisms are unknown, but the authors cautiously discuss membrane-stabilizing or antithrombotic effects of IPE (Bhatt et al., 2019). This trial led to the indication expansion of IPE and approval for usage as an adjunct to maximally tolerated statin treatment to reduce the risk of ischemic events for patients with triglyceride levels ≥150mg/dl (European Medicines Agency, 2021; U.S. Food and Drug administration, 2019).

1.2.5. Transport mechanism of n-3-PUFAs into the brain and consequences of its failure

The central transport mechanism of EPA and DHA across the blood-brain barrier (BBB) is suggested to be mediated by the *major facilitator superfamily domain containing 2a* (Mfsd2a, also known as NLS1). This sodium-dependent transporter is highly expressed in the endothelium of brain microvessels. Notably, it transports n-3 PUFAs only when they are covalently bound to lysophosphatidylcholine (LPC) (Ben-Zvi et al., 2014; Cater et al., 2021; Lagarde et al., 2001; Nguyen et al., 2014). However, there remains controversy over this transport mechanism, as other

findings indicate that non-esterified DHA represents the leading source of brain DHA (Chen, C. T. et al., 2015). Still, only DHA-LPC or DHA-phosphatidylcholine increased cerebral DHA concentrations in rat gavage experiments. Whereas non-esterified DHA, DHA-triacylglycerol (as in fish oil), or di-DHA-phosphatidylcholine would only increase DHA incorporation into the heart and adipose tissue (Sugasini et al., 2017; Sugasini et al., 2019).

Observed consequences of PUFA deficiency in studies with mice and humans suggest that PUFA supplementation might benefit brain development. Mice with lowered DHA concentrations, induced by *Mfsd2a* knockout (KO), exhibit anatomic changes such as microcephaly, decreased density of hippocampal neurons as well as motor dysfunction and behavioral changes such as anxiety, learning and memory difficulties (Nguyen et al., 2014). In line with these findings, humans with inactivating *Mfds2a* mutations also exhibit microcephaly, hypomyelination, developmental delay, and motor dysfunction (Guemez-Gamboa et al., 2015; Harel et al., 2018).

1.2.6. PUFAs in brain's health and disease

In the following decades, PUFAs were also investigated for their role in neuro-pathophysiology, function in CNS maintenance, and therapeutic potential use. The discovery of SPMs was a milestone in PUFA research and pushed it further, as they are assumed to be the missing jigsaw pieces required to explain the biological functions of n-3 PUFAs.

Several studies revealed different cellular and molecular mechanisms by which n-3 PUFAs, particularly DHA, and SPMs benefit neuroinflammation, -protection, and -genesis (Bazinet & Layé, 2014). For instance, DHA inhibits lipopolysaccharide-induced NF-kB activation and the synthesis of PIMs in microglia (Smedt-Peyrusse et al., 2008). It also prevents apoptosis by downregulating caspase-3 activity and upregulating anti-apoptotic genes via neuroprotection D1 (NPD1) in neural cell cultures (Kim et al., 2000; Lukiw et al., 2005). Additionally, DHA promotes the growth of hippocampal neurons *in vitro* (Calderon & Kim, 2004).

Several clinical trials and disease models examine the putative beneficial effects of n-3 PUFAs on neurodegenerative disorders:

In multiple sclerosis (MS), metabololipidomics studies have revealed higher lipid mediator levels in patients with active MS than in healthy subjects (Kooij et al., 2020; Prüss et al., 2013). Intriguingly, a murine experimental autoimmune encephalomyelitis study showed that lipoxin A4 improves clinical signs and attenuates T-cell infiltration into the CNS (Derada Troletti et al., 2021). Furthermore, microglia in obese mice on a Western diet, which has, among other characteristics, a high n-6/n-3 ratio, displayed an impaired capacity for phagocytosis after myelin injury in a lysolecithin model of demyelination (Bosch-Queralt et al., 2021). Following this result, epidemiological studies hint at an association between obesity in early life and the incidence of MS in females (Rasul & Frederiksen, 2018). Still, a link between fatty acid supplementation and

improved disease outcomes could not be reliably established in controlled trials (AlAmmar et al., 2019; Parks et al., 2020). However, limitations of these studies due to substantial variation in the form of n-3 PUFA administration and the chosen outcome criteria hamper a conclusive assessment of the overall role of PUFAs in remyelination and MS (Fitzgerald et al., 2020).

In Alzheimer's disease (AD), the extracellular aggregation of beta-amyloid (Aβ) is one of the neuropathological features. DHA and EPA have been shown to promote microglial phagocytosis of Aβ42 (Hjorth et al., 2013). DHA-derived NPD1 activates the lipid catabolic pathways PPARγ pathways and inhibits β-secretase activity in human neuronal-glial cell culture (Zhao et al., 2011). A study in mice suggested that *APOE4* carriers have a lowered uptake of DHA, which connects this risk factor gene to DHA deficiency (Vandal et al., 2014). A review assessing 25 RCTs suggests that n-3 PUFA-enriched food is a preventative measure against AD but showed no mitigating effect on cognitive impairment in patients already diagnosed with AD (Wood et al., 2021).

In conclusion, *in vitro* and *in vivo* studies in mice show that SPMs and n-3 PUFAs are involved in inflammation resolution and neuroprotection. Accordingly, n-3 PUFA deficiency has fatal consequences for affected humans and mice, ranging from behavioral changes to poor myelination. Due to these findings, the idea of supplementing n-3 PUFAs arose. As some of the mentioned studies indicate that n-3 PUFAs might improve certain aspects of diseases, yet not all randomized placebo-controlled trials reported therapeutic benefits, there is an ongoing controversy with further research required.

2. Myelin and Demyelinating Diseases

2.1. Myelin: The Evolutionary Wonder

The rapid propagation of neural impulses is enabled by myelin membranes wrapped around the axons of neurons in multiple layers. This evolutionary feat in vertebrates allows for fast and energy-efficient nerve conduction. In contrast to other membranes, myelin is unique in that it is composed of 70% lipids, mainly cholesterol, phospholipids, and glycosphingolipids, while proteins, mainly myelin basic protein, 2',3'-cyclic nucleotide 3'-phosphodiesterase, and proteolipid proteins constitute the other 30% (Baumann & Pham-Dinh, 2001; Monasterio-Schrader et al., 2012). As a result of this composition, myelin increases the membrane capacitance along the axon and thus enables rapid saltatory conduction (Huxley & Stämpeli, 1949): In unmyelinated axon regions, the nodes of Ranvier, clusters of structural components such as voltage-dependent sodium channels and ATP-dependent exchange pumps are responsible for building up new action potentials. These are then propagated electrotonically along the myelinated axon sections, the internodes, until the signal is regenerated at the next node of Ranvier. Without myelination, significantly thicker axons would be needed to reach similar conduction speeds (Baumann & Pham-Dinh, 2001). Besides this function in impulse conduction, myelin and oligodendrocytes support axons by supplying them with metabolites and thus prevent neurodegeneration (Griffiths et al., 1998; Lee et al., 2012; Nave, 2010). In accordance, oligodendrocytes were recently suggested to protect neurons from iron-mediated cytotoxicity (Mukherjee et al., 2020).

In the peripheral nervous system (PNS), myelin is produced by Swann cells (Geren, 1954). In contrast, oligodendrocytes generate CNS myelin and coat multiple axons from different neurons with their processes (Bunge et al., 1962). In humans, myelination starts postnatal, peaks in the first year, and extends into adulthood, as MRI studies have shown (Snaidero & Simons, 2014; Sowell et al., 1999). These results suggest that myelination is partially independent of default neural processes, is modifiable, and contributes to brain plasticity. Indeed, growing evidence shows that myelination is responsive to social interaction and environmental learning (Fields, 2008; Schlegel et al., 2012).

2.2. Remyelination: The Second Wonder

The nervous system has regenerative capacities to build new myelin sheaths after an injury. This process is called remyelination and is the endogenous program of tissue repair. The factors determining whether a demyelinated axon section undergoes remyelination remain partially elusive (Franklin & Ffrench-Constant, 2017; Stangel et al., 2017).

2.2.1. Microglia: First aid responders after CNS damage

Microglia are tissue-resident macrophages in the CNS, making up 5-15% of all brain cells (Li & Barres, 2018). They are essential for brain homeostasis and the response to infection and damage. Derived from erythromyeloid progenitors in the yolk sac, they migrate early during embryonic development into the CNS (Ginhoux et al., 2010; Gomez Perdiguero et al., 2015). Microglia are long-lasting cells that continuously scan their environment with motile ramified processes for threats by surveying for damage- or pathogen-associated molecular patterns (Herz et al., 2017; Nimmerjahn, 2005). This first response function in the innate immune system makes them vital for proper brain function. Following a threatening stimulus, they change state, morphology, and gene expression profiles from a "resting" to an "activated" state. This activation can be neuroprotective or -damaging. In remyelination, chronic macrophage activation is associated with impaired oligodendrocyte progenitor cells (OPC) activation and an unfavorable microenvironment (Lloyd & Miron, 2019). Neuroinflammation with persisting microglial activation is damaging and common to neurological diseases such as MS and AD (Heneka et al., 2015).

2.2.2. Mechanisms of remyelination and their failure

Remyelination is the stepwise process of restoring damaged myelin sheaths and is facilitated by oligodendrocytes and microglia. In response to myelin damage, OPCs are activated, migrate to the lesion, and differentiate into mature myelinating oligodendrocytes. Genetic fate mapping analyses have revealed that OPCs are the major source of new oligodendrocytes. However, subventricular zone stem cells and even Schwann cells can contribute to CNS remyelination (Franklin & Ffrench-Constant, 2017). The molecular processes involved in activation, migration, and differentiation are only partially understood. Still, it is assumed that the secretion of signal molecules from microglia and macrophages detecting the myelin damage mediate these steps (Lloyd & Miron, 2019). For myelination, the pre-myelinating oligodendrocytes extend multiple processes searching for axons. Subsequently, they produce myelin proteins and wrap new sheaths around the axons until compacted multi-layered sheaths have been formed (Stadelmann et al., 2019). These new sheaths are morphologically shorter in internodal length and thinner than normal myelin, at least in large-diameter axons (O'Leary & Blakemore, 1997).

Microglia contribute to successful remyelination (Stangel et al., 2017) in several ways: First, they phagocytose myelin debris and degrade accumulating lipids (see 2.2.3.) Clearance of myelin debris is crucial for lesion restitution as myelin inhibits OPC differentiation (Baer et al., 2009; Kotter, 2006). Second, microglia secret growth factors and cytokines such as activin A, galectin 3, TNF, or interleukin 1β which support and mediate oligodendrocytes differentiation and myelination (Lloyd & Miron, 2019; Miron, 2017; Miron et al., 2013).

Despite observations of successful remyelination in animal experiments (Bunge et al., 1961) and patients with MS (Albert et al., 2007; Prineas et al., 1984), its failure contributes to axonal damage, neurodegeneration, and subsequent permanent clinical disability (Friese et al., 2014). Therefore, in search of remyelinating therapies, many studies investigated factors of failed remyelination, hoping to find mechanisms exploitable for pro-remyelinating therapies. The remyelination rate can decline due to recruitment or differentiation failure of OPCs (Franklin, 2002; Kuhlmann et al., 2008; Sim et al., 2002). Several signaling pathways and transcriptional factors that regulate OPS differentiation were identified. For instance, protein LINGO-1 is a negative regulator of myelination (Mi et al., 2005) and was a promising candidate for MS treatment, but did ultimately not prove beneficial in a clinical phase 2 trial in 2020. OPC function also depends on environmental factors such as myelin removal by microglia and macrophages. Three recent studies highlight the role of adequate myelin clearance and cholesterol efflux via Liver-X receptor (LXR) target genes for successful remyelination (Berghoff et al., 2021; Cantuti-Castelvetri et al., 2018; Safaiyan et al., 2016). Moreover, microglia and macrophages need pro-inflammatory activation (Cunha et al., 2020) and an astrocytic signaling environment for activation and recruitment (Skripuletz et al., 2013).

2.2.3. Myelin phagocytosis and cholesterol handling in microglia and macrophages

As myelin is rich in lipids, free cholesterol is one of the main components that accumulates after demyelination. Its concentration is tightly regulated since excess amounts of cholesterol cause tissue damage, e.g., within atherosclerotic plaques (Maguire et al., 2019). Therefore, microglia activate pathways and enzymes processing cholesterol to avoid high concentrations. First, O-acyltransferase 1 (*Soat1*, also called *Acat1*) esterifies free cholesterol into cholesterol esters, which are then stored with FAs in intracellular lipid droplets (Guan et al., 2020; Seo et al., 2001). The inhibition of *Soat1* and the following reduced formation of lipid droplets and foam cells are intensely investigated in atherosclerosis (Rong et al., 2013), prostate cancer research (Eckhardt et al., 2021), and others. Second, cholesterol-derived metabolites activate the LXR pathway after myelin intake, whose target genes are involved in cholesterol efflux and reverse cholesterol transport (Berghoff et al., 2021; Bogie et al., 2012). For example, the genes *ATP-binding cassette transporter A1* (*Abca1*) and *sub-family G1* (*Abcg1*) encode for cholesterol efflux pumps and *apolipoprotein-E* (*ApoE)* for a cholesterol carrier (Beyea et al., 2007). LXR agonism was shown to rescue impaired cholesterol clearance and to restore remyelination in aged mice (Cantuti-Castelvetri et al., 2018).

2.3. Demyelinating Diseases

Considering the central role of myelin in CNS and PNS function, its impairment leads to tremendous consequences in humans. There is a large heterogeneous group of hereditary or

acquired demyelinating diseases with an inflammatory, infectious, toxic, or metabolic etiology. The most prevalent example of an inflammatory pathophysiology is multiple sclerosis.

2.3.1. Multiple sclerosis (MS): epidemiology, etiology, and pathology

MS is the most common inflammatory demyelinating disease of the CNS and the most frequent cause of neurological disability in young patients. In 2020, MS affected 2.8 million people worldwide with increasing prevalence. The average age at diagnosis is 33 years, and twice as many women are affected (Walton et al., 2020). The incidence varies regionally, showing the highest reported numbers in Europe and North America. The etiology is unknown, but several genetic and environmental risk factors are described. Family studies identified higher concordance rates in twins and over 100 risk genetic loci (Ebers et al., 1995; Rothhammer & Quintana, 2016). Epidemiological studies suggest latitudes with lower sun exposure, Vitamin-D deficiency (Hedström et al., 2020), Epstein-Barr virus infection, smoking, pollutants, and gut microbiome as MS risk factors (Belbasis et al., 2015; Rothhammer & Quintana, 2016).

Neuropathological hallmarks are inflammation, demyelination, remyelination, axonal loss, causing permanent clinical disability (Trapp et al., 1998), and glial scar formation (Lassmann et al., 2007). Focal demyelinating plaques in the white and grey matter present with different histopathological features. Active demyelinating plaques are highly inflammatory and characterized by perivascular infiltration of mainly $CD8^+$ lymphocytes, activated microglia and macrophages containing myelin debris, and reactive astrocytes. Chronic-active *smoldering* plaques present without lymphocytes but with myelin-loaded macrophages at the plaque edge. Inactive lesions are sharply circumscribed and show hypocellularity with the loss of oligodendrocytes, myelin and inflammatory cells, and astrogliosis. Remyelinated lesions are called *shadow* plaques and occur regularly in patients with short disease durations (Filippi et al., 2018; Lassmann et al., 2012; Stangel et al., 2017).

The adaptive immune system plays a vital role in MS pathology. Two hypotheses are suggested based on the location of exposure to autoantigens (Hemmer et al., 2015). The CNS intrinsic (inside-out) model proposes an initial immune response within the CNS directed against damaged myelin or oligodendrocytes, leading to microglial activation and subsequently to migration of cells of the adaptive and innate immune system (Barnett & Prineas, 2004; Henderson et al., 2009). In contrast, the CNS extrinsic (outside-in) model states that the initial autoimmune event takes place in the periphery, maybe through bystander activation or molecular mimicry, with subsequent autoreactive T-cell activation and migration into the CNS (Hemmer et al., 2015; Olson et al., 2001). In a seminal paper, Lucchinetti et al. describe four distinct immunopathological patterns in early active lesions, which might contribute to the heterogeneity of course and therapy response in MS (Lucchinetti et al., 2000). Patterns I and II present T-cell- and antibody-mediated autoimmune response features, while III and IV suggest oligodendrocyte death before demyelination.

2.3.2. Multiple sclerosis (MS): symptoms and therapeutic options

The first symptoms might be visual or sensory disturbances, but depending on the localization of lesions, various neurological symptoms are possible, coining MS as "neurology's chameleon". MS occurs in different forms. Relapsing-remitting MS (RRMS) with clearly defined attacks with complete or incomplete recovery is the most common form (about 90% of patients). Some of these patients enter into secondary progressive MS (SPMS) over time. In SPMS, as in primary progressive MS (PPMS), symptoms do not regress but increase steadily over time, which leads to permanent disability. Diagnostics follow the McDonald criteria, assessing spatial and temporal dissemination by patient history, clinical examination, MRI scans, and cerebrospinal fluid analysis (Thompson et al., 2018).

Several therapeutic immunomodulatory, but no curative options exist. Patients with an active relapse are treated with high doses of glucocorticoids, aiming at quicker regression of symptoms. Disease-modifying treatments aim to stop inflammatory attacks, referred to as "NEDA-concept" (no evidence of disease activity: no new MRI lesions, no relapses or expanded disability). Depending on the form and severity of the disease course, various pharmacological agents with different potencies and associated risks of opportunistic infections are chosen to fit the needs and preferences of the individual patient (Hemmer B. et al., 2021). MS course is highly individual, but insufficient remyelination is an established cause of secondary neuronal loss and disability (Friese et al., 2014). As remyelination frequently occurs early after demyelination, when inflammatory processes peak, and remains rare in chronic inactive plaques, which show a loss of inflammatory and myelinating cells (Filippi et al., 2018; Goldschmidt et al., 2009), it is necessary to investigate how the inflammatory response promotes remyelination.

2.4. Demyelinating Animal Models

Experimental models have proven valuable for studying different aspects of remyelination biology. Models for demyelination are either toxin-, virus-, or autoimmune-mediated or genetic. Common toxins used to induce focal demyelination are lysolecithin (s.b.), ethidium bromide, and 6-aminonicotinamide. Systemically used toxins are cuprizone (s.b.) and cholera toxin. Toxin-induced pathologies differ in the extent of astrocyte and oligodendrocyte loss (Blakemore & Franklin, 2008). Virus-mediated models use neurotropic viruses such as Theiler's virus, mouse hepatitis virus, and Semliki Forest virus, which induce demyelination by causing oligodendropathy (Fazakerley & Walker, 2003).

2.4.1. Lysolecithin model of de- and remyelination

In this study, we use the lysolecithin-induced model of de- and remyelination. Since the 1970s, stereotactic injections of lysolecithin (LL) into white matter tracts such as the corpus callosum (CC), the spinal cord, or the cerebellar peduncle have been used to induce focal demyelinating

lesions (Hall, 1972; Hall & Gregson, 1971). LL acts as a membrane dissolver by disrupting myelin lipids in a non-specific manner and by integrating into cellular membranes, which causes an increase in permeability (Plemel et al., 2018). Thus, injections lead to BBB disruption with subsequent infiltration of microglia and macrophages. The resulting ellipsoid-shaped lesions are characterized by astrogliosis and modest axon degeneration (Blakemore et al., 1977; Blakemore & Franklin, 2008). The demyelination process starts rapidly within hours after injection and is completed at 3 to 4 days post injection (dpi). Remyelination starts at around 7 dpi and peaks between 14 dpi and 21 dpi (Cantuti-Castelvetri et al., 2018; Jeffery & Blakemore, 1995). Please see also methods chapter 2.1.2, Fig. 4, and Fig. 5.

2.4.2. Cuprizone model

Oral cuprizone feeding leads to progressive demyelination in distinct brain regions, including CC and cerebellar peduncle (Blakemore, 1972; Goldberg et al., 2015), and is reversible once administration is stopped. The mechanism remains elusive, but it is suggested that cuprizone (bis-(cyclohexanone)-oxaldihydrazone) acts as a chelator of copper, which is required for the functionality of mitochondrial enzymes (Venturini, 1973). Consequently, impaired energy metabolism might induce oligodendrocyte death (Matsushima & Morell, 2001).

2.4.3. Experimental Autoimmune Encephalomyelitis (EAE)

EAE is a heterogeneous family of animal models to study autoimmune processes in the CNS. Due to its pathological and clinical similarities with MS, it is a commonly used disease model (Baxter, 2007). In 1933, Rivers et al. tried to understand cases of paralysis after the administration of Louis Pasteur's rabies vaccine. They found that injections of rabbit brain tissue in primates could induce EAE (Rivers et al., 1933). Generally, EAE is induced by external stimulation of $CD4^+$ T cells against CNS antigens. The active induction scheme uses CNS tissue or myelin antigens and Freund's adjuvant containing inactivated mycobacteria tuberculosis, activating the innate immune system. The passive scheme works with T cells that were prior immunized with myelin antigens, then isolated from the donor and transferred to the recipient animal after T cell stimulation *in vitro* (Stromnes & Goverman, 2006). Neuropathologically, EAE mainly affects the spinal cord and depicts a sequence similar to MS from inflammation and subsequent demyelination toward gliosis and remyelination (Baxter, 2007).

Materials and Methods

1. Materials

1.1. Mouse Lines and Diets

1.1.1. Mouse lines

Line	Source	Identifier
C57BL/6J	Jackson Laboratory, USA; Janvier Labs, France	JAX: 000664
B6.129S2-Alox15tm1Fun/J	Jackson Laboratory, USA	JAX: 002778
B6.129S2-Alox5tm1Fun/J	Jackson Laboratory, USA	JAX: 004155
C57BL/6-Tg (CAG-fat-1)1Jxk/J	Jackson Laboratory, USA	JAX: 020097

1.1.2. Mouse diets

Diet	Company	Catalog Number
Mouse diet with 5 % beef tallow	ssniff Spezialdiäten GmbH	S7007-E022
Mouse diet with 5 % fish oil	ssniff Spezialdiäten GmbH	S7007-E024
Mouse diet with 5 % safflower oil	ssniff Spezialdiäten GmbH	S7007-E021

1.2. Antibodies

1.2.1. Primary antibodies & dyes

Primary Antibody / Dye	Dilution	Company	Catalog Number
anti-APC/CC1 mouse	1:100	Sigma-Aldrich, Germany	OP80-100UG
anti-IBA1 rabbit	1:1000	Wako, Japan	019-19741
anti-OLIG2 rabbit	1:250	Sigma-Aldrich, Germany	AB9610
DAPI (4',6-diamidino-2-phenylindole)	1:1000	Thermo Fisher Scientific, USA	D1306
Fluoromyelin	1:300	Thermo Fisher Scientific, USA	F3465

1.2.2. Secondary antibodies

Secondary Antibody	Dilution	Company	Catalog Number
Donkey anti-rabbit IgG (H+L), Alexa Fluor 647	1:300-1:1000	Thermo Fisher Scientific, USA	A31573
Goat anti-mouse IgG (H+L), Alexa Fluor 555	1:300-1:1000	Thermo Fisher Scientific, USA	A21422
Goat anti-rabbit IgG (H+L), Alexa Fluor 488	1:300-1:1000	Thermo Fisher Scientific, USA	A11008

1.3. Chemicals

Chemical	Company	Catalog Number
Acetylsalicylic acid	Cayman Chemical, USA	Cay70260
Baicalein	Sigma-Aldrich, Germany	465119
Bovine calf serum	Cytiva Life Sciences, USA	SH30073

Bovine serum albumin	Sigma-Aldrich, Germany	A2153
Corn Oil	Sigma-Aldrich, Germany	C8267
Di-sodium hydrogen phosphate dihydrate	Merck Millipore, Germany	1.06580.1000
Docosahexaenoic Acid (DHA)	Cayman Chemical, USA	Cay90310
1-Docosahexaenoyl-2-hydroxy-sn-glycero-3-phosphocholine (DHA-LPC)	Avanti Polar Lipids, USA	790713
Egg Lyso PC (LPC)	Sigma-Aldrich, Germany	830071P
Fab fragment donkey anti-mouse IgG (H+L)	Jackson ImmunoResearch, Germany	715-007-003
Gelatine	Merck Millipore, Germany	104070
Glycerol	Sigma-Aldrich, Germany	65518
Hydrochloric acid	Sigma-Aldrich, Germany	258148
4-(2-hydroxyethyl)-1-piperazine ethanesulfonic acid (HEPES)	Carl Roth, Germany	HN78.2
Leukotriene B4	Cayman Chemical, USA	Cay-20110
Lipoxin A4	Cayman Chemical, USA	Cay-90410
Lysophosphatidylcholine	Sigma-Aldrich, Germany	L4129
Maresin 1	Cayman Chemical, USA	Cay-10878
β-mercaptoethanol	Carl Roth, Germany	4227.1
Monastral blue	Sigma-Aldrich, Germany	274011
Mowiol	Roth, Germany	0713.2
Natriumhydroxid pellets	Roth, Germany	6771.1
Neuroprotectin D1	Cayman Chemical, USA	Cay-1001039
Paraformaldehyde (PFA)	Sigma-Aldrich, Germany	158127
PBS, pH 7,4	Thermo Fisher Scientific, Germany	10010023
Penicillin-Streptomycin	Thermo Fisher Scientific, Germany	15070063
Potassium chloride	Carl Roth, Germany	6781.1
Potassium dihydrogen orthophosphate	Carl Roth, Germany	3904.1
PowerUp SYBR Green Master Mix	Applied Biosystems, Germany	A25742
Resolvin D1	Cayman Chemical, USA	Cay-10012554
Resolvin D2	Cayman Chemical, USA	Cay-10007279
Resolvin D4	Cayman Chemical, USA	Cay-13835
Resolvin E1	Cayman Chemical, USA	Cay-10007848
Sodium chloride	Carl Roth, Germany	957.2
Sodium pyruvate	Thermo Fisher Scientific, Germany	11360070
Sucrose	Sigma-Aldrich, Germany	S0389
Tri-sodium citrate dihydrate	Merck Millipore, Germany	106448
Tris Base	5000AppliChem, Germany	A1379
Triton X100	Sigma-Aldrich, Germany	T8787
Tween® 20	Merck Millipore, Germany	822184
Zileuton	LKT Laboratories Inc., USA	LKT-Z3444

1.4. Buffers and Solutions

1.4.1. Paraformaldehyde (PFA)

The 4% PFA solution was used for transcardial perfusion. A 16 % solution was prepared by dissolution of 160 g PFA in 100 ml of 10x PBS and 900 ml of 65 °C warm ddH20. After mixing for 20 min, pellets of 5 N NaOH were added until the PFA was fully dissolved. The pH was adjusted to 7.4, and the solution was then stored at -20 °C. The 4 % solution was prepared by adding 150 ml of cold 1x PBS to 50 ml of the 16% PFA stock using a Steritop 0.2 µm filter system. The final solution was freshly prepared and kept at 4 °C until usage.

1.4.2. Sucrose solution

For cryoprotection of the tissue, the brains were kept in a 30 % sucrose solution after fixation, prepared by solving 30 g of sucrose in 100 mL of 1x PBS.

1.4.3. Blocking solution (BS)

The BS used for immunohistochemistry was prepared by mixing 12.5 mL of 2.5 % FCS, 12.5 g of 2.5 % BSA, and 12.5 mL of 2.5 % fish gelatin with PBS to 500 ml. The solution was kept at -20 °C.

1.4.4. Phosphate-buffered saline (PBS)

For the 10x PBS stock, 80.06 g of 1.37 M NaCl, 2.01 g of 27 mM KCl, 14.2 g of 100 mM Na_2HPO_4, and 2.45 g of 18 mM KH_2PO_4 were dissolved with dH20 to 1 l. The pH was then adjusted to 7.4. The stock was stored at room temperature (RT) for up to three months.

1.4.5. Sodium citrate buffer

The buffer was used for antigen retrieval during immunohistochemistry. For one liter, 2.94 g of tri-sodium citrate dehydrate was dissolved in dH20 to 1 l, 0.5 ml of Tween20 was added, and the pH was adjusted to 6.0. The solution was stored at RT for a maximum of three months.

1.4.6. Tris-HCl buffer

This buffer was made for mowiol production by dissolving 60.57 g of Tris Base in 350 mL of ddH2O. The pH was adjusted to 7.4 by adding 12 M HCl. The buffer was filled to 0.5 l with ddH2O and stored at 4 °C.

1.4.7. Mowiol solution

Mowiol was used as a mounting medium for IHC and was prepared by mixing 2.4 g of mowiol and 6 g of glycerol in 6 mL of ddH2O for several hours at RT. After adding 12 ml of 0.2 M Tris-HCl (pH 8.5), the solution was incubated for 10 minutes at 60 °C and centrifuged at 4.000 g for 15 min. After aliquoting, mowiol was stored at -20 °C.

1.4.8. HEPES buffer

For myelin purification, a 10 mM HEPES buffer was prepared by dissolving 2.38 g of HEPES in 1 l ddH2O. The pH was adjusted to 7.4.

1.4.9. Gelatine

To stabilize tissue on the sample holder for sectioning at a vibratome, a 12 Wt/% gelatin solution was prepared by slowly dissolving 3 g of gelatine in 28 ml of 1x sterile PBS at 50 °C. The solution was kept at 4 °C.

1.5. Other Materials

1.5.1. Primers

Gene	Primers Sequence (from 5' to 3'), F (forward), R (Reverse)
Abca1	F: tgtctgaaaaaggaggacagtg – R: tgtcactttcatggtcgctg
Abcg1	F: cagacgagagatggtcaaaga – R: tcaaagaacatgacaggcgg
ApoE	F: ctgacaggatgcctagcc – R: tcccagggttggttgctttg
Cyc1	F: ATGGGGAGATGTTCATGCGG – R: CTGAGGTCAGGGGGTAAGC
Soat1	F: TGCTGACGTCTTCCTGTGTC – R: GAGCTGTTGGGGAGTAGGTG

1.5.2. Commercial kits

Kit	Purpose	Company	Catalog Number
Neural Tissue Dissociation Kit (P)	Brain tissue dissociation	Miltenyi Biotech, Germany	130-092-628
RNeasy Plus Mini Kit	RNA isolation from cells	Qiagen, Germany	74134
Superscript III First-Strand Synthesis	cDNA synthesis	Thermo Fisher Scientific, Germany	18080051

1.6. Software and Programs

Material	Application	Company, Source
Adobe Illustrator CS5	Data visualization	Adobe Inc., USA
CellProfiler	Image processing and analysis	CellProfiler
CS ChemDraw Drawing	Molecule Drawer	PerkinElmer, Inc.
FIJI, Image J	Image processing and analysis	Open source, https://imagej.net/Fiji
GraphPad Prism 7	Data analysis, statistics	GraphPad Software, USA
IPython 2.7	Data analysis	Fernando Pérez
Leica Application Suite AF	Image acquisition	Leica Microsystems, Germany
LightCycler 480, 1.5	qPCR data acquisition	Roche Life Science, Switzerland

2. Methods

2.1. Mouse Procedures

2.1.1. Animals

All animal experiments were carried out according to the German animal welfare law and to the District Government of Oberbayern. Mice (male and female) were housed at the animal facility in the German Center for Neurodegenerative Diseases (DZNE), Munich, in 12 h light/dark cycles. At arrival, the animals of the same age and sex were randomly distributed to the experimental groups (5 animals each, if not stated otherwise). Experiments started after one week of acclimation.

C57BL/6J mice were purchased from Jackson (United States) and Janvier Laboratories (France) and were, if not stated otherwise, 6-8 weeks old at the time of stereotactic injection. *Alox5*-/-, *Alox15*-/- and C57BL/6J mice for acetylsalicylic acid or baicalein treatment were 12 months, and *fat-1* transgenic mice were 9-14 weeks old at the time of injection. Genetically modified mice were purchased from Jackson Labs (United States).

2.1.2. Stereotactic injections

To induce inflammatory and demyelinating lesions in mice brains, LL was injected into the CC. The 1 % - LL solution was prepared by sonicating LL with 1x PBS, then stored at -20 °C. Before use, monastral blue was added at a concentration of 0.03 % to dye lesions for tracing during later processing. Mice were anesthetized, head fur was carefully cut, and a skin incision was made. After positioning the skull into a stereotactic apparatus, holes were drilled at coordinates (all from bregma) depending on further analysis: For immunohistochemistry, bilateral lesions at X = ± 0.1 mm (lateral), Y = - 1.0 mm (posterior) and Z = - 1.4 mm (ventral/ deep). For lipidomics analysis of LMs, two bilateral lesions at additionally X = ± 0.58 mm, Y = - 1.22 mm, and Z = - 1.44. To reach complete CC-demyelination for shotgun lipidomics analysis, three bilateral lesions at additionally X = ± 1.0 mm, Y = 1.1 mm, and Z = - 2,3 mm. Please see the location of LL-injection and a histological example in **Fig. 4**. A glass capillary was pulled (using DMZ Universal Puller, Zeitz-Instrumente Vertriebs GmbH, Germany), filled with the LL solution, and injected 1 µl at a rate of 150 nl/min for histology and 200 nl/min for -omics analysis. After administration, the capillary remained for another minute in the hole and was then slowly retracted. Afterward, the cut was sutured, the mice received painkillers and sodium chloride, and were put into a heating box. After 30 minutes, anesthesia was antagonized with AFN. Animals were carefully watched and received painkiller buprenorphine for three days post-surgery.

2.1.3. Perfusion

After anesthesia with ketamine/xylazine, mice were transcardially perfused, using a peristaltic pump (PERIPRO-4LS, World Precision Instruments, Germany), with cold and freshly prepared 1x

PBS until the liver turned pale, then further perfused with 4 % PFA in 1x PBS for six minutes. The brain was isolated and post-fixed in PFA for one day at 4 °C. After washing with PBS, the brain was cryoprotected with 30 % sucrose in PBS at 4 °C, which was daily exchanged for three days, embedded in Tissue-Tek O.C.T. (4583, Sakura Finetek, Germany), frozen on dry ice, and stored at -80 °C.

2.1.4. Diets and Treatments

In three experiments, we modified the diet by pharmacological treatment, changing the chow's fatty acid composition or DHA treatment.

2.1.4.1. Pharmacological treatment with acetylsalicylic acid (ASA) or baicalein (Baic)

12-month-old C57BL/6J mice were fed with standard rodent chow (control) or were treated with additional oral pharmacological treatment (Baic or ASA), which they received for 14 days after stereotactic injection. All food was offered *at libidum*. Baic was ground to powder and admixed at a 1.8 mg/g concentration to the standard chow. ASA was dissolved in water at 0.0857 mg/ml. Assuming a daily food intake of 5 mg/d and water intake of 3.5 ml/d, the target concentrations were set at 300 mg/kg BW for baic, respectively, and 100 mg/kg BW for ASA.

2.1.4.2. Chow with different fatty acid composition

C57BL/6J and *fat-1* transgenic mice were kept on diets with different sources and compositions of fatty acids (beef tallow, safflower oil, fish oil; see **Table 1** for composition). These were purchased from ssniff Spezialdiäten (Germany) and sterilized by radiation. In one experiment, female mice were on a diet from conception until weaning and their offspring until stereotactic injection. In another experiment, 6-8-weeks-old *fat-1* transgenic mice and WT control mice received a safflower diet for four weeks before stereotactic injection.

Table 1: Diet composition.
Data either in the percentage of total weight (a) or in the percentage of total FAs (b). MUFA: monounsaturated fatty acid; sFA: saturated fatty acid.

	Diet 1 – Beef Tallow Low PUFA	**Diet 2 – Safflower Oil High PUFA, high n-6**	**Diet 3 - Fish Oil medium PUFA, high n-3**
Crude protein[a] [%]	17.6		
Crude fiber[a] [%]	5.0		
Crude ash[a] [%]	4.4		
Starch[a] [%]	34.2		
Sugar[a] [%]	11.0		
Crude Fat[a] [%]	7.1		
Source of fatty acids[a] [%]	Beef tallow 5 % Soybean oil 2 %	Safflower oil 5 % Soybean oil 2 %	Fish oil 5 % Soybean oil 2%
sFA + MUFA [b] [%]	78.7	31.4	55.0
PUFA [b] [%]	21.2	68.4	44.6
(sFA + MUFA) / PUFA[b]	**3.7**	**0.5**	**1.2**

n-6 FA[b] [%]	18.1	65.9	22.7
n-3 FA[b] [%]	1.9	1.5	19.9
n-6/ n-3 FA[b]	**9.5**	**43.9**	**1.1**

2.1.4.3. Treatment with DHA and DHA-LPC

12-month-old C57BL/6J mice received daily intraperitoneal (i.p.) injections of corn oil (control), DHA in corn oil, or DHA-LPC in corn oil for 14 days before and either 4 or 14 days after stereotactic injection. For its preparation, DHA-LPC (25 mg/ml, 7 ml) was transferred into a glass vial, and the solvent chloroform evaporated under a gentle nitrogen stream. For dissolution, 1 ml of EtOH was added. DHA-LPC and DHA were further dissolved in slowly added corn oil, to each 1 mg of lipid, either 150 µl (DHA-LPC) or 258 µl (DHA) of corn oil to reach equimolarity. Next, the EtOH was evaporated under nitrogen, and the aliquots were stored at -80 °C under nitrogen. Before i.p. administration, aliquots (150 µl/animal) were warmed up and thoroughly mixed.

2.1.5. Lysophosphatidylcholine

In this study, we use the glycerophospholipid lysophosphatidylcholine (LPC, LL, lysolecithin, $C_{10}H_{22}NO_7P$, **Fig. 3**). Glycerophospholipids display a glycerol backbone to which two fatty acids and one phosphoric acid with a choline headgroup are bound. In LPC, the sn2-positioned fatty acid is removed by the hydrolytic enzyme activity of the PLA2, leaving a free fatty acid and LPC (Gressner, 2019). We use LPC in two different applications:

1. As a membrane-destabilizing detergent, which induces focal demyelination, in this case, we refer to lysophosphatidylcholine as LL.
2. In the DHA treatment experiment as a compound for DHA-LPC, which is the suggested BBB-traversable transport form of DHA.

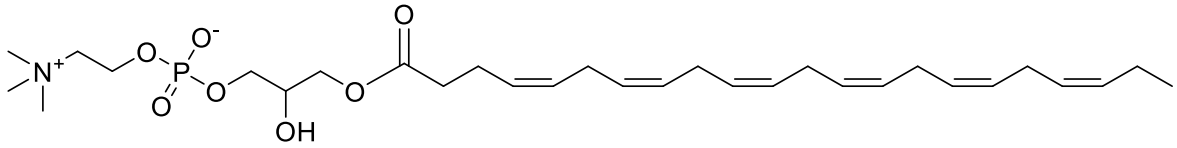

Fig. 3: Chemical structure of DHA-LPC.
The chemical structure of 1-docosahexaenoyl-2-hydroxy-sn-glycero-3-phosphocholine.

2.1.6. Mice medication

For stereotactic injections, animals were anesthetized by i.p. injections of midazolam/ medetomidine/ fentanyl (MMF, 5 / 0.5 / 0.05 mg/kg BW). The anesthesia was antagonized by subcutaneous (s.c.) injections of atipamezole/ naloxone/ flumazenil (AFN, 5 / 1.2 / 0.5 mg/kg BW) and accompanied by 150 µl sodium chloride s.c. injections to avoid dehydration. For analgesia, mice received post-surgery and for a follow-up of three days buprenorphine s.c. (BPN, 0.05 mg/kg BW). For perfusions, lethal anesthesia was carried out with i.p. injections of 10 % ketamine/ 2 % xylazine. All medication solutions were freshly prepared and kept cold until slightly warmed

before injection. Moisture cream was applied for eye protection during stereotactic injections and belly skin protection while i.p.- injections.

2.2. Histological Analysis

2.2.1. Slide Sectioning

Using a cryostat (CryoStar NX70, Thermo Fisher Scientific, USA), brains were cut into coronal sections with a 16-20 µm thickness. The lesion area was generously cut to acquire the entire lesion and identified by the eye-visible monastral blue dye. To allow multiple immunohistochemical analyses, we cut the tissue serially, each series containing the same number of sections. Sections were collected on SuperFrost Plus slides (10149870, Thermo Scientific, Germany), covered with Coverslips (No 1.5, Z692263, Sigma-Aldrich, Germany), air-dried, and stored at -20 °C.

2.2.2. Immunohistochemical staining (IHC)

All steps were performed at room temperature (RT) and with 1x PBS unless stated otherwise. Slides were warmed at 37 °C for 10 minutes and three times washed for five minutes in PBS (3x5'). For IHC with cytoplasmic target proteins, slides were permeabilized with 0.3 % Triton X100 in PBS for 10 minutes and then washed 3x5'. Next, tissue sections were circled with a hydrophobic marker and then, to prevent unspecific binding, incubated with a blocking solution for one hour. If antibodies were made in mice, Fab fragments at a concentration of 1/100 were diluted in the blocking solution, and the incubation time was extended to two hours. After a 3x5' wash, the slides were incubated with the primary antibody diluted in 10 % BS in PBS overnight at 4 °C in a humidified chamber. After a 3x5'wash, the secondary antibody was diluted in 10 % BS in PBS, and the slides were incubated for two hours, then washed 3x5'. Finally, the nuclei were stained with DAPI at 1:1000 in PBS for 10 min or together with Fluoromyelin at 1:300 in PBS for 15 min. After a 3x5' wash in PBS, the slides were dipped into dH20, dried for 15 min, mounted with Mowiol and cover slips, and dried overnight before microscopy. IHC for staining with nuclear proteins (OLIG2, CC1) required heat-induced antigen retrieval for an optimal staining result. After warming up, these slides were incubated in 10 mM sodium citrate buffer at 80 °C for 20 minutes, followed by a cooling and a washing step 3x5'. Triton X100 at a concentration of 0.03 % was added for the incubation with blocking solution. After a 3x5' wash, the primary antibodies were prepared in 1 % Triton in 10 % Blocking Solution in PBS, and the slides were incubated either overnight or for two nights at 4 °C in a humidified chamber. The following steps were performed as stated for cytoplasmatic target proteins.

2.2.3. Image acquisition

All fluorescent images were acquired using the confocal microscopes Leica TCS SP5 (Leica Microsystems, Germany; 20x Air; 0,75 NA objective) or the Zeiss LSM 900 (Carl Zeiss, Germany; 20x Air; 0,8 NA objective). Only images from CC1 and OLIG2 stained slides from the DHA-LPC

experiment were obtained with the epifluorescence microscope Leica DMI6000 B (Leica Microsystems, 10x, 20x Air).

Fluorophores were excited with light of the following wavelengths: DAPI at 405 nm, Alexa488 and Fluoromyelin at 488 nm, Alexa555 at 561 nm, and Alexa647 at 633 nm. To detect the signal of cholesterol crystals, we measured the intensity of reflection light at 410nm or 649nm using the Leica SP5 confocal. For objective and reliable analysis at the Leica SP5 confocal, the following settings remained constant: pinhole at 1 AU, resolution at 16 Bt., format at 1024 x 1024 pixels, scanning speed at 600 Hz, frame average at 3x, zoom factor at 1.4, gain not above 880 V and offset between - 0.2 and - 0.3 %. We used the tile scan option without the smoothing function to acquire the whole lesion onto one image.

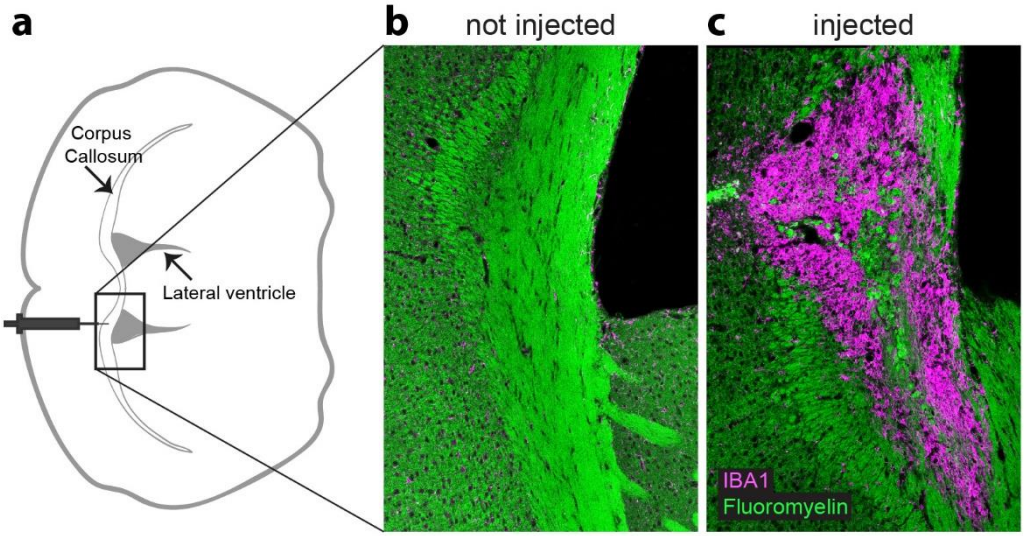

Fig. 4: Location of lysolecithin injection and histological examples.
a Schematic drawing of a coronary section (0.08 mm dorsal from bregma) of a mouse brain, rotated 90° to the left, with the longitudinal fissure pointing to the left. Stereotactic lesions were induced in the Corpus Callosum (CC), dorsal of the lateral ventricle. The area of the black rectangle is magnified in b and c.
b Representative image of a not-injected healthy CC. Fluoromyelin stains the myelin of CC's axons, while IBA1 stains microglia and macrophages, which are hardly present in the CC but in small numbers in the surrounding tissue.
c Representative image of an LL-injected CC 14 days post injection (14 dpi) in old C57BL/6J mice. IBA1$^+$ microglia and macrophages have migrated to the lesion core in the CC. The fluoromyelin signal is reduced in IBA1$^+$ areas. In the middle are accumulations of myelin debris visible.

2.2.4. Image analysis

Image analysis was performed blinded to the tested treatment groups. The lesioned area was identified by manually mapping the negative Fluoromyelin signal and clustered IBA1$^+$ cells. To obtain from these consecutively measured areas the volume of inflammation (IBA1$^+$ volume) and of demyelination (fluoromyelin negative volume), we used this publicly available IPhyton code: https://github.com/lenkavaculciakova/lesion_volume. This code calculated truncated cones from the lesion area's radius, the distance between the sections, and their thickness. The volume of the cones between two consecutive sections was summed up, resulting in the total lesion

volume. The crystal intensity was determined by measuring the Integrated Density value in Fiji, which is the product of the mapped lesion area and the Mean Gray Value. Every 10^6 units were then converted into one arbitrary unit. The cell counting of cells was performed manually using a Cell Counter plug-in of Fiji. The lesion area was obtained in a half-automated manner using a customized FIJI macro. For quantification of microglial density, IBA1 images were thresholded manually, DAPI images automatically, and then analyzed in a custom-made CellProfiler pipeline.

2.3. In vitro and Molecular Biology Analysis

2.3.1. Microglial cell culture

Primary microglial cell cultures were prepared from postnatal 8-12 C57BL/6J mice brains. The single-cell microglial suspension was obtained using the Neural Tissue Dissociation Kit with Papain according to the manufacturer's instructions. Pubs were decapitated, their brain isolated, and the chopped brain tissue dissociated with the enzyme mixes using the gentleMACS™ Dissociator (130-093-235, Miltenyi Biotech, Germany). Next, cells were centrifuged, filtered, and washed. After centrifugation (300 x g for 10 minutes at RT), the pellet was resuspended in 10 ml DMEM/pyruvate medium per C-tube, then twice applied to a 40 µm strainer and twice washed with 5 ml DMEM/pyruvate medium per C-tube. We used magnetic CD11b beads (130-093-634, Miltenyi Biotech, Germany) and a magnetic column to isolate microglia from the whole-brain cell suspension. For every 10^7 cells, the suspension was incubated with 90 µl of DMEM/FCS medium and 8 µl of anti-CD11lb Microbeads for 15 minutes on ice. The cells were then washed with 2 ml of DMEM/FCS medium for every 10^7 cells, centrifuged (300 x g for 12-18 minutes at 4 °C), and the pellet was resuspended in 500 µl of DMEM/FCS medium per 10^7 cells. Placed in LS columns on a magnet, the CD11b positive cells were, following three washes with 3 ml of DMEM/FCS medium, flushed from the column, and 5 ml of DMEM/FCS/L929 medium was added. The cells were counted, diluted to the desired density, and planted onto well plates. The cells were incubated in DMEM/FCS/L929 medium, which was changed twice or three times a week, at 37 °C with 5 % CO_2 until they had grown dense enough for experiments.

2.3.2. Microglial uptake and clearance assay with quantitative PCR

The effects of LMs and pharmacological inhibitors on myelin uptake and clearance in microglia were examined by measuring gene expression levels with quantitative PCR (qPCR). Cells were preincubated with different LMs at 50 nM (in assay #1: RvD1, NPD1, RvD4; in assay #2: RvD2, Mar1, RvE1, LX4, LB4) or pharmacological inhibitors (acetylsalicylic acid at 100 µM, baicalein at 25 µM, zileuton at 10 µM) in DMEM/Pyruvate for two hours. Then, the medium was removed, and the cells were incubated with the same substance and purified myelin at a concentration of 5 µg/ml in DMEM/Pyruvate for two hours. After washing with DMEM/Pyruvate, pre-incubation was repeated, and the cells were post-incubated with the same substance in DMEM/Pyruvate medium

for 24 hours. Cells were washed with cold PBS, collected with β-mercaptoethanol in Buffer RLT-Plus, snap-frozen on dry ice, and stored at -80 °C. Following the entrepreneur's instructions, we used the RNeasy Plus Mini Kit for total RNA isolation. The RNA yield was determined by using a NanoDrop. The SuperScript III First-Strand Synthesis system was used to produce cDNA, with random hexamers as primers and 1 µg of total RNA. The quantitative PCR (qPCR) was performed using the PowerUp SYBR Green Master Mix and a LightCycler 480 Real-Time PCR system (Roche Life Science, Switzerland). qPCR samples were run in technical triplicates, and gene expression fold changes were normalized to the housekeeping gene *CyC1*.

2.3.3. Myelin preparation

Myelin was isolated from 8-week-old C57BL/6J mice, whose brain tissue was homogenized by sonification in 10 mM HEPES buffer. Using a sucrose stepwise gradient of 0.32 M and 0.85 M in 10 mM HEPES, we centrifugated the homogenate at 25000 rpm for 35 minutes at 4 °C with a SW32Ti rotor (369694, Beckman Coulter, Germany). After isolating, the myelin fraction underwent osmotic shock three times by being dissolved in ddH20 and centrifuged at 25000 rpm and then at 10000 rpm for 18 minutes at 4 °C. Supernatants were kept in HEPES at RT overnight. The sucrose gradient method was repeated three times the next day to purify the isolated myelin. To support the resuspension of the precipitated particles, we sonicated the myelin and passed it through a 27 Gauche cannula before being added to cells. Myelin yield, respectively the protein concentration, was determined by using the Bradford assay (500-0006, Biorad, USA).

2.4. Lipidomics Analysis

2.4.1. Corpus callosum isolation

To characterize LL-induced demyelinating lesions, we performed quantitative lipidomics. Young C57BL/6J mice received four (for lipidomics of LMs) or six (for shotgun lipidomics) stereotactic injections into the corpus callosum, which was then isolated at 14 dpi. For CC isolation, animals were anesthetized with ketamine/xylazine and transcardially perfused using a peristaltic pump with cold and freshly prepared 1xPBS to avoid blood contamination until the liver turned pale. To keep tissue degradation to a minimum, we performed the following steps quickly in cool PBS: Brains were isolated, and hemispheres were attached to a sample holder with 15 % gelatine in PBS. Using a vibratome (Leica Microsystems, Germany), 250 µm thick sections were cut at a speed of 1 mm/s. The lesioned CC was dissected from healthy tissue under a stereoscope (Leica KL300 LED, Leica Microsystems, Germany) with fine scalpels and forceps, flash-frozen on dry ice, and stored at -80 °C.

2.4.2. Shotgun Lipidomics

Isolated tissue was weighed and homogenized with 1x sterile PBS in a dounce homogenizator (Tenbroeck, 15 ml, VE 2, 5000006, VWR International, USA) to 5 mg/ml concentration. Samples

were sent to Lipotype GmbH (Dresden, Germany) for further processing and analysis as described previously (Sampaio et al., 2011; Surma et al., 2015). The following texts (2.4.2.1, 2.4.2.2, 2.4.2.3) describe the proceeding and are provided by Lipotype GmbH, Dresden.

2.4.2.1. Lipid extraction for mass spectrometry lipidomics

Lipids were extracted using a two-step chloroform/methanol procedure (Ejsing et al., 2009). Samples were spiked with internal lipid standard mixture containing: cardiolipin 14:0/14:0/14:0/14:0 (CL), ceramide 18:1;2/17:0 (Cer), diacylglycerol 17:0/17:0 (DAG), hexosylceramide 18:1;2/12:0 (HexCer), lysophosphatidate 17:0 (LPA), lysophosphatidylcholine 12:0 (LPC), lysophosphatidylethanolamine 17:1 (LPE), lysophosphatidylglycerol 17:1 (LPG), lysophosphatidylinositol 17:1 (LPI), lysophosphatidylserine 17:1 (LPS), phosphatidate 17:0/17:0 (PA), phosphatidylcholine 17:0/17:0 (PC), phosphatidylethanolamine 17:0/17:0 (PE), phosphatidylglycerol 17:0/17:0 (PG), phosphatidylinositol 16:0/16:0 (PI), phosphatidylserine 17:0/17:0 (PS), cholesterol ester 20:0 (CE), sphingomyelin 18:1;2/12:0;0 (SM), sulfatide d18:1;2/12:0;0 (Sulf), triacylglycerol 17:0/17:0/17:0 (TAG) and cholesterol D6 (Chol). After extraction, the organic phase was transferred to an infusion plate and dried in a speed vacuum concentrator. First, the dry extract was resuspended in 7.5 mM ammonium acetate in chloroform/methanol/propanol (1:2:4, V:V:V), and second dry extract in 33 % ethanol solution of methylamine in chloroform/methanol (0.003:5:1; V:V:V). All liquid handling steps were performed using Hamilton Robotics STARlet robotic platform with the Anti Droplet Control feature for organic solvents pipetting.

2.4.2.2. Mass spectrometry data acquisition

Samples were analyzed by direct infusion on a QExactive mass spectrometer (Thermo Scientific) equipped with a TriVersa NanoMate ion source (Advion Biosciences). Samples were analyzed in both positive and negative ion modes with a resolution of Rm/z=200=280000 for mass spectrometry (MS) MS and Rm/z=200=17500 for tandem mass spectrometry (MSMS) experiments in a single acquisition. MSMS was triggered by an inclusion list encompassing corresponding MS mass ranges scanned in 1 Da increments (Surma et al., 2015). Both MS and MSMS data were combined to monitor CE, DAG, and TAG ions as ammonium adducts; PC, PC O-, as acetate adducts; and CL, PA, PE, PE O-, PG, PI, and PS as deprotonated anions. MS only was used to monitor LPA, LPE, LPE O-, LPI, and LPS as deprotonated anions; Cer, HexCer, SM, LPC, and LPC O- as acetate adducts and cholesterol as ammonium adduct of an acetylated derivative (Liebisch et al., 2006).

2.4.2.3. Data analysis and post-processing

Data were analyzed with in-house developed lipid identification software based on LipidXplorer (Herzog et al., 2012; Herzog et al., 2011). Data post-processing and normalization were performed using an in-house developed data management system. Only lipid identifications with a signal-to-

noise ratio >5 and a signal intensity 5-fold higher than in corresponding blank samples were considered for further data analysis.

For principal component analysis (PCA), the sum of all lipid subspecies within these lipid classes was calculated: CE, CL, DAG, LPA, LPC, LPC O-, LPE, LPE O-, LPG, LPI, LPS, PA, PC, PC O-, PE, PE O-, PG, PI, PS, TAG. Using the median impute method (Kuhn, 2008), missing values were assumed with the caret::preProcess() function. Using singular value decomposition, PCA was quantified with pcaMethods::pca() function (Stacklies et al., 2007). Values were scaled to unit variance and centered.

2.4.3. UPLC-MSMS Metabololipidomics of PUFAs and LMs

Ultra-performance liquid chromatography tandem mass spectrometry (UPLC-MSMS) metabololipidomics analysis was performed by our collaboration partner Prof. Oliver Werz (Department of Pharmacy, Friedrich-Schiller-Universität, Jena, Germany). The following texts (2.4.3, 2.4.3.1) describe the proceeding and are adapted from texts provided by our partner. The CC tissue homogenization was performed in 1 ml ice-cold methanol (10653963, Fisher Chemical, Germany), which included 10 µL of deuterium-labeled LM standard as an internal reference for quantification and sample recovery. These standards comprise 200 nM d_8-5S-hydroxyeicosatetraenoic acid (HETE) (334230, Cayman Chemical, USA), d_4-leukotriene B_4 (320110, Cayman Chemical, USA), d_5-lipoxin A_4 (24936, Cayman Chemical, USA), d_5-resolvin D2 (11184, Cayman Chemical, USA), d_4-prostaglandin E_2 (10007273, Cayman Chemical, USA) and 10 µM d_8-arachidonic acid (390010, Cayman Chemical, USA). In a few words, samples were for 60 minutes at -20 °C to facilitate protein precipitation. After centrifugation (1200 x g for 10 minutes at 4 °C), 8 ml of acidified H_2O was administered to a final pH of 3.5, and solid-phase extraction was performed. Before loading samples into columns, the solid-phase cartridges (Sep-Pak® Vac 6cc 500 mg/ 6 mL C18; Waters Corporation, USA) were equilibrated with 2 ml H_2O and 6 ml methanol. After a wash with 6 ml H_2O and 6 ml *n*-hexane, LMs elution was performed with 6 ml methyl formate. Samples were evaporated (TurboVap LV, Biotage, Sweden), dried, and resuspended in 150 µl of methanol-water (50/50, v/v) for UPLC-MSMS automated injections. Next, the analysis of LM profiling followed with an Acquity™ UPLC system (Waters Corporation, USA) and a QTRAP 5500 Mass Spectrometer (ABSciex, Germany), which was stocked with electrospray ionization and a Turbo V™ Source. LM elution was performed with an ACQUITY UPLC® BEH C18 column (1.7 µm, 2.1 × 100 mm; Waters Corporation, Germany) with a flow rate of 0.3 ml/min at 50 °C. The mobile phase consisted at the beginning of methanol-water-acetic acid 42:58:0.01 (v/v/v) and was then ramped over 12.5 minutes to 86:14:0.01 (v/v/v) and then finally over 3 minutes to 98:2:0.01 (v/v/v) (Werner et al., 2019). The operating mode of the QTrap 5500 was in negative ionization and used scheduled multiple reaction monitoring (MRM) connected with information-dependent acquisition. The MRM window was set to 60 seconds, curtain gas pressure was at

35 psi, and optimized LM parameters (CXP, CE, DP, and EP) were used. For each LM, at least six diagnostic icons and the retention time were validated with an external standard (Cayman Chemical, USA) (Werner et al., 2019).

2.4.3.1. Data analysis

Linear calibration curves quantified each lipid mediator. These gave R2 values for LMs of 0.998 or higher, respectively, for FA of 0.95 or higher. Also, the detectable limits of each LM were determined.

2.5. Data Availability

Please find more information and the complete data, respectively, its deposition set in this publication (Penkert et al., 2021).

2.6. Statistical Testing

Statistical analysis was performed with GraphPad Prism. Detailed information on the tests used in each experiment is found in the legends of the figures. Depending on the number of compared groups, normality, and question, Welch's t-test, one-way ANOVA followed by Dunnett's or Tukey's multiple comparisons test, Kruskal-Wallis test followed by Dunn's multiple comparisons test, or two-way ANOVA followed by Sidak's multiple comparisons test were used. For qPCR, the fold change in gene expression was determined with the ΔΔCt method.

Normality was assessed mainly by eye and because of small sample sizes, only supplementarily by normality tests (Ghasemi & Zahediasl, 2012; Mishra et al., 2019). The probability value of < 0.05 was defined as significant in all tests. The level of significance is indicated in the figures as follows: * = $p < 0.05$, ** = $p < 0.01$, ***= $p < 0.001$, and **** = $p < 0.0001$ and n.s. = no significance. All graphs are plotted as mean ± standard deviation unless stated otherwise. Dots indicate the number of lesions in histological analysis (1-2 per animal), the number of brains in -omics analysis, or technical replicates in cell culture experiments.

Hypothesis and Aims of this Study

Acute inflammation is the protective cellular and humoral response to tissue damage and is ideally self-limited, leading to resolution, functional repair, and the return to homeostasis (Buckley et al., 2014). Growing evidence proposes that the resolution of inflammation is not a passive process following lowering concentrations of pro-inflammatory mediators (PIMs) but actively organized and mediated by n-3 polyunsaturated fatty acids (PUFAs) and their specialized pro-resolving mediators (SPMs) (Serhan, 2017; Serhan & Savill, 2005).

Since persistent inflammation is associated with inadequate remyelination, we wanted to investigate the little-addressed role of n-3 PUFAs and lipid mediators (LMs) in myelin repair. Therefore, we hypothesized in this study that n-3 PUFAs and SPMs could foster lesion recovery and remyelination by facilitating the switch from a pro-inflammatory to a resolving environment in demyelinated tissue.

To test this hypothesis, we assessed the possible role of n-3 and n-6 PUFAs and their bioactive LMs in a mice model of toxin-induced brain demyelinating lesions. Using lipidomic analysis, we first aimed to search for alterations of PUFAs and LMs in these lesions over time. Next, we characterized lesions in knockout mice and inhibited PUFA processing enzymes pharmacologically. Next, we explored *in vitro* potential microglia-mediated mechanisms on lipid buffering that could underlie n-3 PUFA benefits mechanistically. Finally, we tested if a decreased n-6/n-3 PUFA ratio and n-3 PUFA supplementation could support inflammation resolution and remyelination *in vivo*.

Results

1. Characterization of the Lipidome in Demyelinated Lesions Reveals Release of Lysophospholipids and PUFAs

First, we wanted to learn how demyelination affects the lipid profile of lesions. Therefore, we used a mice model of demyelination and induced focal demyelinating lesions by injecting lysolecithin (LL) into the corpus callosum (CC). In injected mice, demyelination and inflammation peak at 3-4 days post injection (dpi), while lesion recovery and remyelination occur at 14 to 21 dpi, as shown in **Fig. 5** (Cantuti-Castelvetri et al., 2018; Jeffery & Blakemore, 1995). To perform lipidomic analysis, we used young C57BL/6J mice and dissected LL-induced demyelinated CC tissue of inflamed (3 dpi) and remyelinating (7 dpi, 14 dpi) lesions and healthy uninjected CC tissue (0 dpi).

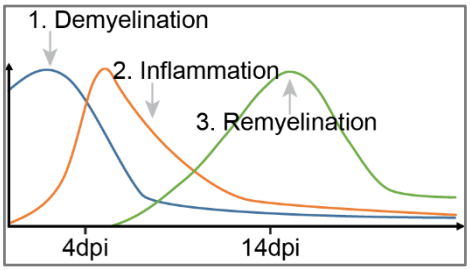

Fig. 5: Course of corpus callosum lesions after lysolecithin-induced demyelination.
After injection, demyelination and inflammation peak 3 to 4 days post injection (dpi). Inflammation resolution and repair processes follow, reaching a maximum at 14 to 21 dpi.

To examine alterations of lipids, polyunsaturated fatty acids (PUFAs), and lipid mediators (LMs) over time, we performed shotgun lipidomics and UPLC-MSMS metabololipidomics analysis. Principal component analysis segregated the lipid profiles of the four different groups (0, 3, 7, 14 dpi) (**Fig. 6a**). We identified the top significantly changed lipid classes by plotting q-values (the p-values corrected for multiple comparisons) against the log2 of the maximum fold change between the groups. We found that lipid profiles were predominantly driven by changes in lysophospholipids and triacylglycerides (**Fig. 6b**). When examining these lipid classes in detail, we discovered that the tissue from 3 dpi is characterized by higher proportions of the lysophospholipids LPC, LPS, LPE, LPE O-, of triacylglycerides and ceramides compared to untreated and remyelinating tissue (**Fig. 6c**).

When phospholipids are hydrolyzed to lysophospholipids, PUFAs are released. Hence, we hypothesized that the increase in lysophospholipids should also be accompanied by an increase in PUFAs. Therefore, we next determined changes in free PUFAs and LMs, which are known to mediate the acute inflammatory response and inflammation resolution. Indeed, the free PUFAs EPA and DHA were increasingly released over time from acute inflammation (3 dpi) towards tissue regeneration and remyelination (7, 14 dpi) (**Fig. 7a**). This release was accompanied by a decreasing ratio of n-6 to n-3 PUFAs (AA / (EPA + DHA)) over time. As age is associated with inadequate remyelination, and therefore, differences between young and aged mice could elucidate reasons for the decline in myelin repair, we repeated this measurement in 12-month-

old mice. In contrast to young mice, we could not observe the decrease of the n-6 / n-3 PUFA ratio in aged mice (**Fig. 7b**). Comparison of the ratio in healthy CC tissue between young and old mice showed a decreased one in aged mice (**Fig. 7b**). Correlated to the release of PUFAs, we measured in young mice an increase of down-stream metabolites such as COX-derived LMs and Alox-derived oxylipins (**Fig. 7c,d**), but not of SPMs (**Fig. 7e**). Thus, demyelination and remyelination profoundly altered the lipid composition in lesioned CC tissue, leading to higher proportions of lysophospholipids at peak inflammation and a release of PUFAs and their LMs during lesion recovery.

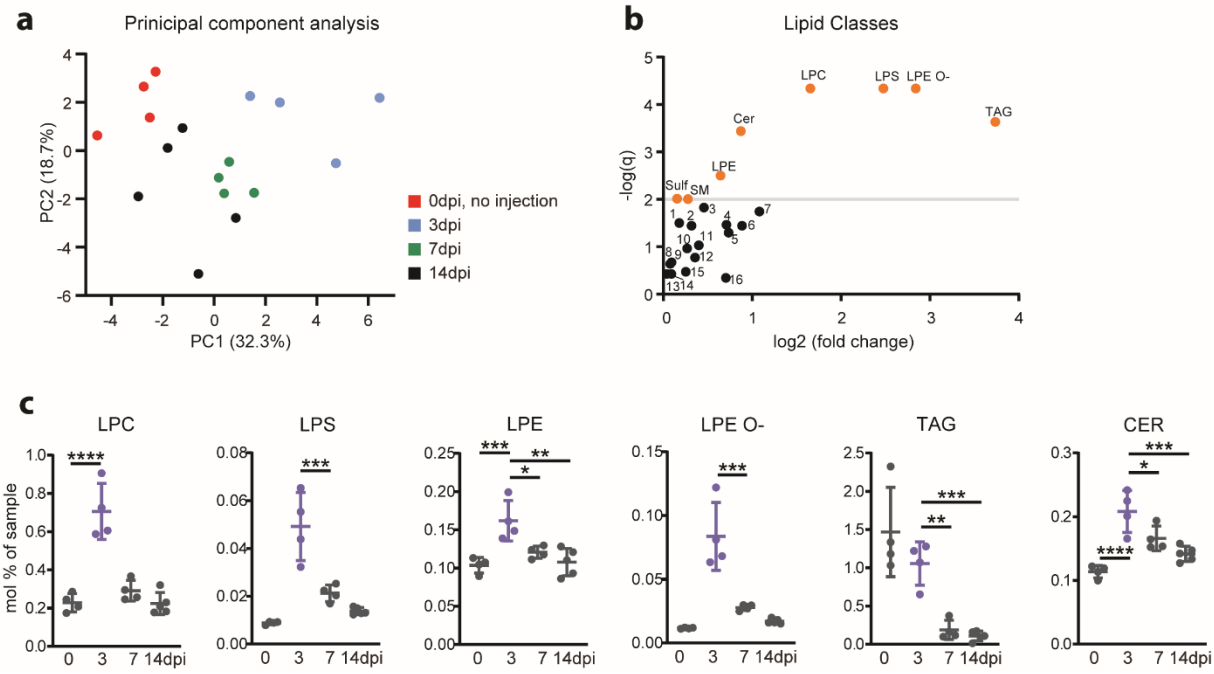

Fig. 6: The lipid profile of demyelinated lesions shows alterations of lysophospholipids during inflammation and its resolution.
Shotgun lipidomics of corpus callosum tissue from young C57BL/6J mice after lysolecithin injection at 3, 7, 14 days post injection (dpi) and without injection (0 dpi). $n_{0dpi}=n_{3dpi}=n_{7dpi}=4$, $n_{14dpi}=5$.
a Principal component analysis based on lipid classes shows distinct lipidomes of the four groups: PC1 discriminates between uninjected (0 dpi, red) and inflamed tissue (3 dpi, blue), and PC2 between uninjected (0 dpi) and remyelinating tissue (7 dpi, green and 14 dpi, black).
b p-values of one-way ANOVA of lipid classes corrected for multiple comparisons ($q \leq 0.01$ in orange) plotted against log2 of maximal fold change between time points. LPC, LPS, LPE, LPE O-, TAG, and CER are identified as drivers of lipidome alterations over time. 1 PE, 2 PC O-, 3 PA, 4 LPI, 5 PG, 6 LPC O-, 7 LPG, 8 Chol, 9 PC, 10 PI, 11 PS, 12 DAG, 13 PE O-, 14 HexCer, 15 LPA, 16 CL.
c Percentage of the sample with altered lipid classes over time. Several lipid classes are changed: One-way ANOVA with Dunnett's multiple comparison test, P-values: *< 0.05, ** < 0.01, *** < 0.001, and **** < 0.0001. Data are represented as mean ± SD. Dots indicate individual brains. LPC: Lysophosphatidylcholine, LPS: lysophosphatidylserine, LPE: lysophosphatidylethanolamine, LPE O-: lysophosphatidylethanolamine ether, TAG: triacylglyceride, CER: ceramide. For other abbreviations, please see the list of abbreviations.
Note: Mathias M. Gerl and Christian Klose from Lipotype GmbH, Dresden, performed lipidomic analysis.

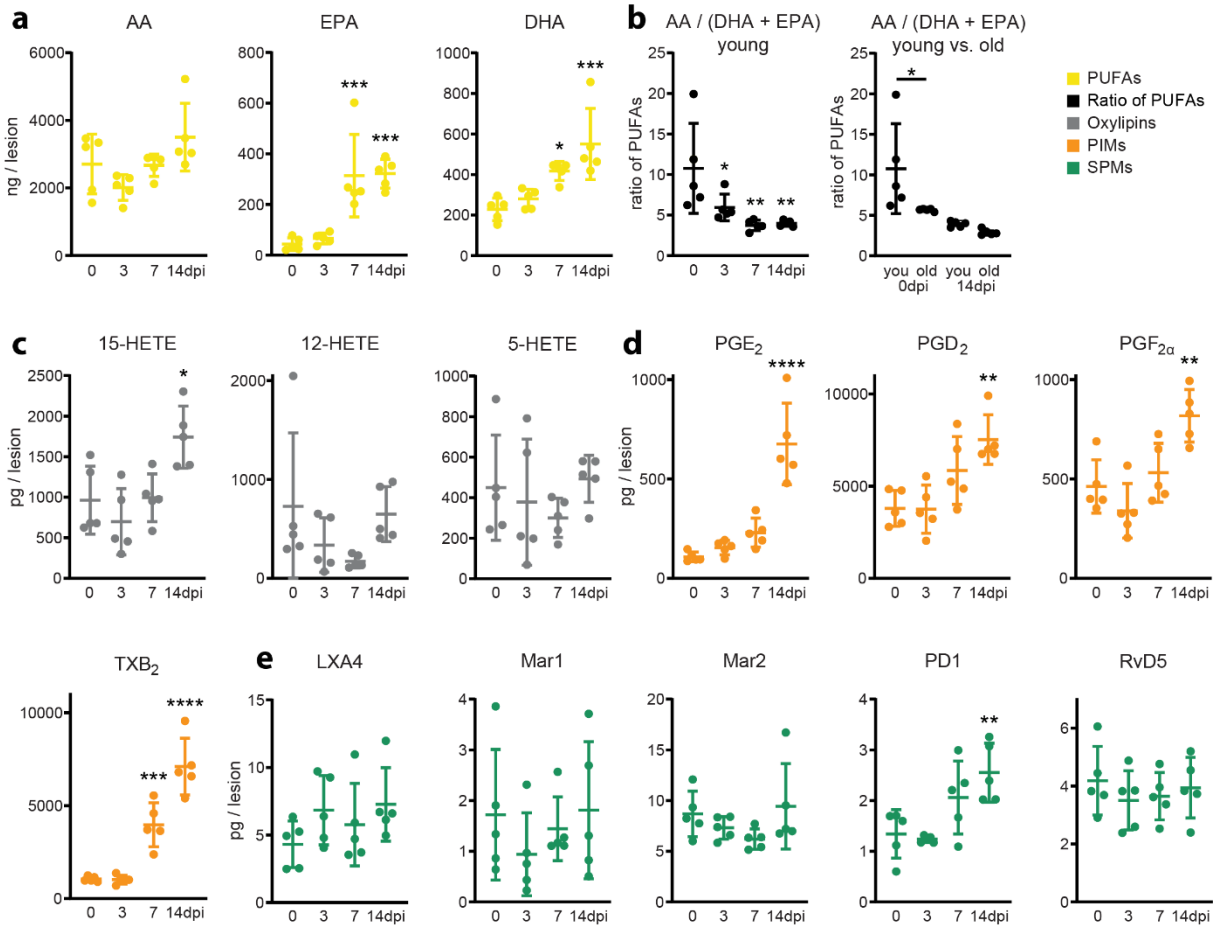

Fig. 7: PUFA and LM profile of demyelinated lesions reveals the release of PUFAs and PIMs during inflammation resolution.

UPLC-MSMS metabololipidomics of corpus callosum tissue from young C57BL/6J mice after lysolecithin injection at 3, 7, 14 days post injection and without injection (0 dpi). $n_{young\ 0,3,7,14dpi}=5$.

a Concentration of the PUFAs AA, EPA, and DHA (yellow) in demyelinated lesions over time. One-way ANOVA with Dunnett's multiple comparisons test were performed. AA: $p_{ANOVA}=0.0356$, EPA: $p_{ANOVA}<0.0001$, $p_{0dpi\ vs.\ 7dpi}=0.0005$, $p_{0dpi\ vs.\ 14dpi}=0.0004$, and DHA: $p_{ANOVA}=0.0004$, $p_{0dpi\ vs.\ 7dpi}=0.0201$, $p_{0dpi\ vs.\ 14dpi}=0.0003$.

b Ratio of AA/(DHA+EPA) (black) in young animals over time. One-way ANOVA with Dunnett's multiple comparisons test: $p_{ANOVA}=0.0053$, $p_{0dpi\ vs.\ 3dpi}=0.0484$, $p_{0dpi\ vs.\ 7dpi}=0.0042$, $p_{0dpi\ vs.\ 14dpi}=0.0056$ (left panel). Ratio in young and 12-month-old mice in healthy (0 dpi) and remyelinating tissue (14 dpi). Two-way ANOVA with Sidak's multiple comparisons test, $n_{old\ 0,14dpi}=5$, $p_{age}=0.0230$, $p_{time}=0.0014$, no significant interaction, $p_{0dpi}=0.0214$, (right panel).

c-e Concentrations of oxylipins (grey, c), PIMs (orange, d), and SPMs (green, e) in demyelinated lesions over time. One-way ANOVA with Dunnett's multiple comparisons test were performed. P-values: *< 0.05, ** < 0.01, *** < 0.001, and **** < 0.0001.

Data are represented as mean ± SD. Dots indicate individual brains. Unless a horizontal bar illustrates otherwise, asterisks illustrate significant results compared to 0 dpi. You: young. Please see the list of abbreviations for abbreviations of lipid mediators.

Note: Horst Penkert performed cerebral injections and vibratome dissection. Paul M. Jordan performed metabololipidomic analysis.

2. Impairment of Lipoxygenases Leads to Persistent Inflammation

After observing the PUFA release upon a demyelinating injury, we wanted to determine if these FAs influence remyelination. Therefore, we examined the effects on phagocyte infiltration and remyelination in lesions with impaired lipoxygenases (Alox) and cyclooxygenases (COX), the enzymes processing these PUFAs. Also, we wanted to investigate if downstream products of the released PUFAs, such as LMs, would affect microglial phagocytosis *in vitro*.

2.1. Pharmacological Inhibition of Lipoxygenases and Cyclooxygenases Leads to a Persisting Inflammatory Infiltrate

We treated 12-month-old mice with baicalein (Baic) or acetylsalicylic acid (ASA), pharmacological inhibitors of Alox12/15 (Sekiya & Okuda, 1982) and COX1/2 (Ferreira et al., 1971; Smith & Willis, 1971; Vane, 1971), and analyzed LL-induced lesions at 14 dpi. We stained immunohistochemically with IBA1, a marker for activated microglia involved in phagocytosis, and fluoromyelin, a marker for myelinated axons. In this and the following experiments, we determined the IBA1$^+$ phagocytic infiltrate and the volume of microglia and macrophages to approximate the extent of *inflammation*. Here, we measured a higher density of IBA1$^+$ cells in the pharmacologically treated groups, indicating an ongoing inflammatory response and impaired lesion restitution in these mice (**Fig. 8a,b**).

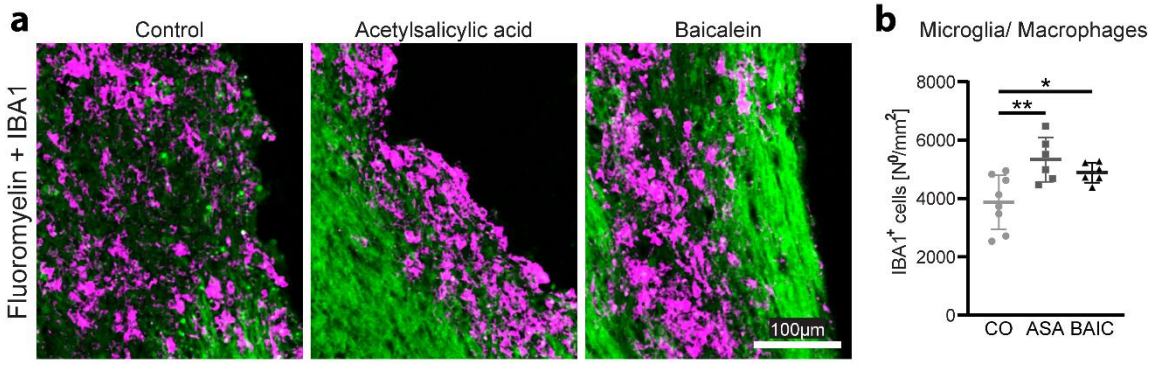

Fig. 8: Pharmacological inhibition of LM synthesis limits phagocyte density.
a Images of corpus callosum lesions showing demyelination (loss of fluoromyelin signal, green) and IBA1$^+$ phagocytic infiltrate (magenta) at 14 dpi in 12-month-old C57BL/6J mice pharmacologically treated with acetylsalicylic acid (ASA), inhibiting COX1/2, or baicalein (BAIC), inhibiting Alox12/15. $n_{CO}=8$, $n_{ASA}=n_{Baic}=6$.
b Analysis of density of IBA1$^+$ phagocytic cells at 14 dpi of mice treated with ASA or BAIC. One-way ANOVA with Dunnett's multiple comparisons test, $p_{ANOVA}=0.0058$, $p_{ASA}=0.0041$, $p_{Baic}=0.0418$.
Data are represented as mean ± SD. Dots indicate individual lesions. All images chosen are representative for the respective cohorts and were selected to present the group's mean.
Note: Horst Penkert performed all steps.

2.2. Lipoxygenases Knockout Results in Persisting Inflammation, Accumulation of Lipids, and Poorer Remyelination

To validate the lipoxygenases effects, we induced demyelinating lesions in young mice with global knockouts (KO) of *Alox15*, transforming AA, EPA, and DHA into SPMs, and *Alox5*, metabolizing AA to pro-inflammatory leukotrienes (Serhan & Petasis, 2011). Because of Alox5's pro-inflammatory properties, we expected a less pronounced inflammatory activity in these KO mice during acute inflammation (4 dpi). However, the density of $IBA1^+$ phagocytic infiltrate was similar compared to wild type (WT) mice, which suggests a comparable $IBA1^+$ inflammatory response (**Fig. 9c**). At 14 dpi, the analysis of *Alox15* and *Alox5* KO mice revealed a higher density of $IBA1^+$ cells compared to WT mice, indicating sustained inflammation (**Fig. 9a-c**). We characterized the phenotype further and noticed cholesterol crystals at the lesion core, whose intensity was increased in *Alox15* KO but not in *Alox5* KO mice (**Fig. 9d,e**).

Having recognized this persistent inflammatory infiltrate and accumulation of lipids, we examined the KO effects on remyelination by studying oligodendrocytes in the lesion. Therefore, we stained with CC1, a marker for mature myelinating oligodendrocytes, and OLIG2, an oligodendrocyte lineage marker, and counted $CC1^+OLIG2^+$ and $CC1^-OLIG2^+$ cells at the lesion core. In this and the following experiments, we use this ratio to determine the percentage of mature oligos as an approximation for *remyelination*. Here, we found that the ratio of mature $CC1^+OLIG2^+$ over all $OLIG2^+$ oligodendrocytes is reduced in *Alox15* KO mice, pointing to poor repair of the myelin damage (**Fig. 9g,h**). To control that this reduced ratio was not artificial due to fewer counted $OLIG2^+$ cells, we determined the $OLIG2^+$ density, which was similar between all groups (**Fig. 9h**).

Taken together, both KOs resulted in poor lesion recovery at 14 dpi by not limiting inflammation, and in *Alox15* KO additionally by impairing myelin debris clearance and remyelination.

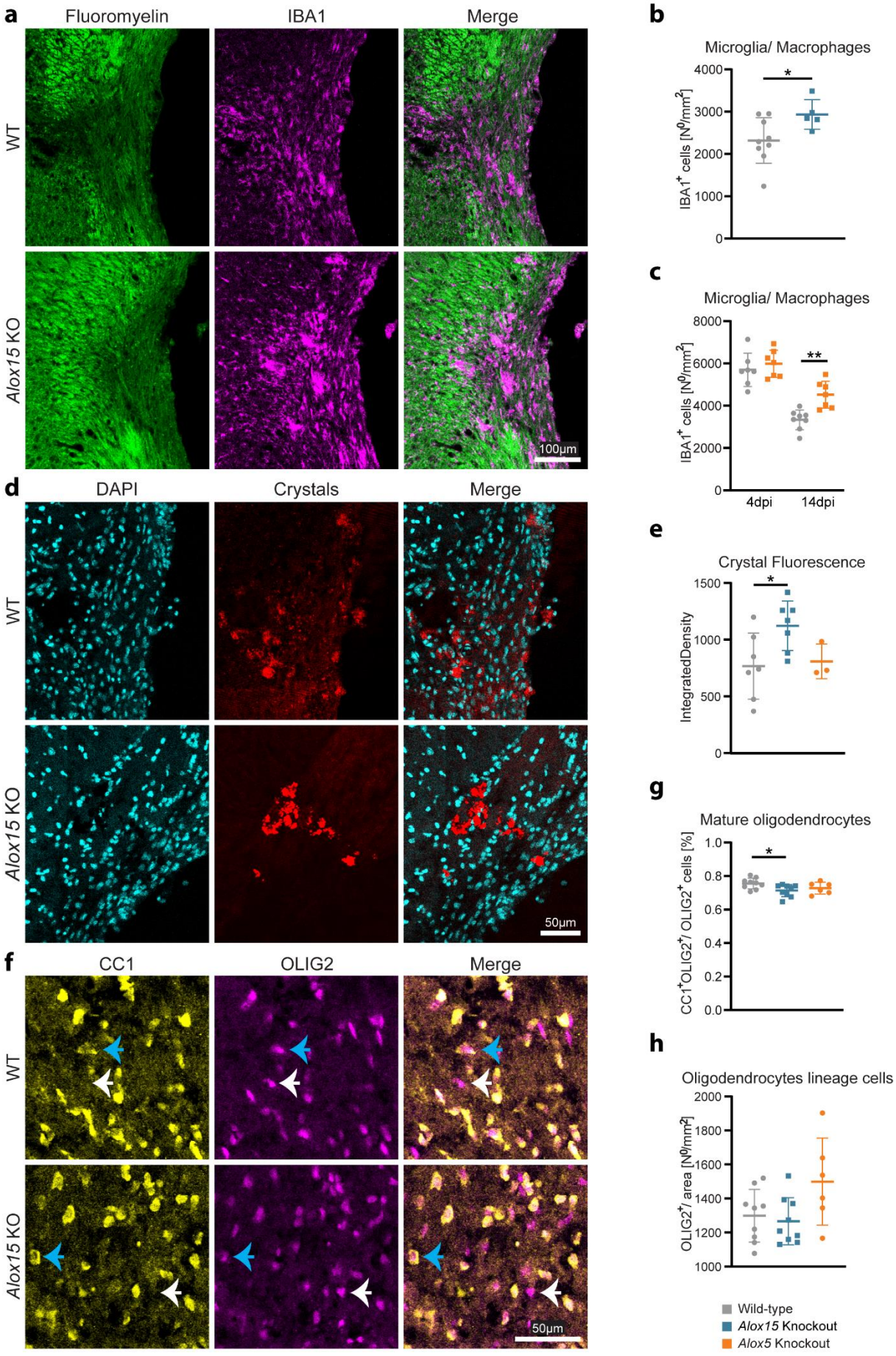
a
Fluoromyelin
IBA1
Merge
WT
Alox15 KO
100µm
b
Microglia/ Macrophages
IBA1+ cells [N0/mm2]
4000
3000
2000
1000
0
*
c
Microglia/ Macrophages
IBA1+ cells [N0/mm2]
8000
6000
4000
2000
0
**
4dpi
14dpi
d
DAPI
Crystals
Merge
WT
Alox15 KO
50µm
e
Crystal Fluorescence
IntegratedDensity
1500
1000
500
0
*
f
CC1
OLIG2
Merge
WT
Alox15 KO
50µm
g
Mature oligodendrocytes
CC1+OLIG2+/ OLIG2+ cells [%]
1.0
0.8
0.6
0.4
0.2
0.0
*
h
Oligodendrocytes lineage cells
OLIG2+/ area [N0/mm2]
2000
1800
1600
1400
1200
1000
Wild-type
Alox15 Knockout
Alox5 Knockout

Fig. 9 (previous page): Inhibition of lipid mediator synthesis by knockouts of Alox15 and Alox5 limits inflammation resolution.
a Images of corpus callosum (CC) lesions showing fluoromyelin (green) and IBA1 (magenta) signal at 14 dpi in WT and *Alox15* KO mice.
b,c Quantification of density of IBA1$^+$ phagocytic cells in WT and KO mice at 4 and 14 dpi. Welch's t-test, $n_{WT}=9$, $n_{Alox15}=5$, $p=0.0250$ (b). Two-way ANOVA with Sidak's multiple comparisons test, $n_{WT,4dpi}=n_{Alox5,4dpi}=n_{Alox5,14dpi}=7$, $n_{WT,14dpi}=8$, $p_{time}<0.0001$, $p_{mouseline}=0.0048$, no significant interaction, $p_{14dpi}=0.0029$ (c).
d,e Images of CC lesions with DAPI-stained nuclei (cyan) and cholesterol crystals (red) at 14 dpi in WT and *Alox15* KO mice (d). Analysis of crystals in WT and KO mice measured as the integrated density of reflected light. One-way ANOVA with Dunnett's multiple comparisons test, $n_{WT}=n_{Alox15}=7$, $n_{Alox5}=3$, $p_{ANOVA}=0.0403$, $p_{WT\ vs.\ Alox15}=0.0313$ (e).
f Images of CC lesions showing CC1 (yellow) and OLIG2 (magenta) signal at 14 dpi in WT and *Alox15* KO mice. Mature oligodendrocytes (CC1$^+$OLIG2$^+$ cells) are marked with a blue arrow, and oligodendrocytes lineage cells (CC1$^-$OLIG2$^+$) with a white arrow.
g,h The ratio of mature oligodendrocytes in WT and KO mice. One-way ANOVA with Dunnett's multiple comparisons test: $p_{ANOVA} = 0.0487$ und $p_{WT\ vs.\ Alox15}=0.0301$ (g). Analysis of OLIG2+ oligodendrocyte lineage cell density in WT and KO mice. One-way ANOVA with Dunnett's multiple comparisons test, $n_{WT}=n_{Alox15}=9$, $n_{Alox5}=6$, $p_{ANOVA}=0.0538$ (h).
Data are represented as mean ± SD. Dots indicate lesions. All images chosen are representative for the respective cohorts and were selected to present the group's mean. Alox: lipoxygenase, KO: knockout, WT: wild type. Please see the list of abbreviations.
Note: Horst Penkert performed injection of mice, processing, and analysis of data shown in a-c.

2.3. Lipid Mediators and Pharmacological Inhibitors Show None to Modest Effects on Myelin Clearance in Microglia *in vitro*

Before remyelination can begin, microglia and macrophages need to phagocytose and degrade accumulating myelin debris, and therefore they activate lipid catabolic pathways (e.g., LXR, PPAR) (Bogie et al., 2012). As we have observed poorer regeneration and persisting inflammation in KO mice, we wondered if the deficiency and limited availability of downstream metabolites of n-3/ n-6 PUFAs would affect microglia's myelin and lipid processing mechanisms. We hypothesized that SPMs would improve while PIMs, Alox, and COX pharmacological inhibitors would impede phagocytic myelin clearance. Therefore, we cultured microglia, incubated them with myelin and LMs or pharmacological inhibitors, and measured the gene expression of LXR target genes *Apoe, Abca1, Abcg1*, and of *Soat1*.

Neither acetylsalicylic acid nor baicalein had effects on the expression of these genes. Only zileuton, an inhibitor of Alox5, increased the fold change of *Abcg1*, mediating cholesterol efflux (**Fig. 10a**). None of the tested LMs affected the expression of *Apoe, Abca1*, or *Abcg1*. Neuroprotectin D1 (NPD1), resolvin D4 (RvD4), and leukotriene B4 (LB4) led to a downregulation of *Soat1* (**Fig. 10b-c**), which encodes for an enzyme esterifying cholesterol molecules for storage in lipid droplets.

These experiments could not provide further consistent and reliable *in vitro* evidence on microglia-mediated mechanisms underlying our *in vivo* observations.

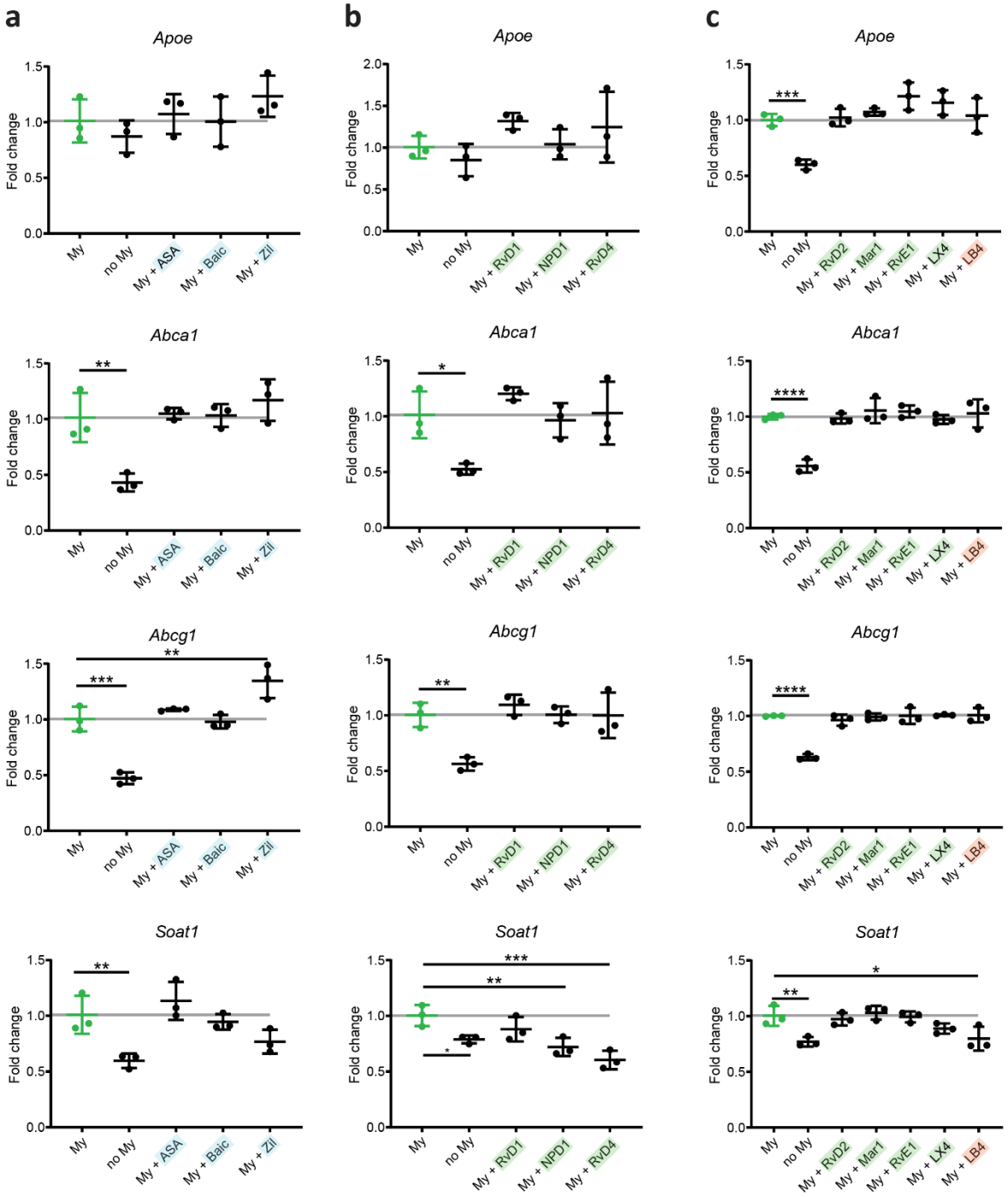

Fig. 10: LMs and pharmacological inhibitors do not affect myelin clearance and cholesterol processing in microglia in vitro.

a-c Quantification of the fold change of mRNA expression of *Apoe* (first row), *Abca1* (second row), *Abcga1* (third row), and *Soat1* (fourth row) 24 hours after myelin (My) administration in microglia either treated with the pharmacological inhibitors (blue, a) acetylsalicylic acid (ASA), baicalein (Baic), zileuton (Zil,) or the SPMs (green, b) RvD1, NPD1, RvD4 or with SPMs (green, red, c) RvD2, Mar1, RvE1, LA4, and PIM LB4. One-way ANOVA with Dunnett's multiple comparisons test was performed in all experiments, n=3 in all cases. *Apoe*: $p_{ANOVA}<0.0001$, $p_{My\ vs.\ NoMy}=0.0009$. *Abca1*: $p_{ANOVA}=0.0007$, $p_{My\ vs.\ NoMy}<0.0019$ (a), $p_{ANOVA}=0.0087$, $p_{My\ vs.\ NoMy}=0.0211$ (b), $p_{ANOVA}<0.0001$, $p_{My\ vs.\ NoMy}<0.0001$ (c). *Abcg1*: $p_{ANOVA}<0.0001$, $p_{My\ vs.\ NoMy}=0.0001$, $p_{My\ vs.\ My+Zil}=0.0036$ (a), $p_{ANOVA}=0.0021$, $p_{My\ vs.\ NoMy}=0.0038$ (b), $p_{ANOVA}<0.0001$, $p_{My\ vs.\ NoMy}<0.0001$ (c). *Soat1*: $p_{ANOVA}=0.0030$, $p_{My\ vs.\ NoMy}=0.0081$ (a), $p_{ANOVA}=0.0018$, $p_{My\ vs.\ NoMy}=0.0361$, $p_{My\ vs.\ My+NPD1}=0.0075$, $p_{My\ vs.\ My+RvD4}=0.0006$ (b), $p_{ANOVA}=0.0013$, $p_{My\ vs.\ NoMy}=0.0047$, $p_{My\ vs.\ My+Lb4}=0.0122$ (c).
Data are represented as mean ± SD. Dots indicate technical replicates. Please see the list of abbreviations.

3. Enhancing n-3 PUFA Supply Fosters Inflammation Resolution and Remyelination

Our previous results demonstrated that PUFAs are released during the recovery stage after demyelination. In addition, we showed that the impairment of PUFA metabolism, i.e., of pro-resolving Alox15 and pro-inflammatory Alox5 and COX1/2, hampers inflammation resolution. Taken together, this led us to the question of whether the need for supply with PUFAs is increased after demyelination to resolve inflammation and enable tissue restoration in our mice model. To test if PUFAs benefit lesion recovery, we performed a genetic intervention, shifting the n-6/n-3 PUFA ratio towards n-3, and a dietary intervention, treating with n-3 PUFA DHA.

3.1. Low n-6/n-3 PUFA Ratio Supports Inflammation Resolution and Remyelination in *Fat-1* Mice

Since SPMs are mainly produced from n-3 PUFAs, we wanted to test if a decreased n-6 to n-3 PUFA ratio can support inflammation resolution. To change this ratio, we fed pregnant mice with three different diets with varying PUFA composition and examined the lesions of their 6-week-old offspring, which were kept on the same diet. At 14 dpi, the IBA1+ density was highest in the group that received a diet high in PUFAs with a high n-6/n-3 PUFA ratio (diet containing safflower oil) compared to the diet groups with either high saturated FAs (sFA) and monounsaturated FAs (MUFA, diet containing beef tallow) or with medium sFA and MUFA and low n-6/n-3 PUFA ratio (diet containing fish oil, **Fig. 11a,d**). Please see **Table 1** for the detailed diet composition.

Next, we wanted to assess whether this safflower diet's high n-6/n-3 PUFA ratio rather than other differences between the diets was the cause for the poorer outcome. Therefore, we used young *fat-1* transgenic mice, which express a desaturase converting n-6 to n-3 PUFAs (Kang et al., 2004), and challenged them with the n-6 PUFA-rich safflower diet for four weeks before injection. At 14 dpi, we measured a smaller IBA1$^+$ phagocytic density in *fat-1* mice, indicating a rescue from the n-6 enriched diet compared to WT mice (**Fig. 11b,d**). We determined the effects on remyelination and quantified a higher ratio of mature oligodendrocytes at 14 dpi while the OLIG2$^+$ density remained similar (**Fig. 11c,e,f**). Thus, *fat-1* mice, which convert n-6 to n-3 PUFAs, showed better lesion recovery than WT mice.

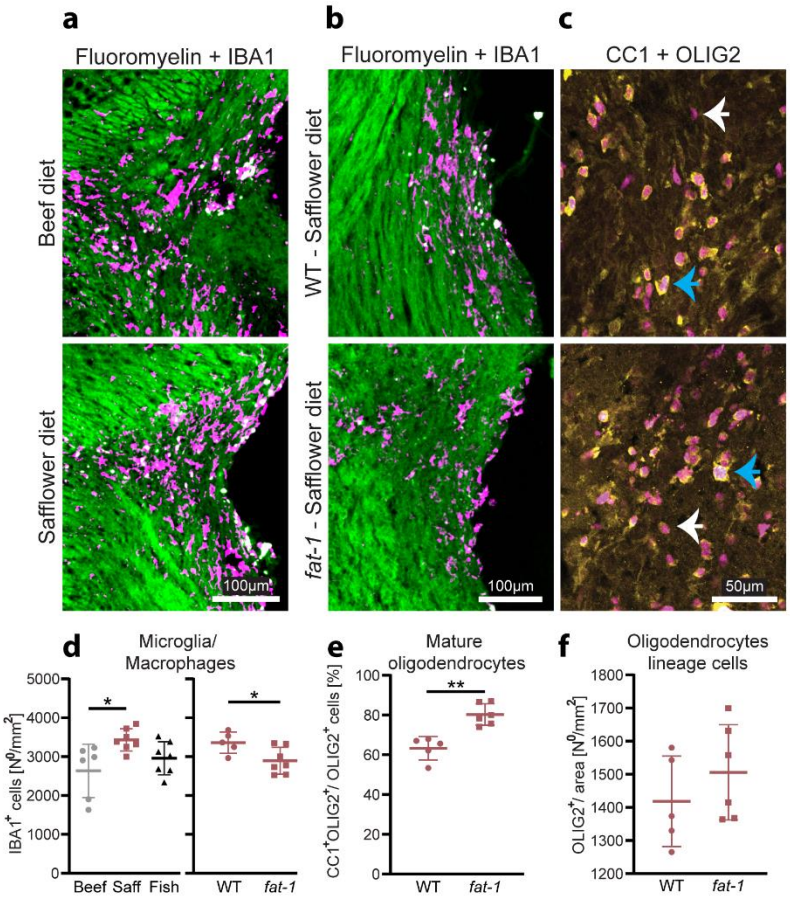

Fig. 11: Fat-1 mice convert n-6 to n-3 PUFAs and show better lesion recovery.
a, b Images of corpus callosum (CC) lesions showing fluoromyelin (green) and IBA1 (magenta) signal at 14 dpi. The left panel (a) shows lesions in C57BL/6J mice on beef tallow or safflower oil (saff) diet, and the right panel (b) in WT and *fat-1* transgenic mice on the saff diet.
d Analysis of IBA1$^+$ phagocytic cell density in WT mice on beef, saff, and fish diet (left side) as well as in WT and *fat-1* mice on saff diet (right side). One-way ANOVA with Tukey's multiple comparison test, n_{Beef}=6, n_{Saff}=n_{Fish}=7, p_{ANOVA}=0.0263, $p_{Saff\ vs.\ Beef}$=0.0219. Welch's t-test, n_{WT}=5, $n_{fat\text{-}1}$=7, p=0.0270.
c Images of CC lesions showing CC1 (yellow) and OLIG2 (magenta) signal at 14 dpi in WT and *fat-1* mice on saff diet. Mature oligodendrocytes (CC1$^+$OLIG2$^+$ cells) are marked with a blue arrow, and oligodendrocytes lineage cells (CC1$^-$OLIG2$^+$) with a white arrow.
e, f Ratio of mature oligodendrocytes in these mice. Welch's t-test, n_{WT}=5, $n_{fat\text{-}1}$=6, p=0.0010 (e). Analysis of OLIG2$^+$ oligodendrocyte lineage cell density in these mice. Welch's t-test, n_{WT}=5, $n_{fat\text{-}1}$=6, p=0.3304 (f).
Data are represented as mean ± SD. Dots indicate lesions. All images chosen are representative for the respective cohorts and were selected to present the group's mean.
Note: Horst Penkert performed injection of mice, processing, and analysis of data shown in a, b, and d. Vini Tiwari performed processing and analysis of data shown in c, e, and f.

3.2. Treatment with DHA-LPC Improves Inflammation Resolution and Remyelination in Old Mice

We then wanted to investigate if treatment with the n-3 PUFA DHA would also limit inflammation. Young animals have better regenerative capacities than old ones, but the reasons are not fully understood. To test the hypothesis that old mice might miss n-3 PUFAs and thus the beneficial effects of PUFAs for myelin repair, we chose to supplement 12-month-old mice with DHA.

Since free DHA is hardly transported over the blood-brain barrier (BBB), we used DHA covalently joined to lysophosphatidylcholine (LPC), which the lipid transporter Mfsd2a actively transports

into the CNS (Cater et al., 2021; Nguyen et al., 2014). We treated mice with daily intraperitoneal injections of either corn oil (control), DHA in corn oil, or DHA-LPC in corn oil for two weeks. We induced demyelination and analyzed the lesions. Early after demyelination (4 dpi), the volumes of demyelination (fluoromyelin-negative area) and inflammation (IBA1$^+$ area) were similar in all groups, suggesting a comparable extent of demyelination and inflammation (**Fig. 12a,b**).

Fig. 12 : Volumes of demyelination and inflammation in DHA-LPC-treated mice at the peak of inflammation.

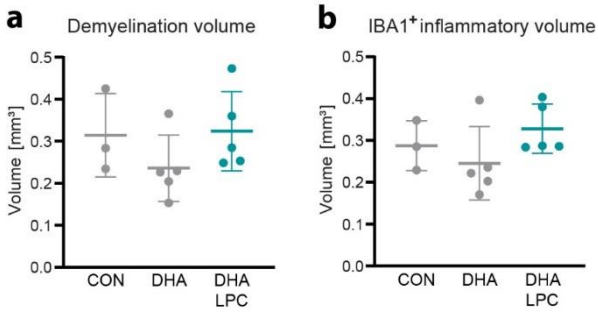

a-b Quantification of fluoromyelin-negative (a) and IBA1$^+$ (b) volume at 4 dpi in 12-month-old C57BL/6J mice i.p. injected with corn oil (CON), corn oil and DHA or DHA-LPC. One-way ANOVA with Tukey's multiple comparisons test, n_{CON}=3, n_{DHA}=$n_{DHA\text{-}LPC}$=5, p=0.2963 (a) and p=0.2387 (b).
Note: Vini Tiwari performed all steps.

At 14 dpi, these volumes shrunk most in the DHA-LPC treated group (**Fig. 13a-c**). Using reflection light microscopy, we also found that cholesterol crystal accumulation was lowest in this group (**Fig. 13d,e**). Further, we measured an increased share of mature oligodendrocytes in DHA and DHA-LPC treated mice, while the OLIG2$^+$ density in this area was similar between all groups (**Fig. 13f-h**). Hence, supplementation with brain-targeted DHA-LPC resulted in enhanced resolution of the IBA1$^+$ phagocytic infiltrate and a higher share of myelinating oligodendrocytes in old mice.

Fig. 13 (next page): Supplementation with BBB-traversable DHA-LPC supports inflammation resolution and lesion recovery.
a Images of corpus callosum (CC) lesions showing fluoromyelin (green) and IBA1 (magenta) signal at 14 dpi in 12-month-old C57BL/6J mice i.p. injected with corn oil (control, CON) or corn oil + DHA-LPC.
b,c Quantification of demyelination and IBA1$^+$ volume from mice treated with CON, DHA, or DHA-LPC. One-way ANOVA with Dunnett's multiple comparison test: n_{CON}=6, n_{DHA}=7, $n_{DHA\text{-}LPC}$=8, p_{ANOVA}=0.0293 $p_{DHA\text{-}LPC\ vs.\ CON}$=0.0183 (b) and n_{CON}=6, n_{DHA}=8, $n_{DHA\text{-}LPC}$=9, p_{ANOVA}=0.0216, $p_{DHA\text{-}LPC\ vs.\ CON}$=0.0121 (c).
d,e Images of CC lesions with DAPI-stained nuclei (cyan) and cholesterol crystals (red) at 14 dpi in 12-month-old C57BL/6J mice i.p. injected with CON or DHA-LPC (d). Analysis of integrated density of reflected light (correlating to the amount of crystals) in mice treated with CON, DHA, or DHA-LPC. One-way ANOVA with Dunnett's multiple comparison test n_{CON}=6, n_{DHA}=7, $n_{DHA\text{-}LPC}$=8, p_{ANOVA}=0.0160, $p_{DHA\text{-}LPC\ vs.\ CON}$=0.0120 (e).
f Images of CC lesions showing CC1 (yellow), OLIG2 (magenta), and also merge with fluoromyelin signal (green) at 14 dpi in 12-month-old C57BL/6J mice i.p. injected with CON or DHA. Mature oligodendrocytes (CC1$^+$OLIG2$^+$ cells) are marked with a blue arrow, and oligodendrocytes lineage cells (CC1$^-$OLIG2$^+$) with a white arrow.
g,h The ratio of mature oligodendrocytes in mice treated with CON, DHA, or DHA-LPC. One-way ANOVA with Dunnett's multiple comparison test, n_{CON}=6, n_{DHA}=7, $n_{DHA\text{-}LPC}$=8, p_{ANOVA}=0.0054, $p_{CON\ vs.\ DHA}$=0.0221, $p_{CON\ vs.\ DHA\text{-}LPC}$=0.0035 (g). The density of CC1$^-$OLIG2$^+$ oligodendrocyte lineage cells in mice treated with CON, DHA, or DHA-LPC. One-way ANOVA with Dunnett's multiple comparison test, n_{CON}=6, n_{DHA}=7, $n_{DHA\text{-}LPC}$=8, p=0.2089 (h).
Data are represented as mean ± SD. Dots indicate lesions. All images chosen are representative for the respective cohorts and were selected to present the group's mean. LPC: lysophosphatidylcholine. Please see the list of abbreviations.

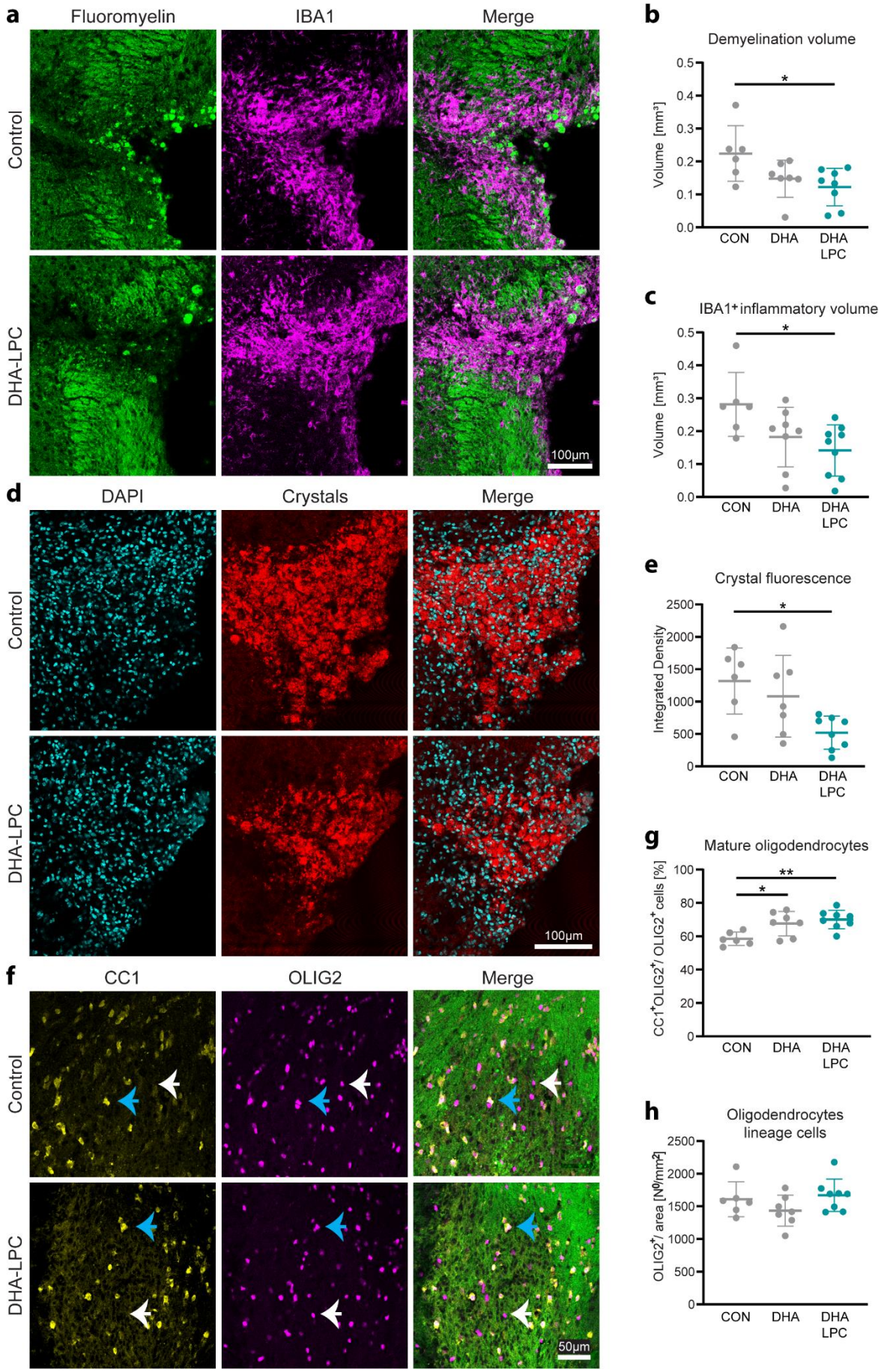
a
Fluoromyelin
IBA1
Merge
Control
DHA-LPC
100µm
b
Demyelination volume
Volume [mm³]
CON
DHA
DHA LPC
c
IBA1⁺ inflammatory volume
d
DAPI
Crystals
Merge
e
Crystal fluorescence
Integrated Density
f
CC1
OLIG2
50µm
g
Mature oligodendrocytes
CC1⁺OLIG2⁺/ OLIG2⁺ cells [%]
h
Oligodendrocytes lineage cells
OLIG2⁺/ area [N⁰/mm²]

3.3. DHA-LPC Treatment Does not Change Free DHA Levels in the CNS

To learn more about the effects of DHA-LPC treatment and LL-injection on FA composition in the CNS, we performed lipidomic analysis at 14 dpi of either not-injected, PBS-injected, LL-injected, or LL-injected + DHA-LPC treated mice. DHA-LPC i.p. treatment was performed as explained above. While the concentration of AA was similar between all groups, we observed in the LL-injected groups trends and statistically significant increases in EPA and DHA concentrations compared to the PBS-injected group (**Fig. 14a**). Also, the n-6/n-3 PUFA ratio was lowered in the LL-injected groups compared to PBS-injected mice. Regarding DHA-LPC treatment, the concentrations of PUFAs and their ratio were similar to only LL-injected mice (**Fig. 14b**). Thus, aside from changes in PIMs and oxylipins (**Fig. 14c**), we could not detect differences in free brain PUFA concentrations after DHA-LPC treatment.

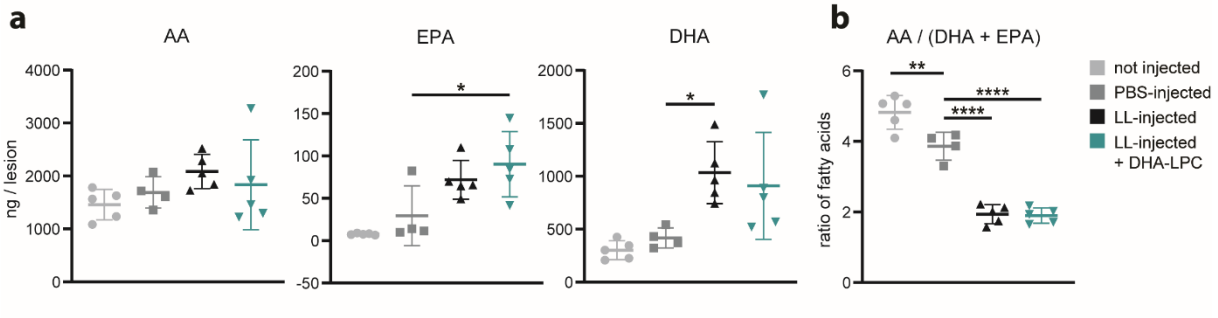

c

0 F_I 10	PBS-inj.	non-injected	F_I	LL-inj.	F_I	LL-inj. + DHA-LPC	F_I
AA	1.689.454 ± 295.743	1.459.609 ± 289.476	0,86	2.085.040 ± 323.969	1,23	1.835.016 ± 848.797	1,09
EPA	29.474 ± 35.314	7.790 ± 972	0,26	71.935 ± 22.773	2,44	90.308 ± 38.580	3,06
DHA	417.483 ± 95.345	301.474 ± 89.435	0,72	1.033.429 ± 292.090	2,48	908.586 ± 504.956	2,18
PGE_2	380 ± 84	104 ± 25	0,27	753 ± 228	1,98	578 ± 233	1,52
$PGF_{2\alpha}$	270 ± 39	240 ± 58	0,89	310 ± 79	1,15	236 ± 112	0,87
PGD_2	3.236 ± 407	2.025 ± 379	0,63	7.514 ± 1.389	2,32	9.626 ± 5.294,9	2,98
TXB_2	1.062 ± 165	581 ± 73	0,55	2.145 ± 286	2,02	3.248 ± 1.412	3,06
epi-t-LTB_4	11,3 ± 0,9	9,4 ± 1,1	0,83	42 ± 52	3,76	12 ± 6,1	1,09
t-LTB_4	9,3 ± 1,6	9,1 ± 1,3	0,98	31 ± 30	3,34	12 ± 4,5	1,27
5-HETE	152 ± 24	126 ± 13	0,83	445 ± 345	2,93	223 ± 111	1,46
5-HEPE	10,5 ± 6,6	5,5 ± 1,1	0,52	20 ± 9,0	1,94	27 ± 15	2,52
17-HDHA	81 ± 27	40 ± 15	0,49	330 ± 335	4,08	262 ± 300	3,23
15-HEPE	10 ± 6,1	5,3 ± 0,5	0,51	24 ± 8,4	2,27	44 ± 42	4,25
15-HETE	620 ± 180	365 ± 32	0,59	1.615 ± 716	2,61	1.490 ± 794	2,4
14-HDHA	51 ± 24	31 ± 4,0	0,61	288 ± 268	5,61	514 ± 884	10
12-HEPE	10 ± 5,6	5,0 ± 0,5	0,5	27 ± 15	2,71	37 ± 46	3,76
12-HETE	278 ± 150	238 ± 49	0,86	843 ± 465	3,03	751 ± 900	2,7
11-HEPE	7,0 ± 3,4	2,9 ± 0,3	0,41	33 ± 9,4	4,67	57 ± 31	8,05
11-HETE	749 ± 172	428 ± 54	0,57	2.038 ± 455	2,72	2.320 ± 1.219	3,1
18-HEPE	14 ± 9,5	6,6 ± 0,9	0,48	29 ± 12	2,06	29 ± 14	2,05
7-HDHA	34 ± 13	21 ± 1,5	0,62	79 ± 69	2,32	30 ± 12	0,89
4-HDHA	55 ± 15	42 ± 6,6	0,77	260 ± 192	4,75	90 ± 42	1,65

Fig. 14 Profiles of PUFA, oxylipin, and LM concentrations after injections and DHA-LPC treatment.
UPLC-MS/MS metabololipidomics of corpus callosum tissue from 12-month-old C57BL/6J mice with either cerebral PBS-injection (dark grey), LL-injection (black), LL-injection + DHA-LPC treatment (blue) or without cerebral injection (light grey). n_{not}=5, n_{PBS}=4, n_{LL}=5, $n_{LL+DHA-LPC}$=5.
a-b Concentrations of the PUFAs AA, EPA, and DHA and the ratio of AA/(DHA+EPA). Results of One-way ANOVA with Dunnett's multiple comparison test: AA: p=0.3065, EPA: p=0.0012, $p_{PBS\ vs.\ LL+DHA-LPC}$=0.0142, DHA: p=0.0046, $p_{PBS\ vs.\ LL}$=0.0235 and Ratio: p <0.0001, $p_{not\ vs.\ PBS}$=0.0026, $p_{PBS\ vs.\ LL}$<0.0001, $p_{PBS\ vs.\ LL+DHA-LPC}$<0.0001.

c Mean concentration (± SD) of PUFAs, LMs, and oxylipins in pg/lesion. F_I=fold increase of mean compared to the mean of PBS-injected mice.
Data are represented as mean ± SD. Dots indicate individual brains. Please see the list of abbreviations for more lipid mediators and oxylipins.
Note: Horst Penkert and Vini Tiwari performed injections of mice and vibratome dissection, Paul M. Jordan performed metabololipidomic analysis.

Discussion

1. Lipidome of Demyelinating Lesions: Surprises and Limitations

We used lipidomics and metabololipidomics to understand lipid metabolism during acute inflammation and its resolution after demyelination and found specific alterations of lipids and FAs. We measured an increase of lysophospholipids during acute inflammation (3 dpi), which might result from phospholipase A2 activity. This enzyme is activated upon inflammation and hydrolyses phospholipids into lysophospholipids and free FAs (Burke & Dennis, 2009; Sun et al., 2018). Indeed, at 7 dpi, the free PUFAs EPA and DHA were released (**Fig. 15**), while the n-6/n-3 PUFA ratio decreased in parallel.

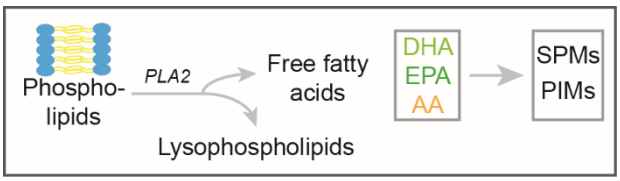

Fig. 15: Activity of phospholipase A2. Upon stimulus, phospholipase A2 (PLA2) hydrolyses phospholipids in lysophospholipids and free fatty acids. These can be oxidized into specialized pro-resolving (SPMs) and pro-inflammatory lipid mediators (PIMs).

Based on the hypothesis that PUFAs are released to facilitate the biosynthesis of SPMs and PIMs, we expected to find increased concentrations of PIMs during acute and of SPMs towards the end of inflammation. However, we could only detect an increase in oxylipins and COX-derived PIMs.

The late increase of PIMs came as a surprise as we expected their peak at 3 dpi and their decrease towards 14 dpi, as suggested by a study in which the authors determined AA metabolites in cuprizone-induced demyelination using ELISA-based assays (Palumbo et al., 2011). However, it is proposed that, e.g., the PIM PGD2 promotes via activation of G protein-coupled receptor Gpr44 PNS myelination (Trimarco et al., 2014). Thus, PIMs could also display features during tissue recovery. Moreover, the increase of Alox15-derived 12-HETE is noteworthy as this oxylipin was recently identified to positively regulate microglial phagocytosis of synaptosomes *in vitro* (Madore et al., 2020). However, more research is required to assess 12-HETE's involvement in our model.

Two explanations for why SPMs did not increase as expected might be their low concentrations at a picogram scale (Serhan, 2017) and their rapid turnover as bioactive LMs in CNS tissue. Therefore, their technical detection is hardly feasible and has been challenging and limiting for others, too (Colas et al., 2014; Mas et al., 2012).

It is crucial to remember that the LL used for injections acts not only as a membrane detergent inducing demyelination but is itself an active mediator in inflammation. Accordingly, LL was shown to possess pro-inflammatory properties by stimulating cytosolic PLA2-dependent AA release *in vitro* (Aiyar et al., 2007). Also, anti-inflammatory effects have been observed, e.g., in a

study where LL supported the anti-oxidative capacity of HDL (Schilcher et al., 2019). Our model does not control for the interference of LL in inflammatory processes and limits the clear distinction of effects due to demyelination from those in response to LL. Furthermore, the injection of LL (synonym: lysophosphatidylcholine, see **2.1.5**) can also contribute to the increased LPC concentrations, regardless of PLA2 activity.

In summary, we show that de- and remyelination are accompanied by altered lipid and FA composition. Increasing PUFA release and the change of its ratio indicates an ongoing switch from n-6 to n-3 derived lipids, even if we could not detect an SPM increase. To further assess and validate oxylipin, SPM, and PIM concentration kinetics after demyelination, we might need even more sensitive lipidomic methods. The next question will be how the altered lipid and FA composition affects cellular and molecular remyelination processes. To elaborate on this, e.g., *in vitro* assays, histological analyses, and lipidome and proteome analyses of single glial cell types would help to reach a better understanding.

2. Role of Lipoxygenases Alox15, Alox5 and Acetylsalicylic Acid

We used *Alox15* and *Alox5* KO mice and pharmacological inhibition by acetylsalicylic acid (ASA) and zileuton to test the hypothesis that the absence of SPMs would impair and of PIMs improve inflammation resolution. Before evaluating our findings, it is crucial to be aware that describing Alox15 or Alox5 as either anti- *or* pro-inflammatory is a simplification to a certain extent. In detail, Alox15 possesses pro-inflammatory characteristics, too, mainly through the synthesis of AA-derived oxylipins 15-HETE, 12-HETE, and 13-HODE (Ivanov et al., 2015). Furthermore, the synthesis of oxylipin and LM is complex and sometimes even requires both Alox isoforms and COX2 (Serhan & Petasis, 2011), which hampers a clear attribution of one LM family to only one enzyme.

Supporting our hypothesis, *Alox15* KO led to persisting inflammation, crystal accumulation, and poorer remyelination. Against our expectations, the KO of the rather pro-inflammatory *Alox5* also led to sustained inflammation during remyelination (14 dpi) but not during acute inflammation (4 dpi). One explanation is that certain Alox5 products, e.g., the SPMs lipoxins, display beneficial effects on inflammation resolution, as mentioned above concerning the complex LM synthesis. Noteworthy, a study in an experimental stroke model showed that following PPARγ-activation (see **2.1**), Alox5 can lead to lipoxin A4-dependent upregulation of CD35 on microglia and macrophages, which promotes phagocytosis activity and thus a resolving phenotype (Ballesteros et al., 2014). Another explanation is based on KOs' general nature, which might lead to unpredictable substrate diversions, putatively impairing lesion repair, or unknown reactions ending in pathogenic products. To learn more about Alox function and their role in remyelination, examining their expression and localization within a demyelinating lesion would be worthwhile, e.g., using *in situ* hybridization technologies. In fact, Alox5 and ALOX5 were identified using microarray hybridizations as a component of inflammatory lesions in microglia from MS and EAE samples (Whitney et al., 2001).

Altogether, our findings support our hypothesis and suggest that Alox5 and Alox15 activity are necessary for inflammation resolution during remyelination (14 dpi). Still, we need to remember a general limitation of our study: we determine remyelination and crystal formation indirectly, namely as fluoromyelin signal and as reflected light in lesions. We could improve the validity of these parameters by measuring the extent and density of myelinated axons, respectively, foam cells directly, e.g., using electron microscopy. This remark affects all experiments where we indicate improved remyelination and crystal formation.

2.1. Alox-Deficiency and Peroxisome Proliferator-activated Receptor Pathway

To the best of our knowledge, the effects of Alox deficiency on de- and remyelination have been investigated only in three EAE studies. Two of these studies explain their findings with effects on

the peroxisome proliferator-activated receptor (PPAR) pathway. These PPARs are lipid sensors and regulate metabolism and inflammation as nuclear receptors in response to several agonists, mainly FAs and lipids (Gross et al., 2017). Activation of PPARγ by, e.g., the AA-metabolites 15-HPETE and 15-HETE (Singh & Rao, 2019) increases insulin sensitivity, promotes lipid storage in adipose tissue, and has an anti-inflammatory effect by inducing NF-kB degradation (Gross et al., 2017; Hou et al., 2012). In contrast, PPARβ/δ activation induces lipid and FA catabolism (Luquet et al., 2003). Both receptors are investigated in remyelination research because of their lipid buffering and, thus, inflammation-resolving capacities. Indeed, studies showed that PPARγ agonists reduce EAE severity (Feinstein et al., 2002) and improve lesion repair in young obese mice in an LL-induced demyelinating model (Bosch-Queralt et al., 2021).

Regarding Alox deficiency, two of three EAE studies support our results, showing worsened disease progression in Alox12/15-deficient (Ivanov et al., 2015) and Alox5-deficient mice (Emerson & LeVine, 2004). They suggest that the absence of PPARγ activators, i.e., Alox downstream effectors such as 15-HETE, decreases its NF-kB-mediated anti-inflammatory effects and impedes clinical severity in EAE (Emerson & LeVine, 2004). However, a third study suggests that Alox12/15 inhibition by baicalein mitigates EAE clinical severity. The authors propose that PPARβ/δ activation suppresses microglial activation and neuroinflammation (Xu et al., 2013). This last result contradicts ours, showing that baicalein leads to a sustained inflammatory infiltrate during remyelination. These differing results might reflect differences in a) the demyelination model used, b) baicalein doses administered, and c) the mode of application. Still, their proposed mechanism is noteworthy and matches studies showing that PPARβ/δ agonists reduce EAE severity (Polak et al., 2005). However, they lack explanations of which agonist is supposed to cause PPARβ/δ activation.

2.2. Acetylsalicylic Acid has Anti-inflammatory and Pro-resolving Effects

Against our expectations, inhibition of COX1/2 and, therefore, of PIM synthesis did not lead to a decreased but to an increased IBA1$^+$ density. Although inhibition of COX2 stops PIM synthesis, the acetylation of COX2 increases the conversion rate of AA into 15-HPETE, which Alox5 can then metabolize to so-called aspirin-triggered lipoxins (Claria & Serhan, 1995; Dennis & Norris, 2015). This aspirin-triggered SPM synthesis is unique among NSAIDs and expanded acetylsalicylic acid's (ASA) imagined mode of action as an anti-inflammatory and pro-resolving drug (Serhan, 2017). However, we would still expect a decreased IBA1$^+$ infiltrate, even if this pathway occurred here.

For the time being, our finding remains without a definitive explanation and suggests that ASA affects inflammation in complex ways. Still, it would be necessary to assess lesions of ASA-treated mice at an earlier time point (4 dpi) to examine its impact during acute inflammation. It is possible

that inflammation is reduced initially but that the resolution program cannot start correctly due to missing PIM signaling.

In conclusion, our findings support the hypothesis that Alox deficiency can harm inflammation resolution and remyelination, strengthening the putatively beneficial role of oxylipins and LMs for these processes. To gain a deeper understanding of our results and to ultimately uncover the underlying mechanisms, it might be interesting to investigate the role of Alox in other MS models, such as EAE, as well as their involvement in lipid buffering in microglia and macrophages, e.g., as activators of PPAR pathways. Furthermore, it would be necessary to analyze the *Alox15* KO during acute inflammation (4 dpi) to assess its role early after demyelination.

3. Spotlight on the n-6/n-3 PUFA Ratio and Aging

Like other regenerative processes, remyelination becomes insufficient with age (Shields et al., 1999; Sim et al., 2002). The two pressing questions are what leads to this decline and whether it is reversible. We have observed a lower n-6/n-3 PUFA ratio in healthy, 12-month-old than in young mice. Moreover, in contrast to the decrease of this ratio after injury in young animals, the old ones do not show this kinetics. Thus, one could ask if this circumstance of a low n-6/n-3 ratio contributes to defective repair after demyelination. Whether this increased n-3 PUFA share results from attempts to enable inflammation resolution or from underlying chronic inflammation is unclear. Nevertheless, we showed that shifting this phenotype to n-3 PUFAs by supplementing with DHA-LPC fostered inflammation resolution and remyelination in old mice.

We further highlight the role of the n-6/n-3 PUFA ratio for remyelination in our *fat-1* mice experiment. These transgenic mice convert n-6 to n-3 PUFAs and showed better lesion recovery than WT mice after being fed a high n-6 PUFA diet. To further investigate the relevance of this finding for aging, one could assess if aged *fat-1* mice reach similar relative improvements. Only one other study investigated n-3 PUFAs for remyelination in *fat-1* mice (Siegert et al., 2017). Even though they showed increased brain levels of EPA, not DHA, they observed a trend towards improved remyelination, but their result lacked statistical significance. The deviation from our results might have to do with differences 1) in the used model of demyelination, 2) the PUFA diet composition, and 3) the quantification method.

Noteworthy, a high n-6/n-3 PUFA ratio might be associated with impaired remyelination: This is characteristic of the Western diet (WD), besides the fact that it is high in sugar, fat, and calories (Madore et al., 2020; Simopoulos, 2008). A recent study showed that WD-induced obesity is associated with impeded remyelination (Bosch-Queralt et al., 2021). Mechanistically, they reveal that WD leads to transforming growth factor-β (TGFβ) mediated downregulation of cholesterol efflux and impaired myelin debris clearance of microglia. Treatment with a TREM2-enhancing antibody, an activator of microglia, restored the clearance function even in old mice. Hence, in light of our findings, it would be worthwhile to investigate the influence of the n-6/n-3 PUFA ratio on TGFβ signaling. So far, this relationship has received very little attention and none regarding the CNS (Cicero et al., 2009; Prabhu & Gopalakrishnan, 2021; Xu et al., 2018).

Taken together, our results from metabololipidomics in young and old mice, *fat-1* mice and DHA-LPC supplementation experiments, favor the idea of increased demand for n-3 PUFAs during remyelination and suggest the relevance of the n-6/n-3 PUFA ratio for future research investigating remyelination failure in age.

4. Diets For Remyelination

4.1. Novel Delivery Form of DHA Improves Lesion Recovery

We show that DHA-LPC treatment supports inflammation resolution and remyelination. One remaining question is how the effect size of DHA vs. DHA-LPC differs. Our results suggest a better outcome for DHA-LPC. Nevertheless, DHA also shows an increased ratio of mature oligodendrocytes and missed significant statistics for the inflammatory volume narrowly ($p_{control\ vs.\ DHA}$ =0.0849). It has been proposed that free n-3 PUFAs can be transformed in the liver into n-3 PUFA-LPC and then become incorporated into membrane lipids in the CNS, but are more likely to diffuse as free FAs over the BBB to be then used for β-oxidation (Chen & Bazinet, 2015; Yalagala et al., 2019). Based on this mechanism, DHA is, in theory, suitable to elevate DHA levels in the brain, but DHA-LPC is the more specific and efficient agent, as also suggested by other studies (Sugasini et al., 2017; Sugasini et al., 2019; Yalagala et al., 2019). Therefore, it is conceivable that in previous studies DHA treatment did not reveal its full potential due to its limited bioavailability in the CNS. In other words, DHA-LPC may lead to more pronounced beneficial effects than free DHA. Hence, further pre-clinical studies are needed to evaluate the assumed DHA-LPC's advantages and to compare DHA and DHA-LPC outcomes. As a side note, one recent study demonstrated a potential climate-friendly manufacturing way of producing DHA-LPC from fishery by-products (Hosomi et al., 2019).

One might ask, why not supplement DHA with its essential precursor FA α-linolenic acid (ALA)? This question remains controversial and is especially discussed in infant formula research. To what extent DHA is obtained from ALA synthesis and dietary intake is unclear. On the one hand, it was shown that feeding human infants with diets containing only ALA, but not DHA, leads to lower cerebral accretion of DHA than in those breastfed (Cunnane et al., 2000). This finding could be a result of the slow conversion rate of DHA from ALA (Gómez Dumm & Brenner, 1975), the many desaturation and elongation steps required for conversion (Sprecher et al., 1995; Sun et al., 2018), or other ingredients of the breast milk. On the other hand, it is suggested that a diet high in ALA covers the brain's need for DHA if the liver functions properly (Rapoport & Igarashi, 2009). Because of this remaining uncertainty, the administration of DHA is considered to be the safer, more controlled, and more specific way of DHA supplementation (Guesnet & Alessandri, 2011; Sun et al., 2018).

Regarding timing and duration of treatment, we saw that administration for 14 days prior and 14 days after myelin damage is sufficient to observe beneficial effects. That suggests that efficient DHA supplementation in adults is possible. Our group showed that feeding mice different diets varying in PUFA composition from conception on does not change the lipid composition in the brain compared to adult mice fed with these diets (Fitzner et al., 2020). Furthermore, it is also

suggested that an even shorter treatment period of only 15 days changes n-3 PUFA composition significantly (Yalagala et al., 2019). That poses a question of clinical importance: Is supplementation only *after* myelin damage sufficient to reach a similar lesion recovery? For this purpose, examining the effects of shorter DHA-LPC treatment time spans and only after LL injection would be interesting.

4.2. Mechanistic Considerations

Our study does not suggest a specific mechanism that explains the beneficial effect of PUFAs on lesion recovery after myelin damage. Since myelin degradation and cholesterol clearance by microglia and macrophages are crucial for inflammation resolution (Stangel et al., 2017), these cells upregulate lipid buffering genes upon myelin loading (Bogie et al., 2012). We investigated the possible effects of LMs and pharmacological inhibitors on these processes *in vitro*. The downregulation of *Soat1*, esterifying free cholesterol into esters for storage, by the LMs NPD1, RvD4, and LB4 was puzzling as we expected its expression to be increased by the SPMs NPD1 and RvD4. The upregulation of *Abcg1*, a cholesterol efflux transporter, by zileuton agrees with the general understanding of Alox5: Inhibiting this pro-inflammatory enzyme supports inflammation resolution and repair. However, this observation contradicts our *in vivo* results from *Alox5* KO mice, showing a higher IBA1$^+$ microglia density at 14 dpi.

To summarize, the few observations made in these *in vitro* experiments are inconclusive, raise questions about other results, and contradict our hypothesis. Nevertheless, before refining our hypothesis, they must be repeated with biological replicates. In particular, we lacked consistent results in our experiment: first, zileuton only affected one target gene, and second, the missing downregulation of *Apoe* after myelin administration suggests technical mistakes. When repeating these cell culture experiments, one should remember that they are artificial and incapable of replicating complex biological processes *in vivo*. We do not recommend higher concentrations as we have used them in order to be comparable to physiological conditions and previous studies.

Still, in a similar experimental set-up using primary microglia cells, DHA and EPA have been shown to inhibit the release of pro-inflammatory cytokines and to improve myelin phagocytosis of microglia (Chen, S. et al., 2015). Furthermore, a recent neurodevelopment study suggested that DHA decreases and AA increases the microglial phagocytosis of synaptosomes *in vitro* (Madore et al., 2020). However, others have suggested that DHA supplementation decreases myelin phagocytosis *in vivo* and in microglia after spinal cord contusion injury (Yip et al., 2019). This surprising finding might result from several methodological differences compared to other studies: 1) low DHA concentrations (at 1-3 µM), 2) microglia cell cultures taken from old mice, 3) another model disease, and 4) different methods of quantification. Notwithstanding the PUFA-

microglia mechanism suggested, the last study also shows a better neurological outcome in rodents after spinal injury, supporting the beneficial role of PUFAs (Yip et al., 2019).

Altogether, our *in vitro* experiments could not yet provide evidence of a link between LMs and microglia. Still, repeating them and testing the PUFAs AA, EPA, and DHA themselves would be interesting. One could also extend the number of genes, e.g., with the stearoyl-CoA desaturase 1, since this enzyme has recently been shown to decrease the abundance of *Abca1* in myelin-loaded microglia and macrophages (Bogie et al., 2020). In addition, histological analysis of myelin-loaded microglia after treatment with PUFAs and LMs could be insightful. Also, using microglia from n-3 deficient mice could enhance the effect size and reveal potential mechanisms.

4.3. Why Does DHA-LPC Treatment Not Increase Free DHA Levels in the Brain?

Despite the benefits of DHA-LPC treatment for lesion recovery in the CNS, we could not measure differences in PUFA concentrations in the brain. Several explanations are conceivable: The one aligned with our central hypothesis is that DHA-LPC had crossed the BBB, was then rapidly metabolized in LM synthesis, and could, therefore, not be measured. However, there is no evidence for this hypothesis at this point. Future research could use labeled DHA-LPC molecules to track their further metabolization and contribution to brain DHA abundance. Nevertheless, it was shown that the lipid composition of the CNS can, in principle, be modified by diets (Fitzner et al., 2020). Thus, our treatment should be able to change the composition, too.

Another probable reason is of a more technical nature. We used a lipidomics technique with liquid chromatography for separation to measure *free* PUFAs. Therefore, PUFAs accumulated in intracellular lipid droplets or biomembranes as well as covalently bound PUFAs were not detected. Others, using shotgun lipidomics, detect *all* fatty acids and can thus show elevated DHA and EPA brain levels after treatment with DHA- and EPA-LPC (Sugasini et al., 2017; Yalagala et al., 2019). Furthermore, radiolabeled LPC and shotgun lipidomics have shown that the knockout of *Mfsd2a*, the gene for a DHA transporter at the BBB, decreases DHA brain levels compared to WT mice (Nguyen et al., 2014).

Another factor to remember is that DHA-LPC is quickly oxidized, which could have happened during preparation or i.p. administration despite all efforts. Oxidation might have led to the creation of other metabolites, which still had a beneficial effect but were not detectable as DHA-LPC anymore. Furthermore, the pharmacokinetic absorption and distribution of i.p. injected DHA-LPC in mice are yet unknown. Nevertheless, other scientists working with DHA supplementation have shown elevated cerebral DHA levels after oral gavage (Sugasini et al., 2017; Sugasini et al., 2019; Yalagala et al., 2019).

Altogether, the proof of concept for elevating PUFA brain levels by PUFA-LPC supplementation has already been developed and repeatedly shown by several scientists. Nevertheless, we could not replicate these findings here, presumably due to methodological differences. Therefore, further research is necessary to investigate the pharmacological uptake of supplemental DHA-LPC and its effects on brain FA composition. New insights into these aspects might be crucial to refine and develop hypotheses on the effects of PUFAs in remyelination.

4.4. Supplementation with n-3 PUFAs: Translation from Mice to Humans

Our study suggests beneficial effects of DHA supplementation on remyelination in mice. However, previous clinical studies led to mixed results with either beneficial, harmful, or no effects of DHA supplementation for remyelination. A recent Cochrane review of dietary interventions for several MS-related outcomes finds no difference between PUFA vs. MUFA, different PUFA types, or n-3 vs. n-6 PUFAs (Parks et al., 2020). Thus, no evidence-based recommendation for supplementation with PUFAs exists for MS patients. This might come as a surprise regarding the mounting evidence from animal studies suggesting the beneficial functions of PUFAs and SPMs.

The lack of translatability can be attributed to various factors, particularly the heterogeneous trial design encompassing differences in 1) inclusion criteria, 2) measured outcomes, 3) duration and timing of intervention, 4) dietary source and supplementation form, and 5) administered doses. Especially point 5) is crucial since several studies indicate dose-dependent effects of DHA in mice and show that too high doses can be harmful (Pan et al., 2011). These can induce toxic or inflammatory responses, which is vital to remember if one wants to study inflammatory processes (Sun et al., 2018). Also, if unphysiological high dosages are used in animals, results can often not be responsibly transferred to humans. Furthermore, other general issues with nutraceutical interventions impede successful translation: Dietary interventions control only one part of the diet, while other parts are not controlled for. Vice versa, it is then challenging to assign positive observations to one specific dietary component.

Altogether, caution is required when interpreting the results of animal and human studies dealing with n-3 PUFA supplementation. The remaining translational divergence and inability to reproduce findings require further research in wet labs and thoughtfully designed clinical studies.

Conclusion

This study was based on the hypothesis that n-3 PUFAs foster inflammation resolution and remyelination in the LL-induced model of demyelination. Using lipidomics, we identified a PUFA release and a dynamic n-6/n-3 PUFA ratio during remyelination. Based on different genetic, pharmacological, and dietary interventions, we established the involvement of PUFAs in inflammation resolution and remyelination *in vivo* (**Fig. 16**). However, we could not yet identify any underlying PUFA- or LM-mediated effects on microglia, which would explain our findings.

The novel contributions of our study to remyelination research are first, that we characterize the lipidome of demyelinating lesions, second that we elucidate the role of PUFA processing enzymes Alox5 and Alox15, third that we show improved lesion recovery with DHA treatment in LL-induced demyelination and last, that we use DHA covalently bound to LPC for this treatment. Our findings suggest a potential advantage of DHA-LPC over DHA in lesion recovery and indicate cautiously that prior nutraceutical approaches with *free* DHA might not reveal DHA's full potential due to the low cerebral bioavailability.

In conclusion, we show that n-3 PUFA DHA is beneficial after myelin damage and supports inflammation resolution and remyelination in our model. Our brain-targeted treatment with DHA-LPC represents a novel possibility for improving remyelination and merits future research to comprehensively understand its uptake and functions.

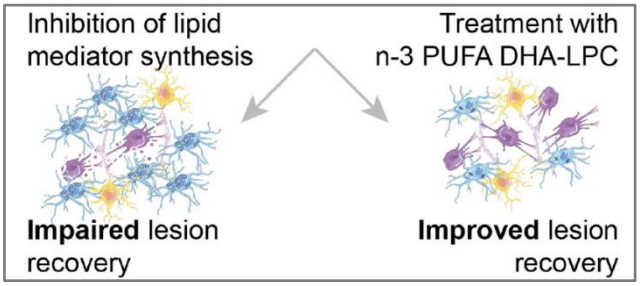

Fig. 16: Effects of PUFAs and LMs on lesion recovery after demyelination.
While inhibition of LM synthesis by *Alox* knockout experiments worsened lesion outcome, intraperitoneal treatment with n-3 PUFA DHA-LPC enhanced inflammation resolution and remyelination.

List of Figures

List of Tables

Copyright

Author contributions

As indicated in the legends of the figures, the following authors made contributions to this study:

- Horst Penkert performed injections, vibratome dissections, and sample processing of young and old mice and mice after different injections for UPLC-MSMS metabololipidomics analysis. Also, he performed injections, processing, and analysis of mice treated with acetylsalicylic acid and baicalein, as well as injections, processing, and analysis of microglia density of Alox5 and Alox15 KO mice and mice on beef tallow, safflower, or fish oil diet, respectively in fat-1 mice on safflower diet.
- Vini Tiwari performed injections, vibratome dissections, and sample processing of mice after different injections for UPLC-MSMS metabololipidomics analysis. Also, she performed processing and analysis of oligodendrocytes of fat-1 mice as well as injections, processing, and analysis of mice treated with DHA and DHA-LPC for 4dpi timepoint analysis.
- Mathias M. Gerl and Christian Klose from Lipotype GmbH, Dresden, analyzed the samples for shotgun lipidomics.
- Paul M. Jordan performed UPLC-MSMS metabololipidomics analysis of young and old mice and of mice after different injections.
- Lenka Vaculčiaková wrote the iPython code to calculate lesion volumes.

All other experiments, injections, vibratome dissections, sample processing, analysis, and data visualization were performed by Alix Bertrand.

Acknowledgements

I would like to thank everyone who supported me during this project. Special thanks go to…

… **Prof. Dr. Mikael Simons** for giving me the opportunity to join his lab, providing excellent research conditions, and introducing me to the world of remyelination. His scientific guidance and advice were pivotal for this project.

… **Dr. Horst Penkert** for his scientific and personal mentorship throughout my project. His endless efforts, instructions, explanations, ideas, and experience were invaluable to me. I am thankful for his commitment and passion, which helped me throughout this journey.

… all members of the Simons Lab: **Agata, Alkmini, Chaitali, Gary, Georg, Jana, Jianping, Lili, Ludo, Mar, Maria, Martina, Minou, Nico, Seiji, Shima, and Vini**. Thank you all for your (experi)mental support and expertise. I would not have succeeded in my project without your help. Special thanks go to Mar, who became a scientist role model for me. To Ludo, the scientist who knows all the details and shares them generously, and to Gary, my partner in crime.

… our collaborators **Stephan Breimann, Dr. Stephan Müller, Dr. Paul Jordan, Dr. Mathias Gerl, Dr. Christian Klose, Prof. Dr. Ilya Levental, Prof. Dr. Stefan Lichtenthaler, and Prof. Dr. Oliver Werz** for their expertise and input.

… **the animal facility team at DZNE** for their help, advice, and for taking good care of our mice.

… **Prof. Dr. Anja Horn-Bochtler** for her support and mentorship.

… **Dr. Frits Kamp** for advice and guidance on the handling of PUFAs.

… **the Friedrich Naumann Foundation for Freedom** for personal and financial support.

… **my family** for their endless love and encouragement.

… **my friends** for their companionship and understanding during the highs and lows of this journey.

References

Aiyar, N., Disa, J., Ao, Z., Ju, H., Nerurkar, S., Willette, R. N., Macphee, C. H., Johns, D. G., & Douglas, S. A. (2007). Lysophosphatidylcholine induces inflammatory activation of human coronary artery smooth muscle cells. *Molecular and Cellular Biochemistry*, *295*(1-2), 113–120. https://doi.org/10.1007/s11010-006-9280-x

AlAmmar, W. A., Albeesh, F. H., Ibrahim, L. M., Algindan, Y. Y., Yamani, L. Z., & Khattab, R. Y. (2019). Effect of omega-3 fatty acids and fish oil supplementation on multiple sclerosis: a systematic review. *Nutritional Neuroscience*, *24*(7), 569–579. https://doi.org/10.1080/1028415X.2019.1659560

Albert, M., Antel, J., Brück, W., & Stadelmann, C. (2007). Extensive Cortical Remyelination in Patients with Chronic Multiple Sclerosis. *Brain Pathology (Zurich, Switzerland)*, *17*(2), 129–138. https://doi.org/10.1111/j.1750-3639.2006.00043.x

Arita, M., Yoshida, M., Hong, S., Tjonahen, E., Glickman, J. N., Petasis, N. A., Blumberg, R. S., & Serhan, C. N. (2005). Resolvin E1, an endogenous lipid mediator derived from omega-3 eicosapentaenoic acid, protects against 2,4,6-trinitrobenzene sulfonic acid-induced colitis. *Proceedings of the National Academy of Sciences of the United States of America*, *102*(21), 7671–7676. https://doi.org/10.1073/pnas.0409271102

Baer, A. S., Syed, Y. A., Kang, S. U., Mitteregger, D., Vig, R., Ffrench-Constant, C., Franklin, R. J. M., Altmann, F., Lubec, G., & Kotter, M. R. (2009). Myelin-mediated inhibition of oligodendrocyte precursor differentiation can be overcome by pharmacological modulation of Fyn-RhoA and protein kinase C signalling. *Brain*, *132*(2), 465–481. https://doi.org/10.1093/brain/awn334

Ballesteros, I., Cuartero, M. I., Pradillo, J. M., La Parra, J. de, Pérez-Ruiz, A., Corbí, A., Ricote, M., Hamilton, J. A., Sobrado, M., Vivancos, J., Nombela, F., Lizasoain, I., & Moro, M. A. (2014). Rosiglitazone-induced CD36 up-regulation resolves inflammation by PPARγ and 5-LO-dependent pathways. *Journal of Leukocyte Biology*, *95*(4), 587–598. https://doi.org/10.1189/jlb.0613326

Bang, H. O., & Dyerberg, J. (1972). Plasma lipids and lipoproteins in Greenlandic west coast Eskimos. *Acta Medica Scandinavica*, *192*(1-2), 85–94. https://doi.org/10.1111/j.0954-6820.1972.tb04782.x

Bang, H. O., Dyerberg, J., & Sinclair, H. M. (1980). The composition of the Eskimo food in north western Greenland. *The American Journal of Clinical Nutrition*, *33*(12), 2657–2661. https://doi.org/10.1093/ajcn/33.12.2657

Barnett, M. H., & Prineas, J. W. (2004). Relapsing and remitting multiple sclerosis: Pathology of the newly forming lesion. *Annals of Neurology*, *55*(4), 458–468. https://doi.org/10.1002/ana.20016

Basak, S., Mallick, R., Banerjee, A., Pathak, S., & Duttaroy, A. K. (2021). Maternal Supply of Both Arachidonic and Docosahexaenoic Acids Is Required for Optimal Neurodevelopment. *Nutrients*, *13*(6), 2061. https://doi.org/10.3390/nu13062061

Baumann, N., & Pham-Dinh, D. (2001). Biology of oligodendrocyte and myelin in the mammalian central nervous system. *Physiological Reviews*, *81*(2), 871–927. https://doi.org/10.1152/physrev.2001.81.2.871

Baxter, A. G. (2007). The origin and application of experimental autoimmune encephalomyelitis. *Nature Reviews Immunology*, *7*(11), 904–912. https://doi.org/10.1038/nri2190

Bazinet, R. P., & Layé, S. (2014). Polyunsaturated fatty acids and their metabolites in brain function and disease. *Nature Reviews. Neuroscience*, *15*(12), 771–785. https://doi.org/10.1038/nrn3820

References

Belbasis, L., Bellou, V., Evangelou, E., Ioannidis, J. P. A., & Tzoulaki, I. (2015). Environmental risk factors and multiple sclerosis: an umbrella review of systematic reviews and meta-analyses. Advance online publication. https://doi.org/10.1016/S1474-4422(14)70267-4 (The Lancet Neurology, 14(3), 263-273).

Ben-Zvi, A., Lacoste, B., Kur, E., Andreone, B. J., Mayshar, Y., Yan, H., & Gu, C. (2014). Mfsd2a is critical for the formation and function of the blood–brain barrier. *Nature*, *509*(7501), 507–511. https://doi.org/10.1038/nature13324

Berghoff, S. A., Spieth, L., Sun, T., Hosang, L., Schlaphoff, L., Depp, C., Düking, T., Winchenbach, J., Neuber, J., Ewers, D., Scholz, P., van der Meer, F., Cantuti-Castelvetri, L., Sasmita, A. O., Meschkat, M., Ruhwedel, T., Möbius, W., Sankowski, R., Prinz, M., … Saher, G. (2021). Microglia facilitate repair of demyelinated lesions via post-squalene sterol synthesis. *Nature Neuroscience*, *24*(1), 47–60. https://doi.org/10.1038/s41593-020-00757-6

Beyea, M. M., Heslop, C. L., Sawyez, C. G., Edwards, J. Y., Markle, J. G., Hegele, R. A., & Huff, M. W. (2007). Selective up-regulation of LXR-regulated genes ABCA1, ABCG1, and APOE in macrophages through increased endogenous synthesis of 24(S),25-epoxycholesterol. *The Journal of Biological Chemistry*, *282*(8), 5207–5216. https://doi.org/10.1074/jbc.M611063200

Bhatt, D. L., Steg, P. G., Miller, M., Brinton, E. A., Jacobson, T. A., Ketchum, S. B., Doyle, R. T., Juliano, R. A., Jiao, L., Granowitz, C., Tardif, J.-C., & Ballantyne, C. M. (2019). Cardiovascular Risk Reduction with Icosapent Ethyl for Hypertriglyceridemia. *New England Journal of Medicine*, *380*(1), 11–22. https://doi.org/10.1056/NEJMoa1812792

Blakemore, W. F. (1972). Observations on oligodendrocyte degeneration, the resolution of status spongiosus and remyelination in cuprizone intoxication in mice. *Journal of Neurocytology*, *1*(4), 413–426. https://doi.org/10.1007/BF01102943

Blakemore, W. F., Eames, R. A., Smith, K. J., & Mcdonald, W. I. (1977). Remyelination in the spinal cord of the cat following intraspinal injections of lysolecithin. *Journal of the Neurological Sciences*, *33*(1-2), 31–43. https://doi.org/10.1016/0022-510X(77)90179-4

Blakemore, W. F., & Franklin, R. J. M. (2008). Remyelination in Experimental Models of Toxin-Induced Demyelination. In M. Rodriguez (Ed.), *Current Topics in Microbiology and Immunology: Vol. 318. Advances in multiple Sclerosis and Experimental Demyelinating Diseases* (pp. 193–212). Springer-Verlag Berlin Heidelberg. https://doi.org/10.1007/978-3-540-73677-6_8

Bogie, J. F. J., Timmermans, S., Huynh-Thu, V. A., Irrthum, A., Smeets, H. J. M., Gustafsson, J.-Å., Steffensen, K. R., Mulder, M., Stinissen, P., Hellings, N., & Hendriks, J. J. A. (2012). Myelin-Derived Lipids Modulate Macrophage Activity by Liver X Receptor Activation. *PloS One*, *7*(9), e44998. https://doi.org/10.1371/journal.pone.0044998

Bogie, J. F.J., Grajchen, E., Wouters, E., Corrales, A. G., Dierckx, T., Vanherle, S., Mailleux, J., Gervois, P., Wolfs, E., Dehairs, J., van Broeckhoven, J., Bowman, A. P., Lambrichts, I., Gustafsson, J.-Å., Remaley, A. T., Mulder, M., Swinnen, J. V., Haidar, M., Ellis, S. R., … Hendriks, J. J.A. (2020). Stearoyl-CoA desaturase-1 impairs the reparative properties of macrophages and microglia in the brain. *Journal of Experimental Medicine*, *217*(5), Article e20191660. https://doi.org/10.1084/jem.20191660

Bosch-Queralt, M., Cantuti-Castelvetri, L., Damkou, A., Schifferer, M., Schlepckow, K., Alexopoulos, I., Lütjohann, D., Klose, C., Vaculčiaková, L., Masuda, T., Prinz, M., Monroe, K. M., Di Paolo, G., Lewcock, J. W., Haass, C., & Simons, M. (2021). Diet-dependent regulation of TGFβ impairs reparative innate immune responses after demyelination. *Nature Metabolism*, *3*(2), 211–227. https://doi.org/10.1038/s42255-021-00341-7

References

Bray, M. A., Cunningham, F. M., Ford-Hutchinson, A. W., & Smith, M.J.H. (1981). Leukotriene B4: A mediator of vascular permeability. *British Journal of Pharmacology*, *72*(3), 483–486. https://doi.org/10.1111/j.1476-5381.1981.tb11000.x

Buckley, C. D., Gilroy, D. W., & Serhan, C. N. (2014). Proresolving lipid mediators and mechanisms in the resolution of acute inflammation. *Immunity*, *40*(3), 315–327. https://doi.org/10.1016/j.immuni.2014.02.009

Bunge, M. B., Bunge, R. P., & PAPPAS, G. D. (1962). Electron microscopic demonstration of connections between glia and myelin sheaths in the developing mammalian central nervous system. *The Journal of Cell Biology*, *12*, 448–453. https://doi.org/10.1083/jcb.12.2.448

Bunge, M. B., Bunge, R. P., & Ris, H. (1961). Ultrastructural study of remyelination in an experimental lesion in adult cat spinal cord. *The Journal of Biophysical and Biochemical Cytology*, *10*(1), 67–94.

Burke, J. E., & Dennis, E. A. (2009). Phospholipase A2 structure/function, mechanism, and signaling. *Journal of Lipid Research*, *50*, S237-S242. https://doi.org/10.1194/jlr.R800033-JLR200

Burr, M. L. (2001). Reflections on the Diet and Reinfarction Trial (DART). *European Heart Journal Supplements*, *3*, D75-D78. https://doi.org/10.1016/S1520-765X(01)90124-5

Burr, M. L., Fehily, A. M., Rogers, S., Welsby, E., King, S., & Sandham, S. (1989). Diet and reinfarction trial (DART): Design, recruitment, and compliance. *European Heart Journal*, *10*(6), 558–567. https://doi.org/10.1093/oxfordjournals.eurheartj.a059528

Calderon, F., & Kim, H.-Y. (2004). Docosahexaenoic acid promotes neurite growth in hippocampal neurons. *Journal of Neurochemistry*, *90*(4), 979–988. https://doi.org/10.1111/j.1471-4159.2004.02520.x

Cantuti-Castelvetri, L., Fitzner, D., Bosch-Queralt, M., Weil, M.-T., Su, M., Sen, P., Ruhwedel, T., Mitkovski, M., Trendelenburg, G., Lütjohann, D., Möbius, W., & Simons, M. (2018). Defective cholesterol clearance limits remyelination in the aged central nervous system. *Science (New York, N.Y.)*, *359*(6376), 684–688. https://doi.org/10.1126/science.aan4183

Cater, R. J., Chua, G. L., Erramilli, S. K., Keener, J. E., Choy, B. C., Tokarz, P., Chin, C. F., Quek, D. Q. Y., Kloss, B., Pepe, J. G., Parisi, G., Wong, B. H., Clarke, O. B., Marty, M. T., Kossiakoff, A. A., Khelashvili, G., Silver, D. L., & Mancia, F. (2021). Structural basis of omega-3 fatty acid transport across the blood–brain barrier. *Nature*, *595*(7866), 315–319. https://doi.org/10.1038/s41586-021-03650-9

Chen, C. T., & Bazinet, R. P. (2015). B-oxidation and rapid metabolism, but not uptake regulate brain eicosapentaenoic acid levels. *Prostaglandins, Leukotrienes, and Essential Fatty Acids*, *92*, 33–40. https://doi.org/10.1016/j.plefa.2014.05.007

Chen, C. T., Kitson, A. P., Hopperton, K. E., Domenichiello, A. F., Trépanier, M.-O., Lin, L. E., Ermini, L., Post, M., Thies, F., & Bazinet, R. P. (2015). Plasma non-esterified docosahexaenoic acid is the major pool supplying the brain. *Scientific Reports*, *5*, 15791. https://doi.org/10.1038/srep15791

Chen, S., Zhang, H., Pu, H., Wang, G., Li, W., Leak, R. K., Chen, J., Liou, A. K., & Hu, X. (2015). n-3 PUFA supplementation benefits microglial responses to myelin pathology. *Scientific Reports*, *4*(1). https://doi.org/10.1038/srep07458

References

Cicero, A., Ertek, S., & Borghi, C. (2009). Omega-3 Polyunsaturated Fatty Acids: Their Potential Role in Blood Pressure Prevention and Management. *Current Vascular Pharmacology*, *7*(3), 330–337. https://doi.org/10.2174/157016109788340659

Claria, J., & Serhan, C. N. (1995). Aspirin triggers previously undescribed bioactive eicosanoids by human endothelial cell-leukocyte interactions. *Proceedings of the National Academy of Sciences*, *92*(21), 9475–9479. https://doi.org/10.1073/pnas.92.21.9475

Colas, R. A., Shinohara, M., Dalli, J., Chiang, N., & Serhan, C. N. (2014). Identification and signature profiles for pro-resolving and inflammatory lipid mediators in human tissue. *American Journal of Physiology-Cell Physiology*, *307*(1), C39-C54. https://doi.org/10.1152/ajpcell.00024.2014

Cunha, M. I., Su, M., Cantuti-Castelvetri, L., Müller, S. A., Schifferer, M., Djannatian, M., Alexopoulos, I., van der Meer, F., Winkler, A., van Ham, T. J., Schmid, B., Lichtenthaler, S. F., Stadelmann, C., & Simons, M. (2020). Pro-inflammatory activation following demyelination is required for myelin clearance and oligodendrogenesis. *Journal of Experimental Medicine*, *217*(5), Article e20191390. https://doi.org/10.1084/jem.20191390

Cunnane, S. C., Francescutti, V., Brenna, J. T., & Crawford, M. A. (2000). Breast-fed infants achieve a higher rate of brain and whole body docosahexaenoate accumulation than formula-fed infants not consuming dietary docosahexaenoate. *Lipids*, *35*(1), 105–111. https://doi.org/10.1007/s11745-000-0501-6

Dennis, E. A., & Norris, P. C. (2015). Eicosanoid storm in infection and inflammation. *Nature Reviews. Immunology*, *15*(8), 511–523. https://doi.org/10.1038/nri3859

Derada Troletti, C., Enzmann, G., Chiurchiù, V., Kamermans, A., Tietz, S. M., Norris, P. C., Jahromi, N. H., Leuti, A., van der Pol, S. M.A., Schouten, M., Serhan, C. N., Vries, H. E. de, Engelhardt, B., & Kooij, G. (2021). Pro-resolving lipid mediator lipoxin A4 attenuates neuro-inflammation by modulating T cell responses and modifies the spinal cord lipidome. *Cell Reports*, *35*(9), 109201. https://doi.org/10.1016/j.celrep.2021.109201

Ebers, G. C., Sadovnick, A. D., & Risch, N. J. (1995). A genetic basis for familial aggregation in multiple sclerosis. *Nature*, *377*(6545), 150–151. https://doi.org/10.1038/377150a0

Eckhardt, C., Sbiera, I., Krebs, M., Sbiera, S., Spahn, M., Kneitz, B., Joniau, S., Fassnacht, M., Kübler, H., Weigand, I., & Kroiss, M. (2021). High expression of Sterol-O-Acyl transferase 1 (SOAT1), an enzyme involved in cholesterol metabolism, is associated with earlier biochemical recurrence in high risk prostate cancer. *Prostate Cancer and Prostatic Diseases.* Advance online publication. https://doi.org/10.1038/s41391-021-00431-3

Ejsing, C. S., Sampaio, J. L., Surendranath, V., Duchoslav, E., Ekroos, K., Klemm, R. W., Simons, K., & Shevchenko, A. (2009). Global analysis of the yeast lipidome by quantitative shotgun mass spectrometry. *Proceedings of the National Academy of Sciences*, *106*(7), 2136–2141. https://doi.org/10.1073/pnas.0811700106

Emerson, M. R., & LeVine, S. M. (2004). Experimental allergic encephalomyelitis is exacerbated in mice deficient for 12/15-lipoxygenase or 5-lipoxygenase. *Brain Research*, *1021*(1), 140–145. https://doi.org/10.1016/j.brainres.2004.06.045

European Medicines Agency (Ed.). (2021). *Human medicine European public assessment report (EPAR): Vazkepa*.

Faki, Y., & Er, A. (2021). Different Chemical Structures and Physiological/Pathological Roles of Cyclooxygenases. *Rambam Maimonides Medical Journal*, *12*(1). https://doi.org/10.5041/RMMJ.10426

References

Fazakerley, J. K., & Walker, R. (2003). Virus demyelination. *Journal of Neurovirology*, *9*(2), 148–164. https://doi.org/10.1080/13550280390194046

Feinstein, D. L., Galea, E., Gavrilyuk, V., Brosnan, C. F., Whitacre, C. C., Dumitrescu-Ozimek, L., Landreth, G. E., Pershadsingh, H. A., Weinberg, G., & Heneka, M. T. (2002). Peroxisome proliferator-activated receptor-? agonists prevent experimental autoimmune encephalomyelitis. *Annals of Neurology*, *51*(6), 694–702. https://doi.org/10.1002/ana.10206

Ferreira, S. H., Moncada, S., & Vane, J. R. (1971). Indomethacin and Aspirin abolish Prostaglandin Release from the Spleen. *Nature New Biology*, *231*(25), 237–239. https://doi.org/10.1038/newbio231237a0

Fields, R. D. (2008). White matter in learning, cognition and psychiatric disorders. *Trends in Neurosciences*, *31*(7), 361–370. https://doi.org/10.1016/j.tins.2008.04.001

Filippi, M., Bar-Or, A., Piehl, F., Preziosa, P., Solari, A., Vukusic, S., & Rocca, M. A. (2018). Multiple sclerosis. *Nature Reviews Disease Primers*, *4*(1). https://doi.org/10.1038/s41572-018-0041-4

Fitzgerald, K. C., Sand, I. K., Senders, A., Spain, R., Giesser, B., Sullivan, P., Baer, D. J., LaRocca, N., Zackowski, K., & Mowry, E. M. (2020). Conducting dietary intervention trials in people with multiple sclerosis: Lessons learned and a path forward. *Multiple Sclerosis and Related Disorders*, *37*, 101478. https://doi.org/10.1016/j.msard.2019.101478

Fitzner, D., Bader, J. M., Penkert, H., Bergner, C. G., Su, M., Weil, M.-T., Surma, M. A., Mann, M., Klose, C., & Simons, M. (2020). Cell-Type- and Brain-Region-Resolved Mouse Brain Lipidome. *Cell Reports*, *32*(11), 108132. https://doi.org/10.1016/j.celrep.2020.108132

Fliesler, A. J., & Anderson, R. E. (1983). Chemistry and metabolism of lipids in the vertebrate retina. *Progress in Lipid Research*, *22*(2), 79–131. https://doi.org/10.1016/0163-7827(83)90004-8

Franklin, R. J. M. (2002). Why does remyelination fail in multiple sclerosis? *Nature Reviews. Neuroscience*, *3*(9), 705–714. https://doi.org/10.1038/nrn917

Franklin, R. J. M., & Ffrench-Constant, C. (2017). Regenerating CNS myelin - from mechanisms to experimental medicines. *Nature Reviews. Neuroscience*, *18*(12), 753–769. https://doi.org/10.1038/nrn.2017.136

Friese, M. A., Schattling, B., & Fugger, L. (2014). Mechanisms of neurodegeneration and axonal dysfunction in multiple sclerosis. *Nature Reviews. Neurology*, *10*(4), 225–238. https://doi.org/10.1038/nrneurol.2014.37

Geren, B. B. (1954). The formation from the schwann cell surfaceof myelin in the peripheral nerves of chick embryos. *Experimental Cell Research*, *7*(2), 558–562. https://doi.org/10.1016/S0014-4827(54)80098-X

Ghasemi, A., & Zahediasl, S. (2012). Normality tests for statistical analysis: A guide for non-statisticians. *International Journal of Endocrinology and Metabolism*, *10*(2), 486–489. https://doi.org/10.5812/ijem.3505

Gilligan, M. M., Gartung, A., Sulciner, M. L., Norris, P. C., Sukhatme, V. P., Bielenberg, D. R., Huang, S., Kieran, M. W., Serhan, C. N., & Panigrahy, D. (2019). Aspirin-triggered proresolving mediators stimulate resolution in cancer. *Proceedings of the National Academy of Sciences*, *116*(13), 6292–6297. https://doi.org/10.1073/pnas.1804000116

Ginhoux, F., Greter, M., Leboeuf, M., Nandi, S., See, P., Gokhan, S., Mehler, M. F., Conway, S. J., Ng, L. G., Stanley, E. R., Samokhvalov, I. M., & Merad, M. (2010). Fate Mapping Analysis Reveals That Adult Microglia Derive from Primitive Macrophages. *Science*, *330*(6005), 841–845. https://doi.org/10.1126/science.1194637

Goldberg, J., Clarner, T., Beyer, C., & Kipp, M. (2015). Anatomical Distribution of Cuprizone-Induced Lesions in C57BL6 Mice. *Journal of Molecular Neuroscience : MN*, *57*(2), 166–175. https://doi.org/10.1007/s12031-015-0595-5

Goldschmidt, T., Antel, J., Konig, F. B., Bruck, W., & Kuhlmann, T. (2009). Remyelination capacity of the MS brain decreases with disease chronicity. *Neurology*, *72*(22), 1914–1921. https://doi.org/10.1212/WNL.0b013e3181a8260a

Gómez Dumm, I. N. T. de, & Brenner, R. R. (1975). Oxidative desaturation of α-linolenic, linoleic, and stearic acids by human liver microsomes. *Lipids*, *10*(6), 315–317. https://doi.org/10.1007/BF02532451

Gomez Perdiguero, E., Klapproth, K., Schulz, C., Busch, K., Azzoni, E., Crozet, L., Garner, H., Trouillet, C., Bruijn, M. F. de, Geissmann, F., & Rodewald, H.-R. (2015). Tissue-resident macrophages originate from yolk-sac-derived erythro-myeloid progenitors. *Nature*, *518*(7540), 547–551. https://doi.org/10.1038/nature13989

Gressner. (2019). *Lexikon der Medizinischen Laboratoriumsdiagnostik*. Springer Berlin Heidelberg.

Griffiths, I., Klugmann, M., Anderson, T., Yool, D., Thomson, C., Schwab, M. H., Schneider, A., Zimmermann, F., McCulloch, M., Nadon, N., & Nave, K. A. (1998). Axonal swellings and degeneration in mice lacking the major proteolipid of myelin. *Science (New York, N.Y.)*, *280*(5369), 1610–1613. https://doi.org/10.1126/science.280.5369.1610

Gross, B., Pawlak, M., Lefebvre, P., & Staels, B. (2017). PPARs in obesity-induced T2DM, dyslipidaemia and NAFLD. *Nature Reviews Endocrinology*, *13*(1), 36–49. https://doi.org/10.1038/nrendo.2016.135

Guan, C., Niu, Y., Chen, S.-C., Kang, Y., Wu, J.-X., Nishi, K., Chang, C. C. Y., Chang, T.-Y., Luo, T., & Chen, L. (2020). Structural insights into the inhibition mechanism of human sterol O-acyltransferase 1 by a competitive inhibitor. *Nature Communications*, *11*(1), 2478. https://doi.org/10.1038/s41467-020-16288-4

Guemez-Gamboa, A., Nguyen, L. N., Yang, H., Zaki, M. S., Kara, M., Ben-Omran, T., Akizu, N., Rosti, R. O., Rosti, B., Scott, E., Schroth, J., Copeland, B., Vaux, K. K., Cazenave-Gassiot, A., Quek, D. Q. Y., Wong, B. H., Tan, B. C., Wenk, M. R., Gunel, M., … Gleeson, J. G. (2015). Inactivating mutations in MFSD2A, required for omega-3 fatty acid transport in brain, cause a lethal microcephaly syndrome. *Nature Genetics*, *47*(7), 809–813. https://doi.org/10.1038/ng.3311

Guesnet, P., & Alessandri, J.-M. (2011). Docosahexaenoic acid (DHA) and the developing central nervous system (CNS) – Implications for dietary recommendations. *Biochimie*, *93*(1), 7–12. https://doi.org/10.1016/j.biochi.2010.05.005

Haeggström, J. Z., & Funk, C. D. (2011). Lipoxygenase and leukotriene pathways: Biochemistry, biology, and roles in disease. *Chemical Reviews*, *111*(10), 5866–5898. https://doi.org/10.1021/cr200246d

Hajeyah, A. A., Griffiths, W. J., Wang, Y., Finch, A. J., & O'Donnell, V. B. (2020). The Biosynthesis of Enzymatically Oxidized Lipids. *Frontiers in Endocrinology*, *11*, 591819. https://doi.org/10.3389/fendo.2020.591819

Hall, S. M. (1972). The effect of injections of lysophosphatidyl choline into white matter of the adult mouse spinal cord. *Journal of Cell Science*, *10*(2), 535–546.

Hall, S. M., & Gregson, N. A. (1971). The in vivo and ultrastructural effects of injection of lysophosphatidyl choline into myelinated peripheral nerve fibres of the adult mouse. *Journal of Cell Science*, *9*(3), 769–789.

Harel, T., Quek, D. Q. Y., Wong, B. H., Cazenave-Gassiot, A., Wenk, M. R., Fan, H., Berger, I., Shmueli, D., Shaag, A., Silver, D. L., Elpeleg, O., & Edvardson, S. (2018). Homozygous mutation in MFSD2A, encoding a lysolipid transporter for

docosahexanoic acid, is associated with microcephaly and hypomyelination. *Neurogenetics*, *19*(4), 227–235. https://doi.org/10.1007/s10048-018-0556-6

Hedström, A. K., Olsson, T., Kockum, I., Hillert, J., & Alfredsson, L. (2020). Low sun exposure increases multiple sclerosis risk both directly and indirectly. *Journal of Neurology*, *267*(4), 1045–1052. https://doi.org/10.1007/s00415-019-09677-3

Hemmer, B., Kerschensteiner, M., & Korn, T. (2015). Role of the innate and adaptive immune responses in the course of multiple sclerosis. *The Lancet Neurology*, *14*(4), 406–419. https://doi.org/10.1016/S1474-4422(14)70305-9

Hemmer B. et al. (2021). Diagnose und Therapie der Multiplen Sklerose, Neuromyelitis-optica-Spektrum-Erkrankungen und MOG-IgG-assoziierten Erkrankungen, S2k-Leitlinie, 2021, in: Deutsche Gesellschaft für Neurologie (Hrsg.), Leitlinien für Diagnostik und Therapie in der Neurologie. Online: www.dgn.org/leitlinien (abgerufen am 09.08.2021).

Henderson, A. P. D., Barnett, M. H., Parratt, J. D. E., & Prineas, J. W. (2009). Multiple sclerosis: Distribution of inflammatory cells in newly forming lesions. *Annals of Neurology*, *66*(6), 739–753. https://doi.org/10.1002/ana.21800

Heneka, M. T., Carson, M. J., Khoury, J. E., Landreth, G. E., Brosseron, F., Feinstein, D. L., Jacobs, A. H., Wyss-Coray, T., Vitorica, J., Ransohoff, R. M., Herrup, K., Frautschy, S. A., Finsen, B., Brown, G. C., Verkhratsky, A., Yamanaka, K., Koistinaho, J., Latz, E., Halle, A., … Kummer, M. P. (2015). Neuroinflammation in Alzheimer's disease. *The Lancet Neurology*, *14*(4), 388–405. https://doi.org/10.1016/S1474-4422(15)70016-5

Herz, J., Filiano, A. J., Smith, A., Yogev, N., & Kipnis, J. (2017). Myeloid Cells in the Central Nervous System. *Immunity*, *46*(6), 943–956. https://doi.org/10.1016/j.immuni.2017.06.007

Herzog, R., Schuhmann, K., Schwudke, D., Sampaio, J. L., Bornstein, S. R., Schroeder, M., & Shevchenko, A. (2012). LipidXplorer: A Software for Consensual Cross-Platform Lipidomics. *PloS One*, *7*(1), e29851. https://doi.org/10.1371/journal.pone.0029851

Herzog, R., Schwudke, D., Schuhmann, K., Sampaio, J. L., Bornstein, S. R., Schroeder, M., & Shevchenko, A. (2011). A novel informatics concept for high-throughput shotgun lipidomics based on the molecular fragmentation query language. *Genome Biology*, *12*(1), R8. https://doi.org/10.1186/gb-2011-12-1-r8

Hjorth, E., Zhu, M., Toro, V. C., Vedin, I., Palmblad, J., Cederholm, T., Freund-Levi, Y., Faxen-Irving, G., Wahlund, L.-O., Basun, H., Eriksdotter, M., & Schultzberg, M. (2013). Omega-3 fatty acids enhance phagocytosis of Alzheimer's disease-related amyloid-β42 by human microglia and decrease inflammatory markers. *Journal of Alzheimer's Disease : JAD*, *35*(4), 697–713. https://doi.org/10.3233/JAD-130131

Hoffmann, F. (1900). Acetyl Salicylic Acid(U.S. Patent No. 644,077, United States Patent Office).

Hosomi, R., Fukunaga, K., Nagao, T., Shiba, S., Miyauchi, K., Yoshida, M., & Takahashi, K. (2019). Effect of Dietary Oil Rich in Docosahexaenoic Acid-Bound Lysophosphatidylcholine Prepared from Fishery By-Products on Lipid and Fatty Acid Composition in Rat Liver and Brain. *Journal of Oleo Science*, *68*(8), 781–792. https://doi.org/10.5650/jos.ess19103

Hou, Y., Moreau, F., & Chadee, K. (2012). PPARγ is an E3 ligase that induces the degradation of NFκB/p65. *Nature Communications*, *3*(1). https://doi.org/10.1038/ncomms2270

Huxley, A. F., & Stämpeli, R. (1949). Evidence for saltatory conduction in peripheral myelinated nerve fibres.

References

Israel, E. (1996). Effect of Treatment With Zileuton, a 5-Lipoxygenase Inhibitor, in Patients With Asthma. *JAMA*, *275*(12), 931. https://doi.org/10.1001/jama.1996.03530360041036

Ivanov, I., Kuhn, H., & Heydeck, D. (2015). Structural and functional biology of arachidonic acid 15-lipoxygenase-1 (ALOX15). *Gene*, *573*(1), 1–32. https://doi.org/10.1016/j.gene.2015.07.073

Jeffery, N. D., & Blakemore, W. F. (1995). Remyelination of mouse spinal cord axons demyelinated by local injection of lysolecithin. *Journal of Neurocytology*, *24*(10). https://doi.org/10.1007/BF01191213

Kang, J. X., Wang, J., Wu, L., & Kang, Z. B. (2004). Fat-1 mice convert n-6 to n-3 fatty acids. *Nature*, *427*(6974), 504. https://doi.org/10.1038/427504a

Kim, H. Y., Akbar, M., Lau, A., & Edsall, L. (2000). Inhibition of neuronal apoptosis by docosahexaenoic acid (22:6n-3). Role of phosphatidylserine in antiapoptotic effect. *The Journal of Biological Chemistry*, *275*(45), 35215–35223. https://doi.org/10.1074/jbc.M004446200

Kooij, G., Troletti, C. D., Leuti, A., Norris, P. C., Riley, I., Albanese, M., Ruggieri, S., Libreros, S., van der Pol, S. M.A., van het Hof, B., Schell, Y., Guerrera, G., Buttari, F., Mercuri, N. B., Centonze, D., Gasperini, C., Battistini, L., Vries, H. E. de, Serhan, C. N., & Chiurchiù, V. (2020). Specialized pro-resolving lipid mediators are differentially altered in peripheral blood of patients with multiple sclerosis and attenuate monocyte and blood-brain barrier dysfunction. *Haematologica*, *105*(8), 2056–2070. https://doi.org/10.3324/haematol.2019.219519

Kotter, M. R. (2006). Myelin Impairs CNS Remyelination by Inhibiting Oligodendrocyte Precursor Cell Differentiation. *Journal of Neuroscience*, *26*(1), 328–332. https://doi.org/10.1523/JNEUROSCI.2615-05.2006

Kuhlmann, T., Miron, V., Cuo, Q., Wegner, C., Antel, J., & Bruck, W. (2008). Differentiation block of oligodendroglial progenitor cells as a cause for remyelination failure in chronic multiple sclerosis. *Brain*, *131*(7), 1749–1758. https://doi.org/10.1093/brain/awn096

Kuhn, H., Banthiya, S., & van Leyen, K. (2015). Mammalian lipoxygenases and their biological relevance. *Biochimica Et Biophysica Acta*, *1851*(4), 308–330. https://doi.org/10.1016/j.bbalip.2014.10.002

Kuhn, M. (2008). Building Predictive Models in R Using the caret Package. *Journal of Statistical Software*, *28*(1), 1–26. https://doi.org/10.18637/jss.v028.i05

Lagarde, M., Bernoud, N., Brossard, N., Lemaitre-Delaunay, D., Thiès, F., Croset, M., & Lecerf, J. (2001). Lysophosphatidylcholine as a Preferred Carrier Form of Docosahexaenoic Acid to the Brain. *Journal of Molecular Neuroscience*, *16*(2-3), 201–204. https://doi.org/10.1385/JMN:16:2-3:201

Lämmermann, T., Afonso, P. V., Angermann, B. R., Wang, J. M., Kastenmüller, W., Parent, C. A., & Germain, R. N. (2013). Neutrophil swarms require LTB4 and integrins at sites of cell death in vivo. *Nature*, *498*(7454), 371–375. https://doi.org/10.1038/nature12175

Lassmann, H., Brück, W., & Lucchinetti, C. F. (2007). The Immunopathology of Multiple Sclerosis: An Overview. *Brain Pathology (Zurich, Switzerland)*, *17*(2), 210–218. https://doi.org/10.1111/j.1750-3639.2007.00064.x

Lassmann, H., van Horssen, J., & Mahad, D. (2012). Progressive multiple sclerosis: pathology and pathogenesis. *Nature Clinical Practice Neurology*, *8*(11), 647–656. https://doi.org/10.1038/nrneurol.2012.168

Lauritzen, L., Brambilla, P., Mazzocchi, A., Harsløf, L., Ciappolino, V., & Agostoni, C. (2016). DHA Effects in Brain Development and Function. *Nutrients*, *8*(1), 6. https://doi.org/10.3390/nu8010006

Lazarus, M., Yoshida, K., Coppari, R., Bass, C. E., Mochizuki, T., Lowell, B. B., & Saper, C. B. (2007). EP3 prostaglandin receptors in the median preoptic nucleus are critical for fever responses. *Nature Neuroscience*, *10*(9), 1131–1133. https://doi.org/10.1038/nn1949

Lee, Y., Morrison, B. M., Li, Y., Lengacher, S., Farah, M. H., Hoffman, P. N., Liu, Y., Tsingalia, A., Jin, L., Zhang, P.-W., Pellerin, L., Magistretti, P. J., & Rothstein, J. D. (2012). Oligodendroglia metabolically support axons and contribute to neurodegeneration. *Nature*, *487*(7408), 443–448. https://doi.org/10.1038/nature11314

Lévesque, H., & Lafont, O. (2000). L'aspirine à travers les siècles: Rappel historique. *La Revue De Médecine Interne*, *21*, S8-S17. https://doi.org/10.1016/S0248-8663(00)88720-2

Li, Q., & Barres, B. A. (2018). Microglia and macrophages in brain homeostasis and disease. *Nature Reviews. Immunology*, *18*(4), 225–242. https://doi.org/10.1038/nri.2017.125

Liebisch, G., Binder, M., Schifferer, R., Langmann, T., Schulz, B., & Schmitz, G. (2006). High throughput quantification of cholesterol and cholesteryl ester by electrospray ionization tandem mass spectrometry (ESI-MS/MS). *Biochimica Et Biophysica Acta (BBA) - Molecular and Cell Biology of Lipids*, *1761*(1), 121–128. https://doi.org/10.1016/j.bbalip.2005.12.007

Liu, J. J., Green, P., John Mann, J., Rapoport, S. I., & Sublette, M. E. (2015). Pathways of polyunsaturated fatty acid utilization: Implications for brain function in neuropsychiatric health and disease. *Brain Research*, *1597*, 220–246. https://doi.org/10.1016/j.brainres.2014.11.059

Lloyd, A. F., & Miron, V. E. (2019). The pro-remyelination properties of microglia in the central nervous system. *Nature Reviews. Neurology*, *15*(8), 447–458. https://doi.org/10.1038/s41582-019-0184-2

Lucchinetti, C., Brck, W., Parisi, J., Scheithauer, B., Rodriguez, M., & Lassmann, H. (2000). Heterogeneity of multiple sclerosis lesions: Implications for the pathogenesis of demyelination. *Annals of Neurology*, *47*(6), 707–717. https://doi.org/10.1002/1531-8249(200006)47:6<707::AID-ANA3>3.0.CO;2-Q

Lukiw, W. J., Cui, J.-G., Marcheselli, V. L., Bodker, M., Botkjaer, A., Gotlinger, K., Serhan, C. N., & Bazan, N. G. (2005). A role for docosahexaenoic acid-derived neuroprotectin D1 in neural cell survival and Alzheimer disease. *The Journal of Clinical Investigation*, *115*(10), 2774–2783. https://doi.org/10.1172/JCI25420

Luquet, S., Lopez-Soriano, J., Holst, D., Fredenrich, A., Melki, J., Rassoulzadegan, M., & Grimaldi, P. A. (2003). Peroxisome proliferator-activated receptor δ controls muscle development and oxydative capability. *The FASEB Journal*, *17*(15), 2299–2301. https://doi.org/10.1096/fj.03-0269fje

Madore, C., Leyrolle, Q., Morel, L., Rossitto, M., Greenhalgh, A. D., Delpech, J. C., Martinat, M., Bosch-Bouju, C., Bourel, J., Rani, B., Lacabanne, C., Thomazeau, A., Hopperton, K. E., Beccari, S., Sere, A., Aubert, A., Smedt-Peyrusse, V. de, Lecours, C., Bisht, K., . . . Layé, S. (2020). Essential omega-3 fatty acids tune microglial phagocytosis of synaptic elements in the mouse developing brain. *Nature Communications*, *11*(1). https://doi.org/10.1038/s41467-020-19861-z

Maguire, E. M., Pearce, S. W.A., & Xiao, Q. (2019). Foam cell formation: A new target for fighting atherosclerosis and cardiovascular disease. *Vascular Pharmacology*, *112*, 54–71. https://doi.org/10.1016/j.vph.2018.08.002

Mas, E., Croft, K. D., Zahra, P., Barden, A., & Mori, T. A. (2012). Resolvins D1, D2, and Other Mediators of Self-Limited Resolution of Inflammation in Human Blood following n-3 Fatty Acid Supplementation. *Clinical Chemistry*, *58*(10), 1476–1484. https://doi.org/10.1373/clinchem.2012.190199

Mashima, R., & Okuyama, T. (2015). The role of lipoxygenases in pathophysiology; new insights and future perspectives. *Redox Biology*, *6*, 297–310. https://doi.org/10.1016/j.redox.2015.08.006

Matsushima, G. K., & Morell, P. (2001). The neurotoxicant, cuprizone, as a model to study demyelination and remyelination in the central nervous system. *Brain Pathology (Zurich, Switzerland)*, *11*(1), 107–116. https://doi.org/10.1111/j.1750-3639.2001.tb00385.x

McNamara, R. K., & Carlson, S. E. (2006). Role of omega-3 fatty acids in brain development and function: Potential implications for the pathogenesis and prevention of psychopathology. *Prostaglandins, Leukotrienes and Essential Fatty Acids*, *75*(4-5), 329–349. https://doi.org/10.1016/j.plefa.2006.07.010

Mi, S., Miller, R. H., Lee, X., Scott, M. L., Shulag-Morskaya, S., Shao, Z., Chang, J., Thill, G., Levesque, M., Zhang, M., Hession, C., Sah, D., Trapp, B., He, Z., Jung, V., McCoy, J. M., & Pepinsky, R. B. (2005). LINGO-1 negatively regulates myelination by oligodendrocytes. *Nature Neuroscience*, *8*(6), 745–751. https://doi.org/10.1038/nn1460

Miron, V. E. (2017). Microglia-driven regulation of oligodendrocyte lineage cells, myelination, and remyelination. *Journal of Leukocyte Biology*, *101*(5), 1103–1108. https://doi.org/10.1189/jlb.3RI1116-494R

Miron, V. E., Boyd, A., Zhao, J.-W., Yuen, T. J., Ruckh, J. M., Shadrach, J. L., van Wijngaarden, P., Wagers, A. J., Williams, A., Franklin, R. J. M., & Ffrench-Constant, C. (2013). M2 microglia and macrophages drive oligodendrocyte differentiation during CNS remyelination. *Nature Neuroscience*, *16*(9), 1211–1218. https://doi.org/10.1038/nn.3469

Mishra, P., Pandey, C. M., Singh, U., Gupta, A., Sahu, C., & Keshri, A. (2019). Descriptive statistics and normality tests for statistical data. *Annals of Cardiac Anaesthesia*, *22*(1), 67–72. https://doi.org/10.4103/aca.ACA_157_18

Monasterio-Schrader, P. de, Jahn, O., Tenzer, S., Wichert, S. P., Patzig, J., & Werner, H. B. (2012). Systematic approaches to central nervous system myelin. *Cellular and Molecular Life Sciences : CMLS*, *69*(17). https://doi.org/10.1007/s00018-012-0958-9

Morimoto, K., Shirata, N., Taketomi, Y., Tsuchiya, S., Segi-Nishida, E., Inazumi, T., Kabashima, K., Tanaka, S., Murakami, M., Narumiya, S., & Sugimoto, Y. (2014). Prostaglandin E 2 –EP3 Signaling Induces Inflammatory Swelling by Mast Cell Activation. *The Journal of Immunology*, *192*(3), 1130–1137. https://doi.org/10.4049/jimmunol.1300290

Mukherjee, C., Kling, T., Russo, B., Miebach, K., Kess, E., Schifferer, M., Pedro, L. D., Weikert, U., Fard, M. K., Kannaiyan, N., Rossner, M., Aicher, M.-L., Goebbels, S., Nave, K.-A., Krämer-Albers, E.-M., Schneider, A., & Simons, M. (2020). Oligodendrocytes Provide Antioxidant Defense Function for Neurons by Secreting Ferritin Heavy Chain. *Cell Metabolism*, *32*(2), 259-272.e10. https://doi.org/10.1016/j.cmet.2020.05.019

Murata, T., Ushikubi, F., Matsuoka, T., Hirata, M., Yamasaki, A., Sugimoto, Y., Ichikawa, A., Aze, Y., Tanaka, T., Yoshida, N., Ueno, A., Oh-ishi, S., & Narumiya, S. (1997). Altered pain perception and inflammatory response in mice lacking prostacyclin receptor. *Nature*, *388*(6643), 678–682. https://doi.org/10.1038/41780

Nave, K.-A. (2010). Myelination and support of axonal integrity by glia. *Nature*, *468*(7321), 244–252. https://doi.org/10.1038/nature09614

Nguyen, L. N., Ma, D., Shui, G., Wong, P., Cazenave-Gassiot, A., Zhang, X., Wenk, M. R., Goh, E. L. K., & Silver, D. L. (2014). Mfsd2a is a transporter for the essential omega-3 fatty acid docosahexaenoic acid. *Nature*, *509*(7501), 503–506. https://doi.org/10.1038/nature13241

Nimmerjahn, A. (2005). Resting Microglial Cells Are Highly Dynamic Surveillants of Brain Parenchyma in Vivo. *Science*, *308*(5726), 1314–1318. https://doi.org/10.1126/science.1110647

O'Brien, J. S., & Sampson, E. L. (1965). Fatty acid and fatty aldehyde composition of the major brain lipids in normal human gray matter, white matter, and myelin_O'Brien&Sampson_1965. *Journal of Lipid Research*.

O'Leary, M. T., & Blakemore, W. F. (1997). Use of a rat Y chromosome probe to determine the long-term survival of glial cells transplanted into areas of CNS demyelination. *Journal of Neurocytology*, *26*(4), 191–206. https://doi.org/10.1023/a:1018536130578

Olson, J. K., Croxford, J. L., Calenoff, M. A., Dal Canto, M. C., & Miller, S. D. (2001). A virus-induced molecular mimicry model of multiple sclerosis. *The Journal of Clinical Investigation*, *108*(2), 311–318. https://doi.org/10.1172/JCI13032

Palumbo, S., Toscano, C. D., Parente, L., Weigert, R., & Bosetti, F. (2011). Time-dependent changes in the brain arachidonic acid cascade during cuprizone-induced demyelination and remyelination. *Prostaglandins, Leukotrienes and Essential Fatty Acids*, *85*(1), 29–35. https://doi.org/10.1016/j.plefa.2011.04.001

Pan, J.-P., Zhang, H.-Q., Wei-Wang, Guo, Y.-F., Na-Xiao, Cao, X.-H., & Liu, L.-J. (2011). Some subtypes of endocannabinoid/endovanilloid receptors mediate docosahexaenoic acid-induced enhanced spatial memory in rats. *Brain Research*, *1412*, 18–27. https://doi.org/10.1016/j.brainres.2011.07.015

Parks, N. E., Jackson-Tarlton, C. S., Vacchi, L., Merdad, R., & Johnston, B. C. (2020). Dietary interventions for multiple sclerosis-related outcomes. *The Cochrane Database of Systematic Reviews*, *5*(5). https://doi.org/10.1002/14651858.CD004192.pub4

Penkert, H., Bertrand, A., Tiwari, V., Breimann, S., Müller, S. A., Jordan, P. M., Gerl, M. J., Klose, C., Cantuti-Castelvetri, L., Bosch-Queralt, M., Levental, I., Lichtenthaler, S. F., Werz, O., & Simons, M. (2021). Proteomic and lipidomic profiling of demyelinating lesions identifies fatty acids as modulators in lesion recovery. *Cell Reports*, *37*(4), 109898. https://doi.org/10.1016/j.celrep.2021.109898

Plemel, J. R., Michaels, N. J., Weishaupt, N., Caprariello, A. V., Keough, M. B., Rogers, J. A., Yukseloglu, A., Lim, J., Patel, V. V., Rawji, K. S., Jensen, S. K., Teo, W., Heyne, B., Whitehead, S. N., Stys, P. K., & Yong, V. W. (2018). Mechanisms of lysophosphatidylcholine-induced demyelination: A primary lipid disrupting myelinopathy. *Glia*, *66*(2), 327–347. https://doi.org/10.1002/glia.23245

Polak, P. E., Kalinin, S., Dello Russo, C., Gavrilyuk, V., Sharp, A., Peters, J. M., Richardson, J., Willson, T. M., Weinberg, G., & Feinstein, D. L. (2005). Protective effects of a peroxisome proliferator-activated receptor-β/δ agonist in experimental autoimmune encephalomyelitis. *Journal of Neuroimmunology*, *168*(1-2), 65–75. https://doi.org/10.1016/j.jneuroim.2005.07.006

Prabhu, Y., & Gopalakrishnan, A. (2021). Can polyunsaturated fatty acids regulate Polycystic Ovary Syndrome via TGF-β signalling? *Life Sciences*, *276*. https://doi.org/10.1016/j.lfs.2021.119416

Prineas, J. W., Kwon, E. E., Cho, E.-S., & Sharer, L. R. (1984). Continual Breakdown and Regeneration of Myelin in Progressive Multiple Sclerosis Plaques. *Annals of the New York Academy of Sciences*, *436*(1 Multiple Scle), 11–32. https://doi.org/10.1111/j.1749-6632.1984.tb14773.x

Prüss, H., Rosche, B., Sullivan, A. B., Brommer, B., Wengert, O., Gronert, K., & Schwab, J. M. (2013). Proresolution lipid mediators in multiple sclerosis - differential, disease severity-dependent synthesis - a clinical pilot trial. *PloS One*, *8*(2), e55859. https://doi.org/10.1371/journal.pone.0055859

Rapoport, S. I., & Igarashi, M. (2009). Can the rat liver maintain normal brain DHA metabolism in the absence of dietary DHA? *Prostaglandins, Leukotrienes and Essential Fatty Acids*, *81*(2-3), 119–123. https://doi.org/10.1016/j.plefa.2009.05.021

Rasul, T., & Frederiksen, J. L. (2018). Link between overweight/obese in children and youngsters and occurrence of multiple sclerosis. *Journal of Neurology*, *265*(12), 2755–2763. https://doi.org/10.1007/s00415-018-8869-9

Rivers, T. M., Sprunt, D. H., & Berry, G. P. (1933). OBSERVATIONS ON ATTEMPTS TO PRODUCE ACUTE DISSEMINATED ENCEPHALOMYELITIS IN MONKEYS. *Journal of Experimental Medicine*, *58*(1), 39–53. https://doi.org/10.1084/jem.58.1.39

Rong, J. X., Blachford, C., Feig, J. E., Bander, I., Mayne, J., Kusunoki, J., Miller, C., Davis, M., Wilson, M., Dehn, S., Thorp, E., Tabas, I., Taubman, M. B., Rudel, L. L., & Fisher, E. A. (2013). ACAT Inhibition Reduces the Progression of Preexisting, Advanced Atherosclerotic Mouse Lesions Without Plaque or Systemic Toxicity. *Arteriosclerosis, Thrombosis, and Vascular Biology*, *33*(1), 4–12. https://doi.org/10.1161/ATVBAHA.112.252056

Rothhammer, V., & Quintana, F. J. (2016). Environmental control of autoimmune inflammation in the central nervous system. *Current Opinion in Immunology*, *43*, 46–53. https://doi.org/10.1016/j.coi.2016.09.002

Safaiyan, S., Kannaiyan, N., Snaidero, N., Brioschi, S., Biber, K., Yona, S., Edinger, A. L., Jung, S., Rossner, M. J., & Simons, M. (2016). Age-related myelin degradation burdens the clearance function of microglia during aging. *Nature Neuroscience*, *19*(8), 995–998. https://doi.org/10.1038/nn.4325

Sampaio, J. L., Gerl, M. J., Klose, C., Ejsing, C. S., Beug, H., Simons, K., & Shevchenko, A. (2011). Membrane lipidome of an epithelial cell line. *Proceedings of the National Academy of Sciences*, *108*(5), 1903–1907. https://doi.org/10.1073/pnas.1019267108

Schilcher, I., Ledinski, G., Radulović, S., Hallström, S., Eichmann, T., Madl, T., Zhang, F., Leitinger, G., Kolb-Lenz, D., Darnhofer, B., Birner-Gruenberger, R., Wadsack, C., Kratky, D., Marsche, G., Frank, S., & Cvirn, G. (2019). Endothelial lipase increases antioxidative capacity of high-density lipoprotein. *Biochimica Et Biophysica Acta (BBA) - Molecular and Cell Biology of Lipids*, *1864*(10), 1363–1374. https://doi.org/10.1016/j.bbalip.2019.06.011

Schlegel, A. A., Rudelson, J. J., & Tse, P. U. (2012). White matter structure changes as adults learn a second language. *Journal of Cognitive Neuroscience*, *24*(8), 1664–1670. https://doi.org/10.1162/jocn_a_00240

Schwab, J. M., Chiang, N., Arita, M., & Serhan, C. N. (2007). Resolvin E1 and protectin D1 activate inflammation-resolution programmes. *Nature*, *447*(7146), 869–874. https://doi.org/10.1038/nature05877

Sekiya, K., & Okuda, H. (1982). Selective inhibition of platelet lipoxygenase by baicalein. *Biochemical and Biophysical Research Communications*, *105*(3), 1090–1095. https://doi.org/10.1016/0006-291X(82)91081-6

Seo, T., Oelkers, P. M., Giattina, M. R., Worgall, T. S., Sturley, S. L., & Deckelbaum, R. J. (2001). Differential Modulation of ACAT1 and ACAT2 Transcription and Activity by Long Chain Free Fatty Acids in Cultured Cells †. *Biochemistry*, *40*(15), 4756–4762. https://doi.org/10.1021/bi0022947

Serhan, C. N. (2014). Pro-resolving lipid mediators are leads for resolution physiology. *Nature*, *510*(7503), 92–101. https://doi.org/10.1038/nature13479

Serhan, C. N. (2017). Discovery of specialized pro-resolving mediators marks the dawn of resolution physiology and pharmacology. *Molecular Aspects of Medicine*, *58*, 1–11. https://doi.org/10.1016/j.mam.2017.03.001

Serhan, C. N., Chiang, N., & van Dyke, T. E. (2008). Resolving inflammation: Dual anti-inflammatory and pro-resolution lipid mediators. *Nature Reviews. Immunology*, *8*(5), 349–361. https://doi.org/10.1038/nri2294

Serhan, C. N., Dalli, J., Colas, R. A., Winkler, J. W., & Chiang, N. (2015). Protectins and maresins: New pro-resolving families of mediators in acute inflammation and resolution bioactive metabolome. *Biochimica Et Biophysica Acta*, *1851*(4), 397–413. https://doi.org/10.1016/j.bbalip.2014.08.006

Serhan, C. N., Dalli, J., Karamnov, S., Choi, A., Park, C.-K., Xu, Z.-Z., Ji, R.-R., Zhu, M., & Petasis, N. A. (2012). Macrophage proresolving mediator maresin 1 stimulates tissue regeneration and controls pain. *FASEB Journal : Official Publication of the Federation of American Societies for Experimental Biology*, *26*(4), 1755–1765. https://doi.org/10.1096/fj.11-201442

Serhan, C. N., & Petasis, N. A. (2011). Resolvins and protectins in inflammation resolution. *Chemical Reviews*, *111*(10), 5922–5943. https://doi.org/10.1021/cr100396c

Serhan, C. N., & Savill, J. (2005). Resolution of inflammation: The beginning programs the end. *Nature Immunology*, *6*(12), 1191–1197. https://doi.org/10.1038/ni1276

Serhan, C. N., Yang, R., Martinod, K., Kasuga, K., Pillai, P. S., Porter, T. F., Oh, S. F., & Spite, M. (2009). Maresins: Novel macrophage mediators with potent antiinflammatory and proresolving actions. *The Journal of Experimental Medicine*, *206*(1), 15–23. https://doi.org/10.1084/jem.20081880

Shields, S. A., Gilson, J. M., Blakemore, W. F., & Franklin, R. J.M. (1999). Remyelination occurs as extensively but more slowly in old rats compared to young rats following gliotoxin-induced CNS demyelination. *Glia*, *28*(1), 77–83. https://doi.org/10.1002/(SICI)1098-1136(199910)28:1<77::AID-GLIA9>3.0.CO;2-F

Siegert, E., Paul, F., Rothe, M., & Weylandt, K. H. (2017). The effect of omega-3 fatty acids on central nervous system remyelination in fat-1 mice. *BMC Neuroscience*, *18*(1), 19. https://doi.org/10.1186/s12868-016-0312-5

Sim, F. J., Zhao, C., Penderis, J., & Franklin, R. J. M. (2002). The Age-Related Decrease in CNS Remyelination Efficiency Is Attributable to an Impairment of Both Oligodendrocyte Progenitor Recruitment and Differentiation. *Journal of Neuroscience*, *22*(7), 2451–2459. https://doi.org/10.1523/JNEUROSCI.22-07-02451.2002

Simopoulos, A. P. (2008). The Importance of the Omega-6/Omega-3 Fatty Acid Ratio in Cardiovascular Disease and Other Chronic Diseases. *Experimental Biology and Medicine*, *233*(6), 674–688. https://doi.org/10.3181/0711-MR-311

Sinclair, A. J. (1975). Incorporation of radioactive polyunsaturated fatty acids into liver and brain of developing rat. *Lipids*, *10*(3), 175–184. https://doi.org/10.1007/bf02534156

Singh, N. K., & Rao, G. N. (2019). Emerging role of 12/15-Lipoxygenase (ALOX15) in human pathologies. *Progress in Lipid Research*, *73*, 28–45. https://doi.org/10.1016/j.plipres.2018.11.001

Skripuletz, T., Hackstette, D., Bauer, K., Gudi, V., Pul, R., Voss, E., Berger, K., Kipp, M., Baumgärtner, W., & Stangel, M. (2013). Astrocytes regulate myelin clearance through recruitment of microglia during cuprizone-induced demyelination. *Brain*, *136*(1), 147–167. https://doi.org/10.1093/brain/aws262

Smedt-Peyrusse, V. de, Sargueil, F., Moranis, A., Harizi, H., Mongrand, S., & Layé, S. (2008). Docosahexaenoic acid prevents lipopolysaccharide-induced cytokine production in microglial cells by inhibiting lipopolysaccharide receptor presentation but not its membrane subdomain localization. *Journal of Neurochemistry*, *105*(2), 296–307. https://doi.org/10.1111/j.1471-4159.2007.05129.x

Smith, J. B., & Willis, A. L. (1971). Aspirin Selectively Inhibits Prostaglandin Production in Human Platelets. *Nature New Biology*, *231*(25), 235–237. https://doi.org/10.1038/newbio231235a0

Snaidero, N., & Simons, M. (2014). Myelination at a glance. *Journal of Cell Science*, *127*(Pt 14), 2999–3004. https://doi.org/10.1242/jcs.151043

Sowell, E. R., Thompson, P. M., Holmes, C. J., Jernigan, T. L., & Toga, A. W. (1999). In vivo evidence for post-adolescent brain maturation in frontal and striatal regions. *Nature Neuroscience*, *2*(10), 859–861. https://doi.org/10.1038/13154

Sprecher, H., Luthria, D. L., Mohammed, B. S., & Baykousheva, S. P. (1995). Reevaluation of the pathways for the biosynthesis of polyunsaturated fatty acids. *Journal of Lipid Research*, *36*(12), 2471–2477. https://doi.org/10.1016/S0022-2275(20)41084-3

Stacklies, W., Redestig, H., Scholz, M., Walther, D., & Selbig, J. (2007). pcaMethods a bioconductor package providing PCA methods for incomplete data. *Bioinformatics*, *23*(9), 1164–1167. https://doi.org/10.1093/bioinformatics/btm069

Stadelmann, C., Timmler, S., Barrantes-Freer, A., & Simons, M. (2019). Myelin in the Central Nervous System: Structure, Function, and Pathology. *Physiological Reviews*, *99*(3). https://doi.org/10.1152/physrev.00031.2018

Stangel, M., Kuhlmann, T., Matthews, P. M., & Kilpatrick, T. J. (2017). Achievements and obstacles of remyelinating therapies in multiple sclerosis. *Nature Reviews. Neurology*, *13*(12), 742–754. https://doi.org/10.1038/nrneurol.2017.139

Stone, N. J. (2000). The Gruppo Italiano per lo Studio della Sopravvivenza nell'Infarto Miocardio (GISSI)-Prevenzione Trial on fish oil and vitamin E supplementation in myocardial infarction survivors. *Current Cardiology Reports*, *2*(5), 445–451. https://doi.org/10.1007/s11886-000-0059-5

Stromnes, I. M., & Goverman, J. M. (2006). Active induction of experimental allergic encephalomyelitis. *Nature Protocols*, *1*(4), 1810–1819. https://doi.org/10.1038/nprot.2006.285

Sugasini, D., Thomas, R., Yalagala, P. C. R., Tai, L. M., & Subbaiah, P. V. (2017). Dietary docosahexaenoic acid (DHA) as lysophosphatidylcholine, but not as free acid, enriches brain DHA and improves memory in adult mice. *Scientific Reports*, *7*(1), 11263. https://doi.org/10.1038/s41598-017-11766-0

Sugasini, D., Yalagala, P. C. R., Goggin, A., Tai, L. M., & Subbaiah, P. V. (2019). Enrichment of brain docosahexaenoic acid (DHA) is highly dependent upon the molecular carrier of dietary DHA: Lysophosphatidylcholine is more efficient than either phosphatidylcholine or triacylglycerol. *The Journal of Nutritional Biochemistry*, *74*, 108231. https://doi.org/10.1016/j.jnutbio.2019.108231

Sun, G. Y., Simonyi, A., Fritsche, K. L., Chuang, D. Y., Hannink, M., Gu, Z., Greenlief, C. M., Yao, J. K., Lee, J. C., & Beversdorf, D. Q. (2018). Docosahexaenoic acid (DHA): An essential nutrient and a nutraceutical for brain health and diseases. *Prostaglandins, Leukotrienes, and Essential Fatty Acids*, *136*, 3–13. https://doi.org/10.1016/j.plefa.2017.03.006

Surma, M. A., Herzog, R., Vasilj, A., Klose, C., Christinat, N., Morin-Rivron, D., Simons, K., Masoodi, M., & Sampaio, J. L. (2015). An automated shotgun lipidomics platform for high throughput, comprehensive, and quantitative analysis of blood plasma intact lipids. *European Journal of Lipid Science and Technology*, *117*(10), 1540–1549. https://doi.org/10.1002/ejlt.201500145

References

Svennerholm, L. (1968). Distribution and fatty acid composition of phosphoglycerides in normal human brain_Svennerholm 1968. *Journal of Lipid Research*.

Thompson, A. J., Banwell, B. L., Barkhof, F., Carroll, W. M., Coetzee, T., Comi, G., Correale, J., Fazekas, F., Filippi, M., Freedman, M. S., Fujihara, K., Galetta, S. L., Hartung, H. P., Kappos, L., Lublin, F. D., Marrie, R. A., Miller, A. E., Miller, D. H., Montalban, X., . . . Cohen, J. A. (2018). Diagnosis of multiple sclerosis: 2017 revisions of the McDonald criteria. Advance online publication. https://doi.org/10.1016/S1474-4422(17)30470-2 (The Lancet Neurology, 17(2), 162-173).

Trapp, B. D., Peterson, J., Ransohoff, R. M., Rudick, R., Mörk, S., & Bö, L. (1998). Axonal transection in the lesions of multiple sclerosis. *The New England Journal of Medicine*, *338*(5). https://doi.org/10.1056/NEJM199801293380502

Trimarco, A., Forese, M. G., Alfieri, V., Lucente, A., Brambilla, P., Dina, G., Pieragostino, D., Sacchetta, P., Urade, Y., Boizet-Bonhoure, B., Martinelli Boneschi, F., Quattrini, A., & Taveggia, C. (2014). Prostaglandin D2 synthase/GPR44: A signaling axis in PNS myelination. *Nature Neuroscience*, *17*(12), 1682–1692. https://doi.org/10.1038/nn.3857

U.S. Food and Drug administration (Ed.). (2007). *Drug approval package: Zileuton*.

U.S. Food and Drug administration (Ed.). (2019). *Drug approval package: Icosapent Ethyl*.

Vandal, M., Alata, W., Tremblay, C., Rioux-Perreault, C., Salem, N., Calon, F., & Plourde, M. (2014). Reduction in DHA transport to the brain of mice expressing human APOE4 compared to APOE2. *Journal of Neurochemistry*, *129*(3), 516–526. https://doi.org/10.1111/jnc.12640

Vane, J. R. (1971). Inhibition of Prostaglandin Synthesis as a Mechanism of Action for Aspirin-like Drugs. *Nature New Biology*, *231*(25), 232–235. https://doi.org/10.1038/newbio231232a0

Venturini, G. (1973). Enzymic activities and sodium, potassium and copper concentrations in mouse brain and liver after cuprizone treatment in vivo. *Journal of Neurochemistry*, *21*(5), 1147–1151. https://doi.org/10.1111/j.1471-4159.1973.tb07569.x

Walton, C., King, R., Rechtman, L., Kaye, W., Leray, E., Marrie, R. A., Robertson, N., La Rocca, N., Uitdehaag, B., van der Mei, I., Wallin, M., Helme, A., Angood Napier, C., Rijke, N., & Baneke, P. (2020). Rising prevalence of multiple sclerosis worldwide: Insights from the Atlas of MS, third edition. *Multiple Sclerosis Journal*, *26*(14), 1816–1821. https://doi.org/10.1177/1352458520970841

Werner, M., Jordan, P. M., Romp, E., Czapka, A., Rao, Z., Kretzer, C., Koeberle, A., Garscha, U., Pace, S., Claesson, H.-E., Serhan, C. N., Werz, O., & Gerstmeier, J. (2019). Targeting biosynthetic networks of the proinflammatory and proresolving lipid metabolome. *FASEB Journal : Official Publication of the Federation of American Societies for Experimental Biology*, *33*(5), 6140–6153. https://doi.org/10.1096/fj.201802509R

Whitney, L. W., Ludwin, S. K., McFarland, H. F., & Biddison, W. E. (2001). Microarray analysis of gene expression in multiple sclerosis and EAE identifies 5-lipoxygenase as a component of inflammatory lesions. *Journal of Neuroimmunology*, *121*(1-2), 40–48. https://doi.org/10.1016/S0165-5728(01)00438-6

Wood, A. H. R., Chappell, H. F., & Zulyniak, M. A. (2021). Dietary and supplemental long-chain omega-3 fatty acids as moderators of cognitive impairment and Alzheimer's disease. *European Journal of Nutrition.* Advance online publication. https://doi.org/10.1007/s00394-021-02655-4

References

Xu, J., Feng, Z.-P., Peng, H.-Y., & Fu, P. (2018). Omega-3 polyunsaturated fatty acids alleviate adenine-induced chronic renal failure via regulating ROS production and TGF-β/SMAD pathway. *European Review for Medical and Pharmacological Sciences*, *22*(15), 5024–5032. https://doi.org/10.26355/eurrev_201808_15645

Xu, J., Zhang, Y., Xiao, Y., Ma, S., Liu, Q., Dang, S., Jin, M., Shi, Y., & Wan, B. (2013). Inhibition of 12/15-lipoxygenase by baicalein induces microglia PPARβ/δ: a potential therapeutic role for CNS autoimmune disease. *Cell Death & Disease*, *4*(4), e569-e569. https://doi.org/10.1038/cddis.2013.86

Xu, Z.-Z., Zhang, L., Liu, T., Park, J. Y., Berta, T., Yang, R., Serhan, C. N., & Ji, R.-R. (2010). Resolvins RvE1 and RvD1 attenuate inflammatory pain via central and peripheral actions. *Nature Medicine*, *16*(5), 592-7, 1p following 597. https://doi.org/10.1038/nm.2123

Yalagala, P. C. R., Sugasini, D., Dasarathi, S., Pahan, K., & Subbaiah, P. V. (2019). Dietary lysophosphatidylcholine-EPA enriches both EPA and DHA in the brain: Potential treatment for depression. *Journal of Lipid Research*, *60*(3), 566–578. https://doi.org/10.1194/jlr.M090464

Yavin, E., Glozman, S., & Green, P. (2001). Docosahexaenoic Acid Accumulation in the Prenatal Brain: Prooxidant and Antioxidant Features. *Journal of Molecular Neuroscience*, *16*(2-3), 229–236. https://doi.org/10.1385/JMN:16:2-3:229

Yip, P. K., Bowes, A. L., Hall, J. C. E., Burguillos, M. A., Ip, T. H. R., Baskerville, T., Liu, Z.-H., Mohamed, M. A. E. K., Getachew, F., Lindsay, A. D., Najeeb, S.-U.-R., Popovich, P. G., Priestley, J. V., & Michael-Titus, A. T. (2019). Docosahexaenoic acid reduces microglia phagocytic activity via miR-124 and induces neuroprotection in rodent models of spinal cord contusion injury. *Human Molecular Genetics*, *28*(14), 2427–2448. https://doi.org/10.1093/hmg/ddz073

Yokoyama, M., Origasa, H., Matsuzaki, M., Matsuzawa, Y., Saito, Y., Ishikawa, Y., Oikawa, S., Sasaki, J., Hishida, H., Itakura, H., Kita, T., Kitabatake, A., Nakaya, N., Sakata, T., Shimada, K., & Shirato, K. (2007). Effects of eicosapentaenoic acid on major coronary events in hypercholesterolaemic patients (JELIS): a randomised open-label, blinded endpoint analysis. *The Lancet*, *369*(9567), 1090–1098. https://doi.org/10.1016/S0140-6736(07)60527-3

Zárate, R., El Jaber-Vazdekis, N., Tejera, N., Pérez, J. A., & Rodríguez, C. (2017). Significance of long chain polyunsaturated fatty acids in human health. *Clinical and Translational Medicine*, *6*(1), 25. https://doi.org/10.1186/s40169-017-0153-6

Zhao, Y., Calon, F., Julien, C., Winkler, J. W., Petasis, N. A., Lukiw, W. J., & Bazan, N. G. (2011). Docosahexaenoic Acid-Derived Neuroprotectin D1 Induces Neuronal Survival via Secretase- and PPARγ-Mediated Mechanisms in Alzheimer's Disease Models. *PloS One*, *6*(1), e15816. https://doi.org/10.1371/journal.pone.0015816